NTNU – Trondheim
Norwegian University of
Science and Technology

An Investigation Into Braess' Paradox and Selfish Routing in Traffic Flow

Solving the non-linear traffic program with
linear cost functions on traffic networks

Anette Østbø Sørensen

Master of Science in Physics and Mathematics
Submission date: June 2014
Supervisor: Helge Holden, MATH

Norwegian University of Science and Technology
Department of Mathematical Sciences

Problem statement

Braess' Paradox is a well known phenomenon in traffic flow. It occurs when extention of a road network by one road, leads to a redistribution of the traffic in such a way that the travel times are increased for everyone.

Selfish routing is another contribution to increased travel time in traffic networks. Comparing travel times at Nash equilibrium and system optimal flow demonstrate how selfish routing may result in increased travel time for some or all travelers.

This study should investigate the occurence of Braess' paradox in traffic flow and how selfish routing affects travel times. In particular,

- on traffic networks of different sizes,
- with suitable/linear cost functions,
- solving the minimization problem for the traffic assignment problems with a suitable method,
- compare different results from the literature.

Preface

This thesis concludes my Master of Science in Applied Physics and Mathematics, with specialication in Industrial Mathematics, at the Norwegian University of Science and Technology (NTNU). The thesis is a continuation of my specialisation project in TMA4500 and is written during the spring of 2014.

I would like to thank my supervisor Helge Holden, Professor of mathematics at NTNU, for guidance and feedback during my work. I would also like to thank Jon Andre Haugen for helpful comments and proofreading.

A special thank to my family and my boyfriend Are Bertheussen for always giving me invaluable support and encouragement. Finally thanks to all my friends and fellow students for five memorable years in Trondheim.

Trondheim, June 2014,
Anette Østbø Sørensen

Sammendrag

Formålet med denne masteroppgaven var å undersøke Braess paradoks i trafikkflyt, og se på innvirkningen "selfish routing" har på reisetiden til brukerene i forhold til optimal fordeling av reisende over rutene i et trafikknettverk.

Braess' paradoks er et godt kjent fenomen i trafikknettverk. Fenomenet inntreffer når en utvidelse av et veinettverk ved tilføring av en link, fører til en redistribusjon av trafikkflyten slik at brukerenes kjøretid øker.

"Selfish routing" handler om at reisende velger reiseruten sin egoistisk basert på hva som er den korteste tilgjengelige ruten. Sammenlignet med reisetid ved systemoptimal flytdistribusjon kan den egoistiske reiseplanleggingen føre til lengre reisetid for alle reisende.

Optimal flytfordeling over rutene i et nettverk ble funnet basert på et ikke-lineært program, hvor Nash likevekt (brukeroptimal flyt) og systemoptimal flyt oppnås med ulike objektfunksjoner. Siden funksjonene for reisetiden er lineære løses det ikke-lineære programmet med kvadratisk programmering. For å løse programmet ble "interior point" metoden brukt, som er basert på en "predictor-corrector" metode. Resultatene for når Braess paradoks inntreffer ble sammenlignet med resultatene fra en matematisk karakterisering av paradokset fra litteraturen.

Fire ulike trafikknettverk ble undersøkt. Det første nettverket var nettverkskmodellen opprinnelig brukt av Braess med ett startpunkt og én destinasjon. Videre, er et nettverk med ett startpunkt og to destinasjoner brukt. Ved at retningen på to av veiene ble snudd, bidro nettverket til to ulike trafikknettverk. Et annet nettverk som ble brukt har to startpunkt og én destinasjon, og bidrar tilsvarende til to ulike nettverk. Det siste nettverket som ble brukt er tre ganger symmetrisk med tre startpunkt-destinasjons par. Hvert av nettverkene ble undersøkt for tilfeller av Braess paradoks og innvirkningen fra egoistiske reisevalg. Analysene ble gjennomført ved å variere parameterene i de lineære reisetidsfunksjonene og etterspørselen.

I arbeidet ble det vist at Braess paradoks inntreffer når etterspørselen er innenfor begrensede intervaller, avhengig av parameterene i reisetidsfunksjonene. Det ser ut til å eksistere en øvre grense for den ekstra reisetiden som inntreffer når en vei blir lagt til i trafikknettverket. Braess paradoks inntreffer når rutene med den tilførte linken blir brukt samtidig med en eller flere andre ruter. "Selfish routing" har innvirkning på reisetid når etterspørselekn er innenfor et begrenset interval. Reisetiden ved systemoptimal flytdistribusjon er i noen intervallre svært ufordelaktig for noen reisende, sammenlignet med reisetiden ved brukeroptimal flyt.

Abstract

The aim of this master thesis was to investigate Braess' Paradox in traffic flow and to look at the effect of selfish routing in optimization of flow distribution on traffic networks.

Braess' Paradox is a well known phenomenon in traffic flow. It occurs when extention of a road network by one road leads to increased travel times for all travelers due to a redistribution of the traffic.

Selfish routing is about how travelers choose their travel route selfishly. Compared to flow distribution at system optimal flow, selfish routing may result in increased travl time for some or all travelers.

The optimal flow distribution was found by a non-linear program, and Nash equilibrium and system optimal flow are achieved with different objective functions. The non-linear program was solved as quadratic programming, since the travel time functions are linear. The method used to solve the program was an interior-point method based on a predictor-corrector method. The results of occurences of Braess' paradox are compared to the results from a mathematical characterization of the paradox from the litterature.

Four different traffic networks was investigated. The first network was the network model originally used by Braess with one origin and one destination. Furthermore, a network of one origin and two destinations was used, which contributed to two different networks when the direction of two roads were changed. Another network is of two origins and one destination, which also contributed to two networks. Lastly, a three times symmetric network was used, with three origin-destination pairs. Each of the networks were investigated to find occurences of Braess' paradox, and to investigate the effect of selfish routing. In the analyses the values of function parameters and demand between origin and destination was changed.

In the work it was showed that Braess' paradox occurs at some limited intervals of demand, which is dependent on the parameters in the travel time functions. It seems to exist an upper limit for the increase in travel time caused by the added road. The paradox occurs when the path with the additional road is utilized together with and at the same time as one or several other paths. Selfish routing affects the travel time when demand is within a limited interval. The travel times at system optimal flow distribution is in some intervals most unfavorable for some of the travelers, compared to the travel time at user optimal flow.

Contents

List of Figures

List of Tables

Chapter 1

Introduction

The aim of this master thesis was to investigate occurences of Braess' paradox in traffic flow and how selfish routing affects travel time.

The Braess Paradox is a well known phenomenon in traffic flow on road networks. However, the paradox has also been observed in other non-traffic systems, such as mechanical systems [5], economic systems and electrical circuits [5, 16].

In traffic flow, when the travel time for crossing a link is independent of the amount of travelers wanting to traverse the road, adding a road to the network cannot increase the travel time. However, this is not true when travel time is dependent on number of travelers, as Braess' paradox shows [3]. The paradox occurs when extention of a road network by one link, leads to a redistribution of the traffic in such a way that travel times are increased.

The paradox was suggested by Dietrich Braess in 1968 [3] (English translation in 2005 [4]). The paradox was followed up by Murchland in 1970 [11], and has since been refered to as Braess' Paradox.

Braess demonstrated occurence of the paradox in the simple road network shown in Figure 1.1. Link u_5 is the additional road in the network. The time it takes to travel across a link is given by a cost function. The link cost may be either dependent or independent of the number of vehicles wanting to cross the link per time unit. In most studies the cost functions have been linear (e.g.[4, 7, 9, 11, 19]), but also quadratic [7] and other non-linear functions have been studied [19, 21]. The linear cost functions used by Braess were $f_1(x) = f_4(x) = 10x$, $f_2(x) = f_3(x) = x + 50$ and $f_5(x) = x + 10$. The functions are symmetric over the network, in such a way that link u_1 and u_4 has equal function parameters, and similar for link u_2 and u_3.

Murchland modified Braess' example by changing the linear cost functions slightly. The costs were changed to be either constant of the form $f(x) = B$ or functions on the form $f(x) = Ax$. In addition, travel time on link u_5 was set to zero, which also has been studied later by others (e.g. [16]). The increase in travel

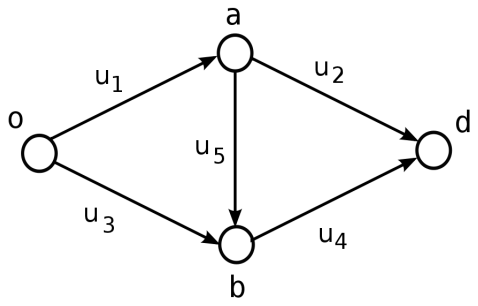

Figure 1.1: Braess' original network model.

time after adding link u_5 to the network was then larger than in Braess' original example.

Braess' paradox has been described by mathematical characterizations given linear cost functions on the network links [7]. It has been shown that Braess' Paradox only occurs when total demand is within certain intervals [7, 14]. The size and the location of the intervals would depend on the parameters in the travel time functions.

It has been shown that Braess' Paradox is as likely to occur as not to occur [21]. This was shown on a general transportation network. Under reasonable assumptions, there has been given some necessary and sufficient conditions for the paradox to occur.

Braess' paradox has also been shown to exist in a simple queueing network [6]. The network in question contained two types of servers, either first-come-first-served or infinite-server queue. The users were assumed to enter the network as Poisson flows. In the first-come-first-served queue, waiting time would be dependent on the number of individuals in the line, whilst in the infinite-server queue average waiting time would not depend on this number. When a link was added to the network, the resulting waiting time increased, as in the Braess Paradox.

The interpretation of the travel time functions is essential to understand the connection between theory and real road network. Linear functions contain two terms, ax and b. In traffic flow, parameter a is refered to as a congesting parameter as the term is dependent on flow x. Parameter b is the noncongesting parameter. A large value of the congesting parameter suggests that the road is narrow [16], since the travel time then increases rapidly when the number of travelers increases. A small value of the congesting parameter suggests that the road is wider, since the road can take more travelers without increasing the travel time excessively. A large value of the noncongesting parameter suggests that the road is long, since

it results in a large travel time independent on the number of travelers. A small value of the noncongesting parameter is therefore understood as a shorter road.

There have been suggested different measures to prevent Braess' paradox from occuring [14, 16]. Such measures could for instance be to charge users with either a fixed toll, or with the marginal cost or variable toll to ensure the system optimal flow.

Other paradoxes in traffic flow have also been shown. One of these is based on a modified definition of Braess' Paradox [9]. The modification would include multiple origins and destinations, multiple traveler types, and general cost functions and networks. The definition still includes Braess' original example and all other examples of the paradox in the literature. As a consequence of the modification, the flow distributions and occurences of the paradox differ slightely from the original Braess paradox.

Selfish routing and how it affected the users travel times was investigated by Rouhghgarden and Tardos in 2002 [19]. They found relations between the total travel cost at Nash equilibrium and at system optimal flow. When the costs were linear functions, there would be an upper limit for this ratio. When the costs were only assumed to be non-decreasing, continuous functions, they showed that this ratio may be unbounded.

In this thesis we investigated occurences of Braess' paradox in traffic flow and the influence of selfish routing on travel times. The analyses were executed on four different traffic networks and included analyses on depenency of origin-destination demands and function parameters. The optimal flow distributions were found solving a non-linear minimization program with quadratic programming.

Chapter 2 presents the notations used throughout the paper, some general theory on the traffic assignment problem and theory concerning Braess' paradox.

In Chapter 3 the methods used in this thesis is described. The methods inlcude the mathematical characterization to find flow distributions on Braess' network model, and the quadratic programming used to solve the non-linear program on general traffic networks with linear travel functions.

Chapter 4 presents the results obtained in the analyses on four different traffic networks with one, two and three origin-destination pairs.

The results are discussed in Chapter 5.

The conclusion is given in Chapter 6.

In Chapter 7 some thoughts concerning further work is given.

Chapter 2

Theory

In 1968 Braess described a paradoxical occurence in traffic planning [3, 4], commonly referred to as Braess' Paradox. Braess showed that the extention of a road network by adding one road, may redistribute the traffic in a way that results in increased travel times. This was demonstrated using a simple road network.

This chapter gives an introduction to some notations and concepts in road traffic that will be used throughout the paper. The well known concepts Nash equilibrium and Wardrop's principles will be described, along with the theory of Braess' paradox, the consept of selfish routing and a mechanical network example.

2.1 Notations

This section gives an overview of the notations used throughout the paper. The general network notations are given in Table 2.1, and some of the terms are further described below.

A road network is commonly described by directed graphs, where roads are represented by oriented links and street intersections are represented by nodes. The amount of travelers wanting to travel through the road network is called *traffic flow*, with number of vehicles per time as denomination. All flow variables are non-negative.

The flow ϕ_α on a link u_α is dependent on how many routes U_β the link is a part of, and the total flow Φ_β on these routes. The relation may be described with the arcpath incidence matrix $\boldsymbol{D}$, whose coefficients are defined as,

$$d_{\alpha\beta} = \begin{cases} 1 & \text{if link } u_\alpha \text{ is contained in path } U_\beta \\ 0 & \text{otherwise.} \end{cases} \tag{2.1}$$

It follows that flow ϕ_α on a link u_α will be

$$\phi_\alpha = \sum_\beta d_{\alpha\beta}\Phi_\beta, \tag{2.2}$$

or in vector form,

$$\boldsymbol{\phi} = \boldsymbol{D}\boldsymbol{\Phi}. \tag{2.3}$$

The *total flow* traversing the network between origin-destination pair $\{o_\nu, d_\nu\}$ is defined by

$$|\Phi_\nu| = \sum_{\beta\in\mathcal{B}_\nu} \Phi_\beta, \tag{2.4}$$

where $\mathcal{B}_\nu$ represent the index sets containing all paths between the origin and destination of ν.

Demand κ_ν is understood as the amount of traffic flow, or in other words number of users per time, wanting to travel between each origin-destination (OD) pair ν. Total flow is the same as demand for each OD pair when the flow distribution meets the demand. As we assume total flow always meets the demand, the notations $|\Phi_\nu|$ and κ_ν is understood as the same throughout the paper. Depending on the circumstances, demand may be either elastic or fixed [15]. In the literature considered and the calculations made in this thesis, the demand has been fixed.

Travel cost on a route may depend on several factors, such as length of road, travel time, road width, intersections, traffic lights, etc. There are two possible types of link cost functions f in a road network. The first type gives an *uncongesting network*, where the travel costs do not vary with the traffic flow $\boldsymbol{\phi}$ using the links [11, 16], that is $f(\boldsymbol{\phi}) = B =$ constant. The opposite case gives a *congesting network*, when the travel costs depend on the traffic flow using the links, i.e. $f = f(\boldsymbol{\phi})$. Most often, travel cost is identified by travel time as a function of flow. The *link-travel time* $t_\alpha(\phi)$ is the time it would take to cross a link u_α carrying the flow $\phi = \phi_\alpha$. The vector of components t_α is denoted $\boldsymbol{t}$.

Path-travel time T_β for getting from o_ν to d_ν on path U_β is dependent on the amount of traffic on each link in the path, and may therefore be expressed by the arcpath incidence matrix D defined in equation (2.1). Travel time on a path will then be,

$$T_\beta(\boldsymbol{\Phi}) = \sum_\alpha d_{\alpha\beta}t_\alpha(\phi_\alpha), \tag{2.5}$$

where the functional relationship $\phi_\alpha = \phi_\alpha(\Phi)$ is given by equation (2.2). Let $\boldsymbol{T}$ denote the vector of components T_β for all paths U_β.

The most unfavorable travel time for traveling between the origin-destination (OD) pair of ν on the paths $\{U_\beta, \beta \in \mathcal{B}_\nu\}$, describes how well the traffic flows are distributed on a road network. This travel time is given by

$$|\boldsymbol{T}^\nu(\boldsymbol{\Phi})| = \max\{T_\beta^\nu(\Phi); \beta \in B_\nu, \Phi_\beta \neq 0\}. \tag{2.6}$$

Let $C(\mathbf{\Phi})$ denote the *system cost*, i.e. the total travel cost summed over all travelers. Then $C(\mathbf{\Phi})$ can be written as,

$$C(\mathbf{\Phi}) = \sum_{\beta} \Phi_\beta T_\beta(\mathbf{\Phi}) = \mathbf{\Phi}^\top \boldsymbol{T}(\mathbf{\Phi}). \tag{2.7}$$

The system cost may also be obtained by summing over the links,

$$C(\boldsymbol{\phi}) = \sum_{\alpha} \phi_\alpha t_\alpha(\phi) = \boldsymbol{\phi}^\top \boldsymbol{t}(\boldsymbol{\phi}). \tag{2.8}$$

This is readily checked by equations (2.2) and (2.5) in the following way,

$$\begin{aligned} C(\boldsymbol{\phi}) &= \sum_{\alpha} \phi_\alpha t_\alpha(\boldsymbol{\phi}) \\ &= \sum_{\alpha} \left(\sum_{\beta} d_{\alpha,\beta} \Phi_\beta \right) t_\alpha(\boldsymbol{\phi}) \\ &= \sum_{\beta} \Phi_\beta \sum_{\alpha} d_{\alpha,\beta} t_\alpha(\boldsymbol{\phi}) \\ &= \sum_{\beta} \Phi_\beta T_\beta(\mathbf{\Phi}) = C(\mathbf{\Phi}). \end{aligned}$$

2.1.1 Additional notations

The following notations were given by Frank [7], and will only be used in Section 3.2. The travel time functions here are defined as $t_\alpha(\boldsymbol{\phi}) = A_\alpha \phi_\alpha + B_\alpha$ with $A_\alpha > 0$ and $B_\alpha \geq 0$ for each link u_α and flow ϕ_α, $\alpha = 1, 2, 3, 4, 5$, in the 5-link traffic network (see Figure 2.1).

$$\Sigma = A_1 + A_2 + A_3 + A_4 \tag{2.9a}$$
$$T(u, v, w) = f_3(u) - f_1(v) - f_5(w) \tag{2.9b}$$
$$T(0) = B_3 - B_1 - B_5 \tag{2.9c}$$
$$T(0)^* = B_2 - B_4 - B_5 \tag{2.9d}$$
$$T = T(0)(A_1 + A_5)^{-1} \tag{2.9e}$$
$$S = A_4 T(0) + A_3 T(0)^* \tag{2.9f}$$
$$S^* = A_1 T(0)^* + A_2 T(0) \tag{2.9g}$$
$$\Delta = A_1 A_4 - A_2 A_3 = \Delta^* \tag{2.9h}$$
$$\theta = (A_1 + A_5) T(0)^* - (A_4 + A_5) T(0) = -\theta^* \tag{2.9i}$$
$$\Lambda = (A_1 + A_3)(A_2 + A_4) + A_5 \Sigma = \Lambda^* > 0 \tag{2.9j}$$
$$G = A_3(A_4 + A_5) + A_4(A_1 + A_5) > 0. \tag{2.9k}$$

Table 2.1: Network notations

$a_i,\ i = 1, 2, ...$	nodes in the network
$\mathcal{N}$	set of nodes a_i in the network
u_α	oriented links in the network
$\mathcal{A}$	set of oriented links in the network
$\{o_\nu, d_\nu\}$	origin-destination (OD) pair in the network
$\nu = 1, 2, ...$	OD index
$\mathcal{B}_\nu$	index sets containing all paths between OD pair j
ϕ_α	flow on link u_α
$\boldsymbol{\phi} = \{\phi_\alpha\}$	vector of ϕ_α
U_β	routes containing links once or less
$\boldsymbol{U} = \{U_\beta\}$	vector of U_β
Φ_β	flow along the path U_β
$\Phi = \{\Phi_\beta\}$	vector of Φ_β
$\boldsymbol{D} = \{d_{\alpha,\beta}\}$	arcpath/link-path incidence matrix
$\kappa_\nu,\ \lvert\Phi_\nu\rvert$	demand and total flow traversing the network between OD pair ν
$t_\alpha(\boldsymbol{\phi})$	link-travel time
$T_\beta(\boldsymbol{\Phi})$	path-travel time
$C(\boldsymbol{\Phi}),\ C(\boldsymbol{\phi})$	system cost

2.2 Nash equilibrium

The *Nash equilibrium* is a principle from game theory, but it has been connected to other areas as well, such as economics and traffic flow. The theory was presented by John Nash in 1951 [12], and shows that a non-cooperative game with a finite number of players, where each player acts independently without communication or cooperation with each other, will at least have one equilibrium point. The equilibrium point may or may not be unique, and is such that the strategy of each player is optimal against those of the others.

If we put this in the context of road traffic, each player is a traveler on the network, and none of the travelers communicate with each other. The best strategy in the sense of road traffic would be to use the path of shortest travel time. There is of course a finite number of travelers, and we assume every traveler have perfect information about travel costs. Then there will be at least one Nash equilibrium, such that every traveler use the path with the shortest possible travel time compared to the path choices of the others. That is, no traveler can find a path with less travel time.

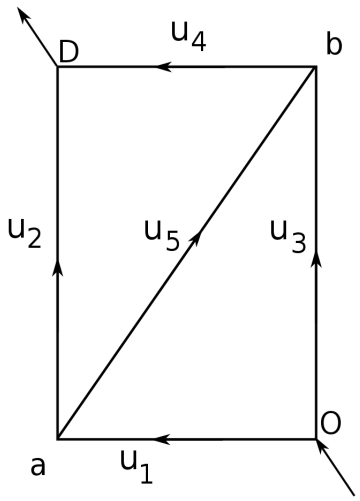

Figure 2.1: Traffic network of five links.

2.3 Wardrop's principles

In 1952, Wardop wrote about mathematical and statistical aspects concerning research on road traffic [23]. One of these aspects concerned the process of evaluating some future improvement on a road system, by adding new roads. Such an extention of the network will lead to a redistribution of traffic from some of the already existing roads to new roads. In the evaluation process it is necessary to estimate the distribution of traffic on the affected roads, both new and existing ones. The problem will be to find out how one may expect the traffic to distribute itself over alternative routes, and if the expected distribution is the most efficient one.

The following criteria have been called *Wardrop's principles*, and suggests two possible criteria to follow when one is to find the optimal distribution on the routes between any two points in a road network. In Wardrop's own words, they read:

(1) "The journey times on all the routes actually used are equal, and less than those which would be expected by a single vehicle on any unused route."

(2) "The average journey time is a minimum." [23, p. 345]

By criteria (1) it is understood that the flow distribution has reached an equilibrium situation where no user can find a route of shorter travel time. Solution of the problem where criteria (1) is satisfied is called the *descriptive solution* [7], and gives the *user optimal* flow distribution. In the sense of game theory, a Wardrop equilibrium coincides with a Nash equilibrium [9].

Criteria (2) indicates that the total travel time is minimal among all the flow distributions. Solution of the problem where criteria (2) is satisfied is called the *normative solution* [7], and gives the *system optimal* flow distribution.

2.4 Braess' Paradox

In this section Braess' Paradox is presented, as given by Braess in 1968 [3] (English translation in 2005 [4]).

Braess identifies cost by travel time as a function of traffic flow, and the travel time was assumed to have the following properties:

I. $t_\alpha \geq 0$.

II. t_α is a nondecreasing function with respect to flow.

III. t_α is semicontinuous, i.e. $\lim_{\phi \to \phi_0; \phi < \phi_0} t_\alpha(\phi) = t_\alpha(\phi_0)$.

Assumption I and II are natural in the sense of traffic modeling, whilst assumption III is used in Braess to simplify the mathematical treatment.

Optimal flow gives a flow distribution such that the travel time for all drivers is as short as possible, also refered to as system optimal flow. Braess suggests two definitions of this optimum, which may be measured by the most unfavorable travel time, or by using the mean value of the travel time. The two definitions of optimal flow is,

Definition 1. The flow Φ is optimal if the relation,

$$|T(\Phi)| \leq |T(\Psi)|, \tag{2.10}$$

holds for all Ψ with $|\Phi| = |\Psi|$.

Definition 2. The optimal flow is determined by the mean value of the travel times, so the inequality,

$$\frac{1}{|\Phi|} \sum_\beta \Phi_\beta T_\beta(\Phi) \leq \frac{1}{|\Psi|} \sum_\beta \Psi_\beta T_\beta(\Psi), \tag{2.11}$$

holds for all Ψ with $|\Phi| = |\Psi|$.

The most unfavorable travel time $|T_\nu(\mathbf{\Phi})|$ is defined in equation (2.6), and the total flow in given in equation (2.4).

These definitions of optimal flow are based on Wardrop's second principle on system optimal flow, and find the distribution of flow which gives the minimum

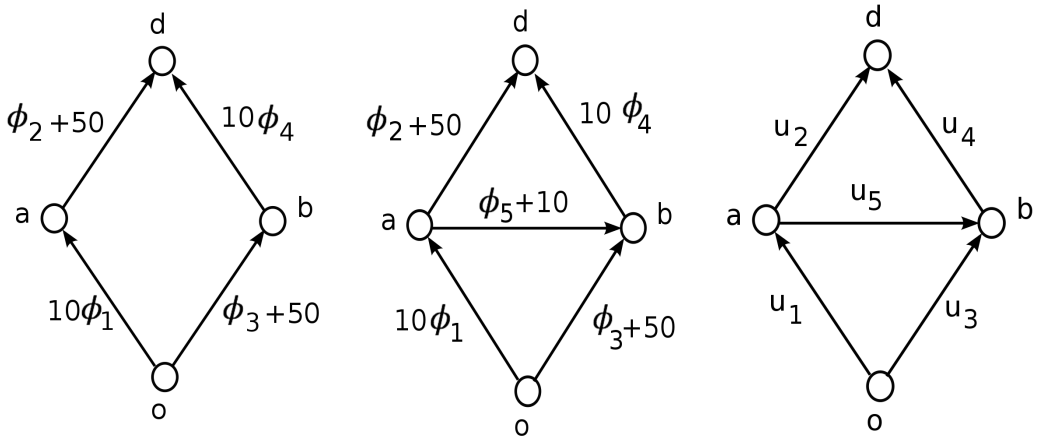

(a) Initial 4-link network (b) Augmented 5-link network (c) Network with link numbers.

Figure 2.2: Braess' original network model with cost functions.

travel time for all drivers. It is known that the system optimal distribution does not need to be equal to the user optimal flow, and consequently, some paths may have shorter travel times than others. In real life each driver is concerned with finding the most favorable route for himself, therefore if there exists a path of less travel time which is known to the driver, the driver will switch route and destroy the system optimum. To find the flow distribution for user optimum, Braess introduced *critical flow* defined as,

Definition 3. The flow $\mathbf{\Phi}$ is a critical flow if for all paths U_β

$$\begin{aligned} T_\beta(\mathbf{\Phi}) &= |T(\mathbf{\Phi})|, \qquad \text{if } \Phi_\beta \neq 0, \\ T_\beta(\mathbf{\Phi}) &\geq |T(\mathbf{\Phi})|, \qquad \text{if } \Phi_\beta = 0. \end{aligned}$$

In practice, critical flow means that all utilized routes have the same travel time, while non-utilized routes have travel times equal to or greater than the other paths. A single vehicle using a path of zero flow would experience a greater travel time than any other user, which is equivalent to Wardrop's first principle.

Braess demonstrates an occurence of the paradox on a simple road network. Braess' original network model contains directed links from origin o to destination d, as shown in Figure 2.2. Before extending the road network with one road the initial network contains 4 links with linear travel cost functions for each link, as illustrated in Figure 2.2(a). After adding a road, the augmented network will be as shown in Figure 2.2(b), with linear travel cost function for the added link.

The nodes of the network in Figure 2.2 are $\{o, a, b, d\}$, and with the oriented links $\{u_1, u_2, u_3, u_4, u_5\}$, the routes of the network are,

$$\begin{aligned} U_{oad} &= u_1 - u_2, \\ U_{obd} &= u_3 - u_4, \\ U_{oabd} &= u_1 - u_5 - u_4. \end{aligned}$$

The flow vector of the routes is $\boldsymbol{\Phi} = (\Phi_{oad}, \Phi_{obd}, \Phi_{oabd})$, so total flow will be $|\boldsymbol{\Phi}_{(o,d)}| = \Phi_{oad} + \Phi_{abd} + \Phi_{oabd}$. From equation (2.2) it follows that the link flows can be written as,

$$\boldsymbol{\phi} = \boldsymbol{D}\boldsymbol{\Phi}_{(o,d)}$$

$$\begin{bmatrix} \phi_1 \\ \phi_2 \\ \phi_3 \\ \phi_4 \\ \phi_5 \end{bmatrix} = \begin{bmatrix} 1 & 0 & 1 \\ 1 & 0 & 0 \\ 0 & 1 & 0 \\ 0 & 1 & 1 \\ 0 & 0 & 1 \end{bmatrix} \begin{bmatrix} \Phi_{oad} \\ \Phi_{obd} \\ \Phi_{oabd} \end{bmatrix}.$$

Using equation (2.5) the path-travel times are obtained to be,

$$\boldsymbol{T}_{(o,d)} = \boldsymbol{D}^\top \boldsymbol{t}.$$

In the Braess example, the total traffic flow is $|\boldsymbol{\Phi}| = 6$, and the link travel times given in Figure 2.2 is denoted,

$$t_1(\boldsymbol{\phi}) = 10\phi_1, \tag{2.12a}$$
$$t_2(\boldsymbol{\phi}) = \phi_2 + 50, \tag{2.12b}$$
$$t_3(\boldsymbol{\phi}) = \phi_3 + 50, \tag{2.12c}$$
$$t_4(\boldsymbol{\phi}) = 10\phi_4, \tag{2.12d}$$
$$t_5(\boldsymbol{\phi}) = \phi_5 + 10. \tag{2.12e}$$

The resulting system optimal flow distribution by optimization Definition 1, is given by,

$$\boldsymbol{\Phi} = (3, 3, 0). \tag{2.13}$$

The travel time for each route then becomes,

$$T_{oad}(3,3,0) = t_1(3) + t_2(3) = 83, \tag{2.14a}$$
$$T_{obd}(3,3,0) = t_3(3) + t_4(3) = 83, \tag{2.14b}$$
$$T_{oabd}(3,3,0) = t_1(3) + t_4(3) + t_5(0) = 70. \tag{2.14c}$$

The maximum travel time a vehicle can experience will then be $|\boldsymbol{T}(\Phi)| = 83$. At the system optimal distribution the travel time on the paths with traffic load

is 83 on both paths, while the travel time is less on the non-utilized path. Since travelers act in a selfish manner, they will choose the route of less travel time. As a result, travelers switch to the path U_{oabd}, and destroy the optimal flow.

The critical flow distribution will be 2 units on each of the three paths, so the travel time for each path becomes,

$$T_{oad}(2,2,2) = t_1(4) + t_2(2) = 92, \tag{2.15a}$$
$$T_{obd}(2,2,2) = t_3(2) + t_4(4) = 92, \tag{2.15b}$$
$$T_{oabd}(2,2,2) = t_1(4) + t_4(4) + t_5(2) = 92. \tag{2.15c}$$

The result is in accordance with Wardrops user optimal principle, as used routes have equal travel times. The maximum travel time a vehicle can experience will then be $|\boldsymbol{T}(\Phi)| = 92$, which is greater than for the system optimal flow. We thereby see that selfish routing by travelers may increase the travel time compared to a system optimal distribution.

However, when removing link u_5 from the network given in Figure 2.2(c), we observe that the critical flow becomes equal to the system optimal flow. The system optimal distribution of flow becomes $\Phi = (\Phi_{oad}, \Phi_{obd}) = (3,3)$, so the path travel times are

$$T_{oad}(3,3) = T_{obd}(3,3) = 83. \tag{2.16}$$

The user optimal flow distribution on the 4-link network will be 3 units on each path, and so the travel times are the same.

The example shows that travel time gained by selfish travelers are less when link u_5 is removed from the road network. When link u_5 is a part of the network, user optimal flow distribution chosen by selfish network users leads to longer travel times for all users.

This result reveals the paradoxical fact that expanding a road network by one link can cause an increase in travel time for all users.

2.4.1 A modified example

Already in 1970, two years after Braess published his paper, Murchland wrote about the Braess' paradox [11].

Murchland modified the example by changing the link travel time functions slightly. As a consequence the increase in travel time after adding a link to the network is larger than in the original Braess example. In the modified example, the linear travel times are changed to purely uncongesting or congesting, such that

the travel time functions are,

$$t_1(\boldsymbol{\phi}) = A_1\phi_1 = (23/3)\phi_1, \tag{2.17a}$$
$$t_2(\boldsymbol{\phi}) = B_2 \quad = 46, \tag{2.17b}$$
$$t_3(\boldsymbol{\phi}) = B_3 \quad = 46, \tag{2.17c}$$
$$t_4(\boldsymbol{\phi}) = A_4\phi_4 = (23/3)\phi_4, \tag{2.17d}$$
$$t_5(\boldsymbol{\phi}) = B_5 \quad = 0. \tag{2.17e}$$

Travel time function t_1 and t_4 are congesting and t_2 and t_3 are uncongesting, while the cost on link u_5 is zero.

The traffic demand between origin and destination is as before $\kappa = 6$, so the flow distribution is $(\Phi_{oad}, \Phi_{obd}) = (3, 3)$ on the initial network of 4-links and $(\Phi_{oad}, \Phi_{obd}, \Phi_{oabd}) = (0, 0, 6)$ on the augmented 5-link network. These distributions result in the following travel times on the 4-link network,

$$T_{oad}(3) = t_1(3) + t_2(3) = 69, \tag{2.18a}$$
$$T_{obd}(3) = t_3(3) + t_4(3) = 69. \tag{2.18b}$$

and on the 5-link network,

$$T_{oad}(0) = t_1(6) + t_2(0) \quad = 92, \tag{2.19a}$$
$$T_{obd}(0) = t_3(0) + t_4(6) \quad = 92, \tag{2.19b}$$
$$T_{oabd}(6) = t_1(6) + t_4(6) + t_5(6) = 92. \tag{2.19c}$$

In the 5-link network the travel times are all equal, and satisfies Wardrops first principle, which is also true for the 4-link network. The increase in travel time after adding one link is $92 - 69 = 23$ units, which is $23/69 = 1/3$ or about 33 %. In comparison with the original Braess example, the same increase is $9/83$ or about 11 %. The result shows that by "adding a link of zero travel time (at any flow) will increase all travel times by a third" [11].

2.5 Mechanical network example

The paradox in traffic networks described by Braess has also been showed to occur in mechanical networks. Such network examples were first presented by Cohen and Horowitz in 1991 [5].

The mechanical network of strings and springs is illustrated in Figure 2.3(a). The upper spring is attached to a fixed point, while the lower spring is attached to a weight. The back-up (longest) strings each of length $L_1 = 1$ m are, deliberately, long enough to be limp when the linking string of length $L_2 = 3/8$ m is intact.

The strings are assumed to be massless and perfectly inelastic, while the springs are assumed to be massless, ideally elastic and have zero unstretched length. Each spring is assumed to have a spring constant k, such that the extension x is related to the applied force F on the spring by $F = kx$. The spring constant is for simplicity chosen to be $k = 1$.

When the linking string is cut, one would intuitively expect the weight to drop slightly, since the back-up strings are hanging limply when the linking string is intact. What really happens, is that the weight is slightly lifted, such that the total distance X between the fixed point and the weight is shorter. This is illustrated in Figure 2.3(b).

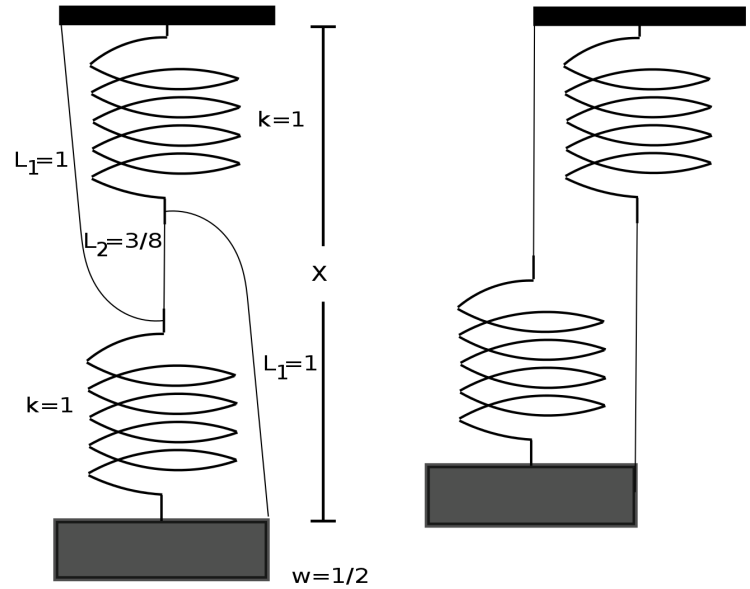

(a) Linking string intact, back-up strings limp.

(b) After cutting the linking string.

Figure 2.3: Mechanical network example showing the occurence of Braess' paradox. When the linking string is cut, the weight is lifted slightly, instead of dropped as would be expected.

The physical explanation is that each spring now carries half of the weight. The result is shown by some simple calculations. The weight is assumed to exert a force $F = 1/2$ N. When the system is intact, as shown in Figure 2.3(a), each spring will cary the full weight. The extention of each spring is then,

$$x_s = \frac{F}{k} = \frac{1}{2} \text{ m}.$$

The total distance X between the fixed point and the weigth is found to be,

$$X = x_s + L_2 + x_s = 1\tfrac{3}{8} \text{ m}.$$

After the linking string is cut, each spring carries half of the weight, and is therefore extended with,

$$x_s' = \frac{1}{2}\frac{F}{k} = \frac{1}{4} \text{ m}.$$

The total distance between fixed point and the weight is now,

$$X = L_1 + x_s' = 1\tfrac{1}{4} \text{ m}.$$

So the distance X is 1/8 m shorter after the linking string is cut and the springs only are connected to the back-up strings.

The translation between the mechanical network and the traffic network can be made in the following way. In the traffic network given in Figure 2.2(c), we can choose travel functions such that link u_1 and u_4 has congesting travel times, $t_\alpha = t_\alpha(\boldsymbol{\phi})$, while link u_2, u_3 and u_5 has non-congesting travel times, $t_\alpha = B_\alpha$. In such a network, t_2, t_3 and t_5 translates to the lengths of the inelastic strings, while t_1 and t_4 translates to lengths of the elastic springs. The traffic flow translates to the force exerted on the springs in the mechanical network.

Similar examples have shown that the paradox also occurs in electrical and hydraulic networks [5].

2.6 A modified definition of Braess' paradox

The viewpoint of Braess in 1968 was that more roads could make traffic flow worse. Hagstrom and Abrams took an inversed viewpoint, to show that fewer roads (or more restricted roads) can make traffic better [9].

The modified definition of Braess' paradox still including Braess' original example and all other examples of the paradox in the literature. However, in addition the definition allow for multiple origins and destinations, multiple traveler types, and general cost functions and networks. The method specifically finds situations in which the total cost of traffic congestion is reduced without adding cost to any traveler. To obtain such situations the traffic is redirected, which in practice can be enforced by restricting access to certain links in the network or introducing tolls. In such situations, the flow distribution is not required to be at equilibrium, in contrast to what is often used in other known Braess examples.

Let a flow equilibrium distribution be a distribution of flows that satisfies Wardrop's first principle (user optimal flow) and meets the demands on the network. It is known that flow distribution at minimal system cost does not need to

be identical to an equilibrium distribution. A total-cost distribution must make some travelers better off than at equilibrium, while instead it usually makes some travelers worse off. As Hagstrom and Abrams did not think this to be paradoxical, they adjusted the requirements for finding occurences of Braess' paradox.

The society may benefit from redistributing traffic such that the total travel cost is minimized. But if such a distribution results in some travelers obtaining longer travel times, some travelers would strongly object to any such solution of travel conditions. It would therefore be beneficial to find a flow distribution where no users are worse off than at equilibrium.

The generalization of the paradox is about improving the flow distribution in such a way that (i) some of the travelers on some of the routes obtain lower travel costs, and (ii) none of the travelers on any route gets a higher travel cost, compared to the user equilibrium distribution. In some examples (e.g. [9, Ex. 1]), the total-cost minimizing distribution will some times lead to longer travel time for some users compared to travel time at the user equilibrium distribution. The modified definition of Braess distribution reads,

> "Given an equilibrium distribution of flows on a traffic network, a Braess paradox occurs if there exists another feasable distribution of flows that meet the demands and for which some travelers have a cost of travel less than in equilibrium and no traveler has a cost higher than in equilibrium. Any such distribution of flow that improves some travelers' costs while not increasing others' costs will be called a *Braess distribution*."[9, p. 837]

With this generalized definition, it is not necessary to add or delete a link to observe that the Braess' paradox occurs.

2.7 Selfish routing

This section presentes a brief account of some of the results and methods about selfish routing by Roughgarden and Tardos from 2002 [19].

As mentioned earlier selfish network users, which travelers often are assumed to be, do not follow the system optimal flow distribution which would give the shortest travel time for all users. It is therefore interesting to investigate how this selfish routing affects the travel times at Nash equilibrium (user optimal flow) compared to the system optimal flow distribution.

The problem of finding a system optimal flow is equivalent to several minimization problems. Braess used the most unfavorable travel time of all paths to minimize over all distributions, as given in Definition 1. Another method is to minimize the system cost from equation (2.8) [19, 9], which is used in this thesis.

The user optimal flow, which is equivalent to Nash equilibrium, can be obtained from minimizing,

$$\sum_{\alpha} \int_0^{\phi_\alpha} t_\alpha(x)\mathrm{d}x,$$

[19, 7]. The following non-linear program is the general program used to find both the minimal system cost and the Nash equilibrium,

$$\begin{aligned} \min \ & \sum_{u_\alpha} g(\phi_\alpha) \\ \text{subject to:} \\ & \sum_{\beta \in B_\nu} \Phi_\beta = |\Phi_\nu| \qquad \forall \nu \in \{1, ..., k\} \\ & \phi_\alpha = \sum_{\beta} c_{\alpha\beta} \Phi_\beta \qquad \forall \alpha \\ & \Phi_\beta \geq 0. \end{aligned}$$

The method to solve the non-linear program and find both the Nash equilibrium and the system optimal flow is thoroughly described in Chapter 3.

Given a directed network $\mathcal{G}$, a set of total OD flows $r = \{|\Phi_\nu|\}$ for all OD pairs ν and a set of link cost functions $\boldsymbol{t} = \{t_\alpha\}$, we denote the optimal flow at minimal system cost as ϕ^*, and the flow at Nash equilibrium as $\tilde{\phi}$. The cost ratio between these flows can then be defined as,

$$\rho = \rho(\mathcal{G}, r, \boldsymbol{t}) = \frac{C(\tilde{\phi})}{C(\phi^*)}.$$

This ratio will satisfy the property,

$$\rho(\mathcal{G}, r, \boldsymbol{t}) \leq \gamma,$$

if the instance $(\mathcal{G}, r, \boldsymbol{t})$ and the constant $\gamma \geq 1$ satisfy,

$$\phi_\alpha t_\alpha(\boldsymbol{\phi}) \leq \gamma \int_0^{\phi_\alpha} t_\alpha(x)\mathrm{d}x,$$

for all links u_α and all positive real numbers ϕ_α [19, Corollary 2.7].

When assuming that the link travel costs are linear functions, the maximum limit γ for the ratio ρ between total travel time for the user optimal flow distribution and the system optimal distribution was shown to be 4/3 [19].

Another interesting result was found when the link travel times were assumed to be non-decreasing, continuous functions. If $\tilde{\boldsymbol{\phi}}$ is a flow at Nash equilibrium for $(\mathcal{G}, r, \boldsymbol{t})$ and $\boldsymbol{\phi}^*$ is an optimal flow for $(\mathcal{G}, (1+\delta)r, \boldsymbol{t})$, then the relation between the total costs will be $C(\tilde{\boldsymbol{\phi}}) \leq \frac{1}{\delta} C(\boldsymbol{\phi}^*)$. Consequently, the cost ratio may be unbounded.

Chapter 3

Method

This chapter will present descriptions of the methods used in this paper. Section 3.1 gives a general presentation of the non-linear program used to find both user optimal and system optimal flow distribution. Section 3.2 presents a mathematical characterization of flow distributions where Braess paradox occurs for the original Braess example network with linear travel time functions. The characterization is a method to obtain the system optimal flow. Section 3.3 gives a description of the method used to solve the non-linear program for Nash equilibrium on general traffic networks. The method is modified in Section 3.4 to find the system optimal flow distribution.

Throughout the paper we will consider linear travel cost functions of the form,

$$t_\alpha(\boldsymbol{\phi}) = A_\alpha \phi_\alpha + B_\alpha. \tag{3.1}$$

3.1 Non-linear program

The following non-linear program (NLP) is the general program used to find both the minimal system cost and the Nash equilibrium [19],

$$\begin{aligned}
\min \quad & \sum_\alpha g(\phi_\alpha), && && \text{(3.2a)}\\
\text{subject to} \quad & \sum_{\beta \in \mathcal{B}_j} \Phi_\beta = |\Phi_j|, && \forall j \in \{1, ..., \nu\}, && \text{(3.2b)}\\
& \phi_\alpha = \sum_\beta d_{\alpha\beta} \Phi_\beta, && \forall \alpha, && \text{(3.2c)}\\
& \Phi_\beta \geq 0. && && \text{(3.2d)}
\end{aligned}$$

The system optimal flow distribution is obtained when minimizing the system cost. The function g will then be,

$$g(\phi_\alpha) = \phi_\alpha t_\alpha(\boldsymbol{\phi}), \tag{3.3}$$

and the objective function becomes,

$$C(\boldsymbol{\phi}) = \sum_{\alpha} \phi_\alpha t_\alpha(\boldsymbol{\phi}).$$

Nash equilibrium, also known as the user optimal flow distribution, is obtained when,

$$g(\phi_\alpha) = \int_0^{\phi_\alpha} t_\alpha(x)\mathrm{d}x, \tag{3.4}$$

and the objective function becomes,

$$\tilde{C}(\boldsymbol{\phi}) = \sum_{\alpha} \int_0^{\phi_\alpha} t_\alpha(x)\mathrm{d}x.$$

The objective function for Nash equilibrium is the sum of the integrals of the link-travel times. The function has no intuitive explanation or interpretation either economical or behavioural, and should only be viewed as a mathematical formulation to solve optimization/equilibrium problems.

The non-linear program in (3.2) is a convex program when all travel time functions are semi-convex. The definition of semiconvexity is as following,

> A function $c : \mathcal{R}^+ \to \mathcal{R}^+$ is semiconvex if $x \cdot c(x)$ is convex [18, p.24].

Let the link travel times $t_\alpha(x)$ be linear functions for all α with $A_\alpha > 0$ and $B_\alpha \geq 0$, and let $\lambda \in [0, 1]$. For all $x_1, x_2 \in [0, \kappa]$, the function $f_\alpha = x \cdot t_\alpha(x)$ will satisfy

$$f(\lambda x_1 + (1-\lambda)x_2) = \lambda f(x_1) + (1-\lambda)f(x_2) - A_i\lambda(1-\lambda)(x_1 - x_2)^2 \tag{3.5}$$
$$\leq \lambda f(x_1) + (1-\lambda)f(x_2), \tag{3.6}$$

so f_i are convex functions. The non-linear program in equations (3.2a)-(3.2d) is then a convex program, when all travel times are assumed to be linear functions.

3.2 Mathematical characterization

In this section, the mathematical characterization of Braess' paradox, suggested by Frank in 1981 [7], is presented.

Let the travel times be linear functions as given in (3.1), with $A_\alpha > 0$ and $B_\alpha \geq 0$. Figure 3.1 shows the Braess network model, where the right OD path is denoted $U_R = U_{obd}$, the left OD path is denoted $U_L = U_{oad}$, and the path utilizing link u_5 is denoted $U_Z = U_{oabd}$. The case of the 4-link network is referred to as network problem P_{I}, and the case of the 5-link network is referred to as network problem P_{II}.

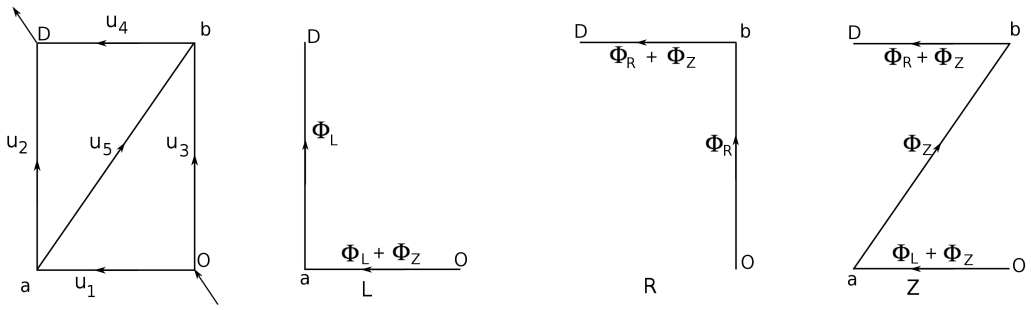

(a) 5-link network. (b) Left OD path U_L. (c) Right OD path U_R. (d) OD path U_Z.

Figure 3.1: Braess' network model, and the OD paths U_L, U_R and U_Z.

3.2.1 Braess flow

Let c_{I} denote the minimal OD cost per unit for problem P_{I}, and let c_{II} denote the minimal OD cost per unit for problem P_{II}. The minimal OD cost is understood as the minimal path travel time over all paths connecting origin O an destination D. A *Braess flow* may be defined as a total OD flow κ with the property that [7, Definition 3.1]

$$c_{\mathrm{II}} > c_{\mathrm{I}}. \tag{3.7}$$

The value of c_{I} is obtained by

$$c_{\mathrm{I}} = t_1(\Phi_L) + t_2(\Phi_L) = t_3(\kappa - \Phi_L) + t_4(\kappa - \Phi_L),$$

resulting in the expression

$$c_{\mathrm{I}} = \frac{(A_1 + A_2)(A_3 + A_4)\kappa + (A_1 + A_2)(B_3 + B_4) + (A_3 + A_4)(B_1 + B_2)}{\Sigma}, \tag{3.8}$$

where Σ is defined in (2.9).

The value of c_{II} is equal to the travel cost on the utilized paths and is less than the travel cost on non-utilized paths. Minimum OD cost per unit for P_{II} when path U_L is utilized is,

$$c_{\mathrm{II}} = t_1(\Phi_L + \Phi_Z) + t_2(\Phi_L). \tag{3.9}$$

Minimum OD cost per unit for P_{II} when path U_R is utilized is,

$$c_{\mathrm{II}} = t_4(\Phi_R + \Phi_Z) + t_3(\Phi_R). \tag{3.10}$$

When paths U_Z is utilized such that $\Phi_Z > 0$, the minimal OD cost satisfy,

$$c_{\mathrm{II}} = t_1(\Phi_L + \Phi_Z) + t_5(\Phi_Z) + t_4(\Phi_R + \Phi_Z). \tag{3.11}$$

If any path p is not utilized, then $\Phi_p = 0$ and the minimal OD cost satisfy,

$$c_{\text{II}} \leq \text{OD cost along } p. \tag{3.12}$$

Equations (3.9)-(3.12) all satisfy Wardrops user equilibrium.

We introduce the ΔSS^*-conditions for a Braess flow [7, Theorem 4.7]. The conditions state that an interior Braess flow exists if and only if

$$\text{(i) } \Delta > 0, \qquad \text{(ii) } S > 0, \qquad S^* > 0, \tag{3.13}$$

where Δ, S and S^* is given in (2.9).

Assuming the network of P_{I} is symmetric, such that $t_1(x) = t_4(x) = A_1x + B_1$ and $t_2(x) = t_3 = A_2x + B_2$, equation (3.13) leads to,

$$0 < \Delta = A_1^2 - A_2^2 \quad \& \quad A_1,\ A_2 > 0 \ \Rightarrow\ A_1 > A_2,$$

and,

$$\begin{aligned} 0 < S &= S^* \\ &= A_1(B_2 - B_1 - B_5) + A_2(B_2 - B_1 - B_5) \\ &= (A_1 + A_2)(B_2 - B_1 - B_5), \end{aligned}$$

and given that $(A_1 + A_2) > 0$ we obtain that,

$$0 < B_5 < B_2 - B_1,$$

resulting in,

$$B_1 < B_2.$$

Consequently, given a symmetric network as described above, a Braess flow exists if and only if $A_1 > A_2$. $B_5 < B_2 - B_1$ and $B_1 < B_2$ [7, Corollary 4.8].

3.2.2 Optimal Nash flow on 4-link network

The initial 4-link network encompass the directed links $\{u_1, u_2, u_3, u_4\}$. The objective function is found by equations (3.2a) and (3.4),

$$\begin{aligned} \tilde{C}_{\text{I}}(\boldsymbol{\phi}) &= \sum_{\alpha} \int_0^{\phi_\alpha} t_\alpha(x)\mathrm{d}x \\ &= \int_0^{\phi_1} t_1(x)\mathrm{d}x + \int_0^{\phi_2} t_2(x)\mathrm{d}x + \int_0^{\phi_3} t_3(x)\mathrm{d}x + \int_0^{\phi_4} t_4(x)\mathrm{d}x. \end{aligned} \tag{3.14}$$

By the optimization criteria of equation (3.2c) and the arcpath incidence matrix D, or intuitively by examining the network, it is clear that,

$$\phi_1 = \phi_2 = \Phi_L, \qquad \phi_3 = \phi_4 = \Phi_R. \tag{3.15}$$

The total OD demand will be denoted κ, and by the optimization requirement of equation (3.2b) it is understood that,

$$\kappa = |\Phi_{(o,d)}| = \Phi_L + \Phi_R, \qquad \Phi_R = \kappa - \Phi_L. \tag{3.16}$$

From equations (3.14), (3.15) and (3.16), the objective function is obtained to be,

$$\tilde{C}_{\mathrm{I}}(\boldsymbol{\phi}) = \int_0^{\Phi_L} t_1(x) + t_2(x)\mathrm{d}x + \int_0^{\kappa-\Phi_L} t_3(x) + t_4(x)\mathrm{d}x. \tag{3.17}$$

The problem of finding the optimal Nash flow on the initial 4-link network becomes,

$$\begin{aligned} \min \quad & \tilde{C}_{\mathrm{I}}(\boldsymbol{\phi}), && (3.18)\\ \text{subject to} \quad & \Phi_L \geq 0, && (3.19)\\ & \kappa - \Phi_L \geq 0. && (3.20) \end{aligned}$$

This minimization problem has only Φ_L as unknown, and may therefore be found by a simple derivation. This is because the constraints can be relaxed and the objective function can be solved as an unconstrained problem [20, p. 63]. If the solution satisfies the constraints, then the solution is valid for the constrained problem as well.

When the flow is interior so that $0 < \Phi_L < \kappa$, then $C'(\boldsymbol{\phi}) = 0$. When the flow is on the boundary so that either $\Phi_L = \kappa$ or $\Phi_L = 0$, then $C'(\boldsymbol{\phi}) \leq 0$ or $C'(\boldsymbol{\phi}) \geq 0$, respectively. Below it is proven that the flow must be interior for a Braess flow to exist. The flow therefore satisfy

$$\begin{aligned} 0 &= \frac{\mathrm{d}\tilde{C}_{\mathrm{I}}(\boldsymbol{\phi})}{\mathrm{d}\Phi_L} && (3.21)\\ &= t_1(\Phi_L) + t_2(\Phi_L) - t_3(\kappa - \Phi_L) - t_4(\kappa - \Phi_L), && (3.22) \end{aligned}$$

which results in the optimal flow distribution

$$\begin{aligned} \Phi_L &= [\kappa(A_3 + A_4) - B_1 - B_2 + B_3 + B_4]\Sigma^{-1} && (3.23)\\ \Phi_R &= \kappa - \Phi_L, && (3.24) \end{aligned}$$

where Σ is defined in equation (2.9a).

Proof of interior flow

This section gives a proof on the statement that the optimal Nash flow on the 4-link network must be interior.

Proof. Assume right boundary flow on the path $U_R = U_{obd}$ on the 4-link network, such that $\Phi_L = 0$ and $\Phi_R = \kappa$. The minimal OD cost per unit is then,

$$c_{\mathrm{I}} = f_3(\kappa) + f_4(\kappa) \leq f_1(0) + f_2(0). \tag{3.25}$$

The definition of Braess flow from equation (3.7) is $c_{\mathrm{II}} > c_{\mathrm{I}}$. We use that the flow on path U_R of the 5-link network may be either utilized or non-utilized.

First, let the path flow on U_R be $y_R > 0$ on the 5-link network and, as before, $\kappa = y_L + y_R + y_Z$. The minimal OD cost is then,

$$\begin{aligned} c_{\mathrm{II}} &= f_4(y_R + y_Z) + f_3(y_R) \\ &= A_4(\kappa - y_L) + B_4 + A_3(\kappa - y_L - y_Z) + B_3 \\ &= f_4(\kappa) - A_4 y_L + f_3(\kappa) - A_3(y_L + y_Z) \\ &= c_{\mathrm{I}} - A_4 y_L - A_3(y_L + y_Z) \\ &\leq c_{\mathrm{I}}, \end{aligned}$$

from equation (3.10).

Second, let the path flow on U_R be $y_R = 0$, and $y_L > 0$. The minimal OD cost is then,

$$\begin{aligned} c_{\mathrm{II}} &= f_1(y_L + y_Z) + f_2(y_L) \\ &= f_1(\kappa) + f_2(y_L), \end{aligned} \tag{3.26}$$

from equation (3.9), and from equation (3.12) the minimal OD cost satisfies,

$$\begin{aligned} c_{\mathrm{II}} &\leq f_4(y_R + y_Z) + f_3(y_R) \\ &\leq f_4(y_Z) + f_3(0). \end{aligned} \tag{3.27}$$

By comparing equations (3.26) and (3.27) the following is obtained,

$$\begin{aligned} f_1(\kappa) + f_2(y_L) + (A_4 y_L + A_3\kappa) &\leq f_4(y_Z) + f_3(0) + (A_4 y_L + A_3\kappa) \\ \kappa(A_1 + A_3) + y_L(A_2 + A_4) + B_1 + B_2 &\leq A_4(y_Z + y_L) + B_4 + A_3\kappa + B_3 \\ &\leq f_4(\kappa) + f_3(\kappa) \end{aligned}$$

Applying equation (3.25) to the right hand side it is obtained that,

$$\kappa(A_1 + A_3) + y_L(A_2 + A_4) + B_1 + B_2 \leq B_1 + B_2.$$

The resulting relation,

$$\kappa(A_1 + A_3) + y_L(A_2 + A_4) \leq 0,$$

states that $y_L = 0$, (when assuming $A_i > 0$), which is a contradiction to the assumption that $y_L > 0$. Consequently, if $y_R = 0$ then $y_L = 0$ and $y_Z = \kappa$. Assuming $y_R = 0$ and $y_Z > 0$, the minimal system cost from equations (3.11) and (3.12) can be compared. The minimal OD cost then satisfy,

$$c_{\text{II}} = f_1(\kappa) + f_5(\kappa) + f_4(\kappa)$$

and,

$$\begin{aligned} c_{\text{II}} &\leq f_4(\kappa) + f_3(0) \\ &\leq f_4(\kappa) + f_3(0) + A_3\kappa = c_{\text{I}} \\ &\Downarrow \\ c_{\text{II}} &\leq c_{\text{I}} \end{aligned}$$

□

The proof shows that when the traffic flow is on the right boundary $\Phi_R = \kappa$ then,

$$\begin{aligned} y_R > 0 : c_{\text{II}} \leq c_{\text{I}} &\nLeftrightarrow c_{\text{II}} > c_{\text{I}}, \\ y_R = 0 : c_{\text{II}} \leq c_{\text{I}} &\nLeftrightarrow c_{\text{II}} > c_{\text{I}}. \end{aligned}$$

Consequently, a flow distribution will never result in a Braess flow. The same result is obtained for left boundary flow [7, p. 289].

3.2.3 Optimal Nash flow on 5-link network

The directed links of the augmented 5-link network are $\{u_1, u_2, u_3, u_4, u_5\}$. The objective function is found by equations (3.2a) and (3.4),

$$\begin{aligned} \tilde{C}_{\text{II}}(\boldsymbol{\phi}) &= \sum_{\alpha} \int_0^{\phi_\alpha} t_\alpha(x)\mathrm{d}x \\ &= \int_0^{\phi_1} t_1(x)\mathrm{d}x + \int_0^{\phi_2} t_2(x)\mathrm{d}x + \int_0^{\phi_3} t_3(x)\mathrm{d}x + \int_0^{\phi_4} t_4(x)\mathrm{d}x \\ &\quad + \int_0^{\phi_5} t_5(x)\mathrm{d}x. \end{aligned}$$

By the optimization criteria of equation (3.2b), we have the following equalities,

$$\kappa = |\Phi_{(o,d)}| = \Phi_{oad} + \Phi_{obd} + \Phi_{oabd}, \tag{3.28}$$

$$\Phi_{oabd} = \kappa - \Phi_{oad} - \Phi_{obd}. \tag{3.29}$$

From the optimization criteria of equation (3.2c), and the arcpath incidence matrix, or inspection of the traffic network, the link flows are

$$\phi_1 = \Phi_{oab} + \Phi_{oabd} = \kappa - \Phi_{obd}, \tag{3.30a}$$
$$\phi_2 = \Phi_{oad}, \tag{3.30b}$$
$$\phi_3 = \Phi_{obd}, \tag{3.30c}$$
$$\phi_4 = \Phi_{obd} + \Phi_{oabd} = \kappa - \Phi_{oad}, \tag{3.30d}$$
$$\phi_5 = \Phi_{oabd} = \kappa - \Phi_{oad} - \Phi_{obd}. \tag{3.30e}$$

The objective function of the augmented 5-link network is obtained by equations (3.28) and (3.30), and results in

$$\begin{aligned}\tilde{C}_{\mathrm{II}}(\boldsymbol{\phi}) = &\int_0^{\kappa-\Phi_{obd}} t_1(x)\mathrm{d}x + \int_0^{\Phi_{oad}} t_2(x)\mathrm{d}x + \int_0^{\Phi_{obd}} t_3(x)\mathrm{d}x \\ &+ \int_0^{\kappa-\Phi_{oad}} t_4(x)\mathrm{d}x + \int_0^{\kappa-\Phi_{oad}-\Phi_{obd}} t_5(x)\mathrm{d}x.\end{aligned} \tag{3.31}$$

The problem of finding the optimal Nash flow on the augmented 5-link network becomes,

$$\begin{aligned} \min \quad & \tilde{C}_{\mathrm{II}}(\boldsymbol{y}) \\ \text{subject to} \quad & y_L \geq 0 \\ & y_R \geq 0 \\ & \kappa - y_L - y_R \geq 0. \end{aligned}$$

The interior solution will then be $(y_L, y_R) = (\Phi_L, \Phi_R)$ if and only if

$$\frac{\partial \tilde{C}_{\mathrm{II}}}{\partial y_L} = \frac{\partial \tilde{C}_{\mathrm{II}}}{\partial y_R} = 0, \tag{3.33}$$

such that $\Phi_L > 0$, $\Phi_R > 0$, $\kappa - \Phi_L - \Phi_R = \Phi_Z > 0$. When the solution flow is on some boundary, one of the partial derivatives becomes ≥ 0 depending on which boundary that has zero flow.

Partial derivatives of the objective function are

$$\frac{\partial \tilde{C}_{\mathrm{II}}}{\partial y_L} = t_2(y_L)\partial_{y_L} y_L + t_4(\kappa - y_L)\partial_{y_L}(\kappa - y_L) + t_5(\kappa - y_L - y_R)\partial_{y_L}(\kappa - y_L - y_R),$$

and

$$\frac{\partial \tilde{C}_{\mathrm{II}}}{\partial y_R} = t_1(\kappa - y_R)\partial_{y_R}(\kappa - y_R) + t_3(y_R)\partial_{y_R} y_R + t_5(\kappa - y_L - y_R)\partial_{y_R}(\kappa - y_L - y_R).$$

Interior flow

Assuming first that the solution is interior, the interior constrains become

$$\Phi_L > 0, \qquad \Phi_R > 0, \qquad \Phi_Z > 0, \tag{3.34}$$

and the equilibrium equations obtained from (3.33) are,

$$\frac{\partial \tilde{C}_{\mathrm{II}}}{\partial y_L}(\Phi_L, \Phi_R) = t_2(\Phi_L) - t_4(\kappa - \Phi_L) - t_5(\Phi_Z) = 0, \tag{3.35}$$

and,

$$\frac{\partial \tilde{C}_{\mathrm{II}}}{\partial y_R}(\Phi_L, \Phi_R) = -t_1(\kappa - \Phi_R) + t_3(\Phi_R) - t_5(\Phi_Z) = 0, \tag{3.36}$$

where,

$$\Phi_Z = \kappa - \Phi_L - \Phi_R. \tag{3.37}$$

Inserting equation (3.1) into equations (3.35) and (3.36), and solving for Φ_L gives,

$$\begin{aligned} 0 &= A_2\Phi_L + B_2 - A_4(\kappa - \Phi_L) - B_4 - A_5(\kappa - \Phi_L - \Phi_R) - B_5, \\ \Phi_L &= \frac{\kappa(A_4 + A_5) - (B_2 - B_4 - B_5) - A_5\Phi_R}{A_2 + A_4 + A_5}. \end{aligned} \tag{3.38}$$

Solving for Φ_R gives,

$$0 = -A_1(\kappa - \Phi_R) - B_1 + A_3\Phi_R + B_3 - A_5(\kappa - \Phi_L - \Phi_R) - B_5,$$

and inserting equation (3.38) results in,

$$\begin{aligned} 0 &= [\Phi_R(A_1 + A_3 + A_5) + (B_3 - B_1 - B_5) - \kappa(A_1 + A_5) + A_5 \times \{(3.38)\}] \\ &\quad \times (A_2 + A_4 + A_5), \\ \Phi_R &= \frac{\kappa\,[A_2(A_1 + A_5) + A_1(A_4 + A_5)] + A_5T(0)^* - T(0)(A_2 + A_4 + A_5)}{(A_1 + A_3)(A_2 + A_4) + A_5\Sigma}, \end{aligned}$$

where $T(0)$ and $T(0)^*$ are given in equation (2.9). Introducing the notations in equation (2.9), and inserting Φ_R into equation (3.38), we obtain the interior user optimal flow distribution,

$$\Phi_L = \Lambda^{-1}[G\kappa - (S + \theta)], \tag{3.39}$$

$$\Phi_R = y_L^* = \Lambda^{-1}[G^*\kappa - (S^* - \theta)], \tag{3.40}$$

$$\Phi_Z = \Lambda^{-1}[-\Delta\kappa + S + S^*]. \tag{3.41}$$

Component Φ_Z is obtained from the relation in equation (3.37), such that,

$$\Phi_Z = \kappa - \Phi_L - \Phi_R, \tag{3.42}$$

$$= \frac{\kappa(\Lambda - G - G^*) + S + S^*}{\Lambda}, \tag{3.43}$$

where $\Lambda - G - G^* = -\Delta$ is readily checked.

Boundary flow

Given interior solutions for P_{I}, and the solution of P_{II} is on the boundary of the constraint set, the flow distribution is categorized [7]. The solution of P_{II} then becomes,

(i) *left boundary* flow when $\Phi_L > 0$, $\Phi_R = 0$, $\Phi_Z > 0$,

(ii) *right boundary* flow when $\Phi_L = 0$, $\Phi_R > 0$, $\Phi_Z > 0$,

(ii) *extreme boundary* flow when $\Phi_L = 0$, $\Phi_R = 0$, $\Phi_Z > 0$.

If a Braess flow exists, the solution flows of P_{II} must utilize path U_Z [7, Lemma 3.2]. It is therefore understood that all flows, left, right and extreme, have $\Phi_Z > 0$ [21].

For the case of right boundary flow, the equilibrium equations become,

$$\frac{\partial \tilde{C}_{\mathrm{II}}}{\partial y_L}(\Phi_L, \Phi_R) \geq 0, \qquad \frac{\partial \tilde{C}_{\mathrm{II}}}{\partial y_R}(\Phi_L, \Phi_R) = 0,$$

with constraints,

$$\Phi_L = 0, \qquad 0 < \Phi_R < \kappa, \qquad \Phi_Z = \kappa - \Phi_R. \tag{3.44}$$

Component Φ_R is obtained by equation (3.36),

$$\begin{aligned} 0 &= \frac{\partial \tilde{C}_{\mathrm{II}}}{\partial y_R}(0, \Phi_R) \\ &= -A_1(\kappa - \Phi_R) - B_1 + A_3(\Phi_R) + B_3 - A_5(\kappa - \Phi_R) - B_5 \\ &= \Phi_R(A_1 + A_3 + A_5) - \kappa(A_1 + A_5) + (B_3 - B_1 - B_5). \end{aligned}$$

Component Φ_Z is obtained by the relation in equation (3.44), and by introducing the notations in equation (2.9). Then,

$$\Phi_R = \frac{(A_1 + A_5)\kappa - T(0)}{A_3 + A_1 + A_5}, \qquad \Phi_Z^r = \frac{T(0) + A_3\kappa}{A_3 + A_1 + A_5}, \tag{3.45}$$

becomes the resulting user optimal distribution with right boundary flow.

For left boundary flow the equilibrium equations become,

$$\frac{\partial \tilde{C}_{\mathrm{II}}}{\partial y_L}(\Phi_L, \Phi_R) = 0, \qquad \frac{\partial \tilde{C}_{\mathrm{II}}}{\partial y_R}(\Phi_L, \Phi_R) \geq 0,$$

with constraints,

$$0 < \Phi_L < \kappa, \qquad \Phi_R = 0, \qquad \Phi_Z = \kappa - \Phi_L. \tag{3.46}$$

Component Φ_L is obtained by equation (3.35),

$$\begin{aligned} 0 &= \frac{\partial \tilde{C}_{\mathrm{II}}}{\partial y_L}(\Phi_L, 0) \\ &= \Phi_L(A_2 + A_4 + A_5) + (B_2 - B_4 - B_5) - \kappa(A_4 + A_5). \end{aligned}$$

Component Φ_Z is obtained by the relation in equation (3.46). By introducing the notations in equation (2.9) the resulting flow distribution becomes,

$$\Phi_L = \frac{(A_4 + A_5)\kappa - T(0)^*}{A_2 + A_4 + A_5} = \Phi_R^*, \qquad \Phi_Z^l = \frac{T(0)^* + A_2\kappa}{A_2 + A_4 + A_5} = \Phi_Z^{r*}. \tag{3.47}$$

which is the perturbated results of right boundary flow.

When the boundary flow is extreme, the distribution is obviously $\Phi_L = \Phi_R = 0$ and $\Phi_Z = \kappa$. The existance of an extreme Braess flow is dependent on whether the following criterias [7, Theorem 6.8] are satisfied,

$$\begin{aligned} &\text{(i) } T > 0 \text{ and } T^* > 0, \\ &\text{(ii) } \Delta > \Delta_0, \end{aligned}$$

where,

$$\Delta_0 = \max\left\{ \frac{(A_3 + A_4)\theta}{T(0)}, -\frac{(A_1 + A_2)\theta}{T(0)^*} \right\}. \tag{3.48}$$

3.2.4 Braess flow intervals

Let *critical intervals* (or Braess flow intervals) be intervals in $\mathbb{R}^+$ where Braess flows exist.

The critical intervals of P_{I} is obtained from $\Sigma \cdot (3.23)$ and $\Sigma \cdot (\kappa - (3.23))$, and solving for κ gives

$$\kappa(A_3 + A_4) = B_1 + B_2 - (B_3 + B_4) + \Sigma x_0,$$

and,

$$\kappa(A_1 + A_2) = -(B_1 + B_2) + B_3 + B_4 + \Sigma(\kappa - x_0).$$

As $x_0 > 0$ and $\kappa - x_0 > 0$ from the interior requirement, and by introducing K_{I} and K_{I}^*, it follows that,

$$\begin{aligned} \kappa &> \frac{B_1 + B_2 - (B_3 + B_4)}{A_3 + A_4} = K_{\mathrm{I}} \geq 0, \\ \kappa &> \frac{B_3 + B_4 - (B_1 + B_2)}{A_1 + A_2} = K_{\mathrm{I}}^* \geq 0, \end{aligned}$$

where the right inequality is a consequence of equation (3.1) where $B_i \geq 0$. Total flow will then satisfy

$$\kappa > \max\{K_{\mathrm{I}}, K_{\mathrm{I}}^*\} \geq 0. \tag{3.49}$$

For the critical intervals of P_{II}, let K_{II} be a flow bound for κ, given by

$$K_{\mathrm{II}} = \frac{S+\theta}{G}. \tag{3.50}$$

First we distinguish between three possible configurations for the components of solution vector $\boldsymbol{y}$ [7]. These are dependent on the value of θ, and are called,

(i) *left-skew* when $\theta < 0$, then $K_{\mathrm{II}} < T^* < T < K_{\mathrm{II}}^*$. (3.51)

(ii) *right-skew* when $\theta > 0$, then $K_{\mathrm{II}} > T^* > T > K_{\mathrm{II}}^*$. (3.52)

(iii) *non-skew* when $\theta = 0$, then $K_{\mathrm{II}} = T^* = T = K_{\mathrm{II}}^*$. (3.53)

The ΔSS^*-conditions from equation (3.13) are necessary for the existence of any Braess flow [7, Theorem 6.5]. The conditions are also sufficient for all Braess flows, with the exception of extreme flows when P_{II} is skew. The conditions determine the critical intervals for Braess flows, [7, Theorem 6.5 & Corollary 6.9], which are defined as:

(i) When P_{II} is right-skew the Braess flow is,

$$\underbrace{K_{\mathrm{R}} < \ \kappa \ \leq \overbrace{K_{\mathrm{II}}}^{\text{interior flow}}}_{\text{right flow}} < \ \kappa \ < K_{\max}. \tag{3.54}$$

(ii) When P_{II} is left-skew the Braess flow is,

$$\underbrace{K_{\mathrm{L}} < \ \kappa \ \leq \overbrace{K_{\mathrm{II}}^*}^{\text{interior flow}}}_{\text{left flow}} < \ \kappa \ < K_{\max}. \tag{3.55}$$

(iii) When P_{II} is non-skew the Braess flow is,

$$\underbrace{K_{\min} < \ \kappa \ \leq \overbrace{K_{\mathrm{II}}}^{\text{interior flow}}}_{\text{extreme flow}} < \ \kappa \ < K_{\max}. \tag{3.56}$$

(iv) If P_{II} is right-skew and extreme Braess flows exist, the critical intervals are given by,

$$\underbrace{K_{\min} < \ \kappa \ \leq \overbrace{T}^{\text{right flow}}}_{\text{extreme flow}} < \ \kappa \ \leq \underbrace{K_{\mathrm{II}}}_{\text{interior flow}} < \ \kappa \ < K_{\max}. \tag{3.57}$$

(v) If P_{II} is left-skew and extreme Braess flows exist, the critical intervals are given such that the Braess flow is,

$$\underbrace{K_{\min} < \ \kappa \ \leq \overbrace{T^*}^{\text{left flow}}}_{\text{extreme flow}} < \ \kappa \ \leq \underbrace{K^*_{\text{II}} < \ \kappa \ < K_{\max}}_{\text{interior flow}}. \tag{3.58}$$

The variables $K_{\max}$ and $K_{\min}$ are given by,

$$K_{\text{R}} = \max(K_{\text{I}}, K^*_{\text{I}}, T, -T(0)A_3^{-1}, Q)), \tag{3.59}$$
$$K_{\text{L}} = K^*_{\text{R}}, \tag{3.60}$$
$$K_{\max} = \frac{S + S^*}{\Delta} = K^*_{\max}, \tag{3.61}$$
$$K_{\min} = \min\left(K_{\text{I}}, K^*_{\text{I}}, \frac{AT + A^*T^*}{A + A^* + \Delta}\right) = K^*_{\min}, \tag{3.62}$$

and Q and A are,

$$Q = \frac{(A_3 + A_4)(S + \theta) - \Delta T(0)}{(A_3 + A_4)G + \Delta A_3}, \tag{3.63}$$
$$A = (A_1 + A_2)(A_1 + A_5). \tag{3.64}$$

3.3 Quadratic programming

The general expression of quadratic programming (QP) can be stated as

$$\min_x \quad q(\boldsymbol{x}) = \frac{1}{2}\boldsymbol{x}^\top \boldsymbol{G}\boldsymbol{x} + \boldsymbol{x}^\top \boldsymbol{c}, \tag{3.65a}$$
$$\text{subject to} \quad \boldsymbol{a}_i^\top \boldsymbol{x} = b_i, \qquad i \in \mathcal{E}, \tag{3.65b}$$
$$\boldsymbol{a}_i^\top \boldsymbol{x} \geq b_i, \qquad i \in \mathcal{I}, \tag{3.65c}$$

where $\mathcal{E}$ and $\mathcal{I}$ are finite sets of indeces for equality and inequality constraints, respectively, $\boldsymbol{G}$ is a symmetric $n \times n$ matrix and $\boldsymbol{c}$, $\boldsymbol{x}$ and $\{\boldsymbol{a}_i\}$, $i \in \mathcal{E} \cup \mathcal{I}$, are vectors in $\mathbb{R}^n$. The quadratic program in equation (3.65) is said to be *convex* if the Hessian matrix $\boldsymbol{G}$ is positive semidefinite.

In the following, the traffic problem will be stated in the same manner as equation (3.65) and solved by the interior point method as described in Section 3.3.1. We continue with the case of one OD-pair, such that $\nu = (o, d)$, and use the 4-link and 5-link networks of the original Braess' problem in Figure 2.2. Later the programming problem will be expanded to operate on larger traffic networks.

Optimization requirement (3.2c) may be written in matrix form. Let $\boldsymbol{\phi} \in \mathbb{R}^n$ and $\boldsymbol{\Phi} \in \mathbb{R}^m$ be the vectors of link flow and path flow, respectively. For the original Braess' network problem in Figure 2.2 the flow vectors are given by,

$$\boldsymbol{\phi} = (\phi_1, \phi_2, \phi_3, \phi_4, \phi_5)^\top, \tag{3.66}$$

$$\boldsymbol{\Phi} = (\Phi_{oad}, \Phi_{obd}, \Phi_{oabd})^\top = (\Phi_1, \Phi_2, \Phi_3)^\top. \tag{3.67}$$

The relation between link flows and path flows may be expressed by the arcpath incidence matrix $\boldsymbol{D} \in \mathbb{R}^{n \times m}$. For the original Braess' network, matrix $\boldsymbol{D}$ becomes,

$$\begin{bmatrix} \phi_1 \\ \phi_2 \\ \phi_3 \\ \phi_4 \\ \phi_5 \end{bmatrix} = \begin{bmatrix} 1 & 0 & 1 \\ 1 & 0 & 0 \\ 0 & 1 & 0 \\ 0 & 1 & 1 \\ 0 & 0 & 1 \end{bmatrix} \begin{bmatrix} \Phi_1 \\ \Phi_2 \\ \Phi_3 \end{bmatrix}, \tag{3.68}$$

$$\boldsymbol{\phi} = \boldsymbol{D}\boldsymbol{\Phi}.$$

Let the link travel times be linear functions written as,

$$t_\alpha(\phi_\alpha) = A_\alpha \phi_\alpha + B_\alpha, \qquad \forall \alpha \in \mathcal{A}. \tag{3.69}$$

The objective function in equations (3.2a) and (3.4) for the 5-link network problem in Figure 2.2(c) may be written as matrices, given linear travel time functions, such that,

$$\begin{aligned}
\tilde{C}(\boldsymbol{\phi}) &= \sum_\alpha \int_0^{\phi_\alpha} t_\alpha(x)\, \mathrm{d}x \\
&= \sum_\alpha \frac{1}{2} A_\alpha \phi_\alpha^2 + B_\alpha \phi_\alpha \\
&= \frac{1}{2} \begin{bmatrix} \phi_1 \\ \phi_2 \\ \phi_3 \\ \phi_4 \\ \phi_5 \end{bmatrix}^\top \begin{bmatrix} A_1 & 0 & 0 & 0 & 0 \\ 0 & A_2 & 0 & 0 & 0 \\ 0 & 0 & A_3 & 0 & 0 \\ 0 & 0 & 0 & A_4 & 0 \\ 0 & 0 & 0 & 0 & A_5 \end{bmatrix} \begin{bmatrix} \phi_1 \\ \phi_2 \\ \phi_3 \\ \phi_4 \\ \phi_5 \end{bmatrix} + \begin{bmatrix} \phi_1 \\ \phi_2 \\ \phi_3 \\ \phi_4 \\ \phi_5 \end{bmatrix}^\top \begin{bmatrix} B_1 \\ B_2 \\ B_3 \\ B_4 \\ B_5 \end{bmatrix} \qquad (3.70) \\
&= \frac{1}{2} \boldsymbol{\phi}^\top \tilde{\boldsymbol{A}} \boldsymbol{\phi} + \boldsymbol{\phi}^\top \boldsymbol{b} \\
&= \frac{1}{2} (\boldsymbol{D}\boldsymbol{\Phi})^\top \tilde{\boldsymbol{A}} (\boldsymbol{D}\boldsymbol{\Phi}) + (\boldsymbol{D}\boldsymbol{\Phi})^\top \boldsymbol{b} \\
&= \frac{1}{2} \boldsymbol{\Phi}^\top (\boldsymbol{D}^\top \tilde{\boldsymbol{A}} \mathrm{D}) \boldsymbol{\Phi} + \boldsymbol{\Phi}^\top (\boldsymbol{D}^\top \boldsymbol{b}) \\
&= \frac{1}{2} \boldsymbol{\Phi}^\top \boldsymbol{G} \boldsymbol{\Phi} + \boldsymbol{\Phi}^\top \boldsymbol{c}. \qquad (3.71)
\end{aligned}$$

Matrix $\tilde{\boldsymbol{A}} \in \mathbb{R}^{n\times n}$ is a diagonal matrix of entries A_α and $\boldsymbol{b} \in \mathbb{R}^n$ is a vector of entries B_α from the linear travel time functions in equation (3.69). And $\boldsymbol{G} \in \mathbb{R}^{m\times m}$ is a symmetrical matrix. Equation (3.71) is obviously true for general network problems of linear travel times.

As both matrix $\tilde{\boldsymbol{A}}$ and $\boldsymbol{G}$ are symmetric, they will be positive definite if the real parts of all eigenvalues are positive. When matrix $\boldsymbol{G}$ is positive definite, the objective function in equation (3.71) will give a *strictly* convex quadratic program.

The equality and inequality constraints in equations (3.2b) and (3.2d) can be expressed as vectors. Given the vector of path flows $\boldsymbol{\Phi} \in \mathbb{R}^m$, and assuming one origin-destination pair, the equality constraints are written,

$$\boldsymbol{e}^\top \Phi = \kappa, \qquad \text{where } \boldsymbol{e} = (1, 1, ...1)^\top \in \mathbb{R}^m, \tag{3.72}$$

and the inequality constraints are,

$$\boldsymbol{e}_i^\top \boldsymbol{\Phi} \geq 0, \qquad \boldsymbol{e}_i = (0, ...0, 1, 0, ...0)^\top \in \mathbb{R}^m,\ i = 1, 2, ...m, \tag{3.73}$$

or

$$\boldsymbol{I}\boldsymbol{\Phi} \geq 0, \qquad \boldsymbol{I} \in \mathbb{R}^{m\times m}, \tag{3.74}$$

where $\boldsymbol{I}$ is the $m \times m$ identity matrix and $\boldsymbol{e}_i$, $i = 1, 2, ...m$ are the columns of I.

Quadratic programs (QP) may be solved in several ways, E.g. the convex combinations method, or Frank-Wolfe method [8] or other methods [15].Some approaches depend on whether the constraints are equality or inequality equations [13]. With purely equality constraints, the QP can be solved directly by factorization methods or iteratively by projected conjugate gradient methods etc. [13, pp. 451-463]. QPs with both equality and inequality constrains may be solved by algorithms such as active-set methods and interior-point methods [13, pp. 463-490].

Active-set methods have been widely used since the 1970s and is suitable for small to medium sized problems. The method will generally require a large number of computational steps, but each search direction is relatively inexpensive to calculate. Interior-point methods are more recent methods for solving quadratic programs, and have been used since the 1990s. These methods are effective on large problems, and uses a small number of expensive computational steps. In comparison, active-set methods are more complicated to implement. And while the interior-point methods are most efficient of the two on very large problems, active-set methods may converge rapidly if an estimate of the solution is available as initial guess.

In this thesis the interior-point method was used to solve the quadratic programming, as described in section 3.3.1. The active-set method described in Appendix C was first tried, but the results were unstable and gave negative flows.

3.3.1 Interior-point method

The interior-point method used is based on Mehrotra's predictor-corrector method, which was originally developed to solve linear programming problems. The method is a practical primal-dual method, solving the KKT-conditions to find solutions of the unknown variable $\boldsymbol{x}$, Lagrange multipliers $\boldsymbol{\lambda}$ and slack vector $\boldsymbol{y}$.

The general problem is as before,

$$\begin{aligned} \min_{x} \quad & q(\boldsymbol{x}) = \frac{1}{2}\boldsymbol{x}^\top \boldsymbol{G}\boldsymbol{x} + \boldsymbol{x}^\top \boldsymbol{c} && \text{(3.75a)} \\ \text{subject to} \quad & \boldsymbol{A}_I \boldsymbol{x} \geq \boldsymbol{b} && \text{(3.75b)} \\ & \boldsymbol{A}_E \boldsymbol{x} = \boldsymbol{\kappa}, && \text{(3.75c)} \end{aligned}$$

where $\boldsymbol{x} \in \mathbb{R}^m$, $\boldsymbol{b} \in \mathbb{R}^p$, $\boldsymbol{\kappa} \in \mathbb{R}^r$, $\boldsymbol{A}_I \in \mathbb{R}^{p \times m}$ represent the inequality constraint matrix and $\boldsymbol{A}_E \in \mathbb{R}^{r \times m}$ represent the equality matrix. The row-dimension of $\boldsymbol{A}_E$ is $r = 1$ in the problem of one OD pair.

With the flow $\boldsymbol{\phi}$ as the unknown variable the Lagrangian function is,

$$\mathcal{L}(\boldsymbol{\phi}, \boldsymbol{\lambda}, \boldsymbol{\rho}) = \frac{1}{2}\boldsymbol{\phi}^\top \boldsymbol{G}\boldsymbol{\phi} + \boldsymbol{\phi}^\top \boldsymbol{c} - \boldsymbol{\lambda}^\top (\boldsymbol{A}_I \boldsymbol{\phi} - \boldsymbol{b}) - \boldsymbol{\rho}\top (\boldsymbol{A}_E \boldsymbol{\phi} - \kappa).$$

The equality and inequality constraints are denoted $\boldsymbol{A}_E$ and $\boldsymbol{A}_I$, with corresponding Lagrange multipliers $\boldsymbol{\rho}$ and $\boldsymbol{\lambda}$, respectively.

To deal with the inequality conditions, a slack vector $\boldsymbol{y} > 0$ is introduced. The solution $(\boldsymbol{\phi}^*, \boldsymbol{y}^*, \boldsymbol{\lambda}^*, \boldsymbol{\rho}^*)$ then satisfy the following KKT-conditions,

$$\begin{aligned} \nabla_\phi \mathcal{L}(\boldsymbol{\phi}^*, \boldsymbol{\lambda}^*) = \boldsymbol{G}\boldsymbol{\phi}^* + \boldsymbol{c} - \boldsymbol{A}_I^\top \boldsymbol{\lambda}^* - \boldsymbol{A}_E^\top \boldsymbol{\rho}^* = 0, && && \text{(3.76a)} \\ \boldsymbol{A}_E \boldsymbol{\phi}^* - \kappa = 0, && && \text{(3.76b)} \\ \boldsymbol{A}_I \boldsymbol{\phi}^* - \boldsymbol{b} - \boldsymbol{y}^* = 0, && && \text{(3.76c)} \\ y_i^* \lambda_i^* = 0, && i \in \mathcal{I}, && \text{(3.76d)} \\ (\boldsymbol{y}^*, \boldsymbol{\lambda}^*) \geq 0, && && \text{(3.76e)} \\ \boldsymbol{\rho}^{*\top} (\boldsymbol{A}_E \boldsymbol{\phi}^* - \kappa) = 0. && && \text{(3.76f)} \end{aligned}$$

At a current iterate $(\boldsymbol{\phi}, \boldsymbol{y}, \boldsymbol{\lambda}, \boldsymbol{\rho})_k$ which satisfies $(\boldsymbol{y}_k, \boldsymbol{\lambda}_k) > 0$, a complementarity measure is defined as,

$$\mu = \frac{\boldsymbol{y}^\top \boldsymbol{\lambda}}{p}, \tag{3.77}$$

where p is the number of inequality constraints.

Let $\mathcal{Y} = \text{diag}(y_i)$ and $\Lambda = \text{diag}(\lambda_i)$ for $i \in \mathcal{I}$, and let σ be some value in the

interval [0,1]. By considering the perturbed KKT-conditions given by,

$$F(\boldsymbol{\phi}, \boldsymbol{y}, \boldsymbol{\lambda}, \boldsymbol{\rho}; \sigma\mu) = \begin{bmatrix} \boldsymbol{G}\phi + \boldsymbol{c} - \boldsymbol{A}_I^\top \boldsymbol{\lambda} - \boldsymbol{A}_E^\top \boldsymbol{\rho} \\ \boldsymbol{A}_E \boldsymbol{\phi} - \kappa \\ \boldsymbol{A}_I \boldsymbol{\phi} - \boldsymbol{b} - \boldsymbol{y} \\ \mathcal{Y}\Lambda e - \sigma\mu e \end{bmatrix} = 0, \tag{3.78}$$

a path-following, primal-dual method is derived. Solutions of equation system (3.78) will, for all positive values of σ and μ, define the central path. As the product $\sigma\mu$ tends to zero, the trajectory defined by the central path will lead to the solution of the quadratic program.

Applying Newtons method to equation system (3.78),

$$\nabla F(\boldsymbol{\phi}, \boldsymbol{y}, \boldsymbol{\lambda}, \boldsymbol{\rho}; \sigma\mu)\Delta\boldsymbol{\phi} = -F(\boldsymbol{\phi}, \boldsymbol{y}, \boldsymbol{\lambda}, \boldsymbol{\rho}; \sigma\mu),$$

while letting μ be fixed, the following linear system is obtained,

$$\begin{bmatrix} \boldsymbol{G} & 0 & -\boldsymbol{A}_I^\top & -\boldsymbol{A}_E^\top \\ \boldsymbol{A}_E & 0 & 0 & 0 \\ \boldsymbol{A}_I & -\boldsymbol{I} & 0 & 0 \\ 0 & \Lambda & \mathcal{Y} & 0 \end{bmatrix} \begin{bmatrix} \Delta\boldsymbol{\phi} \\ \Delta\boldsymbol{y} \\ \Delta\boldsymbol{\lambda} \\ \Delta\boldsymbol{\rho} \end{bmatrix} = - \begin{bmatrix} \boldsymbol{G}\boldsymbol{\phi} + \boldsymbol{c} - \boldsymbol{A}_I^\top \boldsymbol{\lambda} - \boldsymbol{A}_E^\top \boldsymbol{\rho} \\ \boldsymbol{A}_E \boldsymbol{\phi} - \kappa \\ \boldsymbol{A}_I \boldsymbol{\phi} - \boldsymbol{b} - \boldsymbol{y} \\ \mathcal{Y}\Lambda \boldsymbol{e} - \sigma\mu \boldsymbol{e} \end{bmatrix}. \tag{3.79}$$

The right hand side will be denoted $-\boldsymbol{r} = (-\boldsymbol{r}_1, -\boldsymbol{r}_2, -\boldsymbol{r}_3, -\boldsymbol{r}_4)^\top$. The variables/unknowns in equation (3.79) are $\Delta\boldsymbol{\phi} \in \mathbb{R}^m$, $\Delta\boldsymbol{y} \in \mathbb{R}^p$, $\Delta\boldsymbol{\lambda} \in \mathbb{R}^p$ and $\Delta\boldsymbol{\rho} \in \mathbb{R}^r$. So the linear equation system has $(m + p + p + r)$ unknowns, and the same number of equations.

The next iterate is obtained by setting,

$$(\boldsymbol{\phi}, \boldsymbol{y}, \boldsymbol{\lambda}, \boldsymbol{\rho})_{k+1} = (\boldsymbol{\phi}, \boldsymbol{y}, \boldsymbol{\lambda}, \boldsymbol{\rho})_k + \alpha(\Delta\boldsymbol{\phi}, \Delta\boldsymbol{y}, \Delta\boldsymbol{\lambda}, \Delta\boldsymbol{\rho}), \tag{3.80}$$

where α is chosen to satisfy $(\boldsymbol{y}_{k+1}, \boldsymbol{\lambda}_{k+1}) > 0$, as will be explained further below.

Algorithm details

In the following, some of the aspects of the interior-point method used in this paper will be introduced, while the stepwise procedure of the method is given in Algorithm 1.

First step is to compute an affine scaling step $(\Delta\boldsymbol{\phi}, \Delta\boldsymbol{y}, \Delta\boldsymbol{\lambda}, \Delta\boldsymbol{\rho})^{\text{aff}}$ from equation system (3.79) letting $\sigma = 0$. This step is also refered to as the predictor step. From equation (3.76d) we know that the solution must satisfy $y_i\lambda_i = 0$ for $i \in \mathcal{I}$. If we take a full step with the affine step, the updated value will be $y_i^{k+1}\lambda_i^{k+1} = (y_i^k + \Delta y_i^{\text{aff}})(\lambda_i^k + \Delta\lambda_i^{\text{aff}}) = \Delta y_i^{\text{aff}}\Delta\lambda_i^{\text{aff}}$ and not 0 that would be the ideal value. To correct for this deviation, a corrector step $(\Delta\boldsymbol{\phi}, \Delta\boldsymbol{y}, \Delta\boldsymbol{\lambda}, \Delta\boldsymbol{\rho})^{\text{cor}}$ is computed. The

total search direction is then given by the combination of predictor and correcter step, such that $(\Delta\boldsymbol{\phi}, \Delta\boldsymbol{y}, \Delta\boldsymbol{\lambda}, \Delta\boldsymbol{\rho}) = (\Delta\boldsymbol{\phi}, \Delta\boldsymbol{y}, \Delta\boldsymbol{\lambda}, \Delta\boldsymbol{\rho})^{\text{aff}} + (\Delta\boldsymbol{\phi}, \Delta\boldsymbol{y}, \Delta\boldsymbol{\lambda}, \Delta\boldsymbol{\rho})^{\text{cor}}$. This step is obtained from solving the following system,

$$\begin{bmatrix} \boldsymbol{G} & 0 & -\boldsymbol{A}_I^\top & -\boldsymbol{A}_E^\top \\ \boldsymbol{A}_E & 0 & 0 & 0 \\ \boldsymbol{A}_I & -\boldsymbol{I} & 0 & 0 \\ 0 & \Lambda & \mathcal{Y} & 0 \end{bmatrix} \begin{bmatrix} \Delta\boldsymbol{\phi} \\ \Delta\boldsymbol{y} \\ \Delta\boldsymbol{\lambda} \\ \Delta\boldsymbol{\rho} \end{bmatrix} = \begin{bmatrix} -\boldsymbol{r}_1 \\ -\boldsymbol{r}_2 \\ -\boldsymbol{r}_3 \\ -\mathcal{Y}\Lambda\boldsymbol{e} - \Delta\mathcal{Y}^{\text{aff}}\Delta\Lambda^{\text{aff}}\boldsymbol{e} + \sigma\mu\boldsymbol{e} \end{bmatrix}. \quad (3.81)$$

The centering parameter is calculcated from,

$$\sigma = \left(\frac{\mu_{\text{aff}}}{\mu}\right)^3, \quad (3.82)$$

where the complementarity measure μ is calculated from equation (3.77) with current iteration values $\boldsymbol{y}_k$ and $\boldsymbol{\lambda}_k$, and μ_{aff} is calculated by the possible value at the next iterate, such that

$$\mu_{\text{aff}} = (\boldsymbol{y} + \alpha_{\text{aff}}\Delta\boldsymbol{y}^{\text{aff}})^\top(\boldsymbol{\lambda} + \alpha_{\text{aff}}\Delta\boldsymbol{\lambda}^{\text{aff}})/p, \quad (3.83)$$

The step length α_{aff} in equation (3.83) has to satisfy,

$$\alpha_{\text{aff}} = \max\{\alpha \in (0,1] \,|(\boldsymbol{y}, \boldsymbol{\lambda}) + \alpha(\Delta\boldsymbol{y}^{\text{aff}}, \Delta\boldsymbol{\lambda}^{\text{aff}}) \geq 0\}, \quad (3.84)$$

where each value corresponds to iteration step k. The value of α_{aff} will be chosen to 1 if $(\Delta\boldsymbol{y}^{\text{aff}}, \Delta\boldsymbol{\lambda}^{\text{aff}}) > 0$, as the inequality gives,

$$\alpha \geq -\frac{(\boldsymbol{y}, \boldsymbol{\lambda})}{(\Delta\boldsymbol{y}^{\text{aff}}, \Delta\boldsymbol{\lambda}^{\text{aff}})}.$$

This will also be a good choice if the inner product is equal to zero, as the inequality then will hold for any choice of α. However, if $(\Delta\boldsymbol{y}^{\text{aff}}, \Delta\boldsymbol{\lambda}^{\text{aff}}) < 0$ the inequality gives,

$$\alpha \leq \frac{(\boldsymbol{y}, \boldsymbol{\lambda})}{|(\Delta\boldsymbol{y}^{\text{aff}}, \Delta\boldsymbol{\lambda}^{\text{aff}})|},$$

and the step length is chosen by,

$$\alpha_{\text{aff}} = \min\left\{1, \frac{(\boldsymbol{y}, \boldsymbol{\lambda})}{|(\Delta\boldsymbol{y}^{\text{aff}}, \Delta\boldsymbol{\lambda}^{\text{aff}})|}\right\}.$$

To compute the next iterate we may choose to use either step length parameters α^{pri} and α^{dual} or use the same value for both. In this paper we chose to use the

same value, such that $\hat{\alpha} = \min(\alpha_\tau^{\text{pri}}, \alpha_\tau^{\text{dual}})$. The primal and dual values of α_τ are here defined as,

$$\alpha_\tau^{\text{pri}} = \max\{\alpha \in (0,1] : \boldsymbol{y} + \alpha\Delta\boldsymbol{y} \geq (1-\tau)y\}, \tag{3.85a}$$
$$\alpha_\tau^{\text{dual}} = \max\{\alpha \in (0,1] : \boldsymbol{\lambda} + \alpha\Delta\boldsymbol{\lambda} \geq (1-\tau)\lambda\}, \tag{3.85b}$$

where $\tau \in (0,1)$. The values of α_τ^{pri} and $\alpha_\tau^{\text{dual}}$ are found using the same reasoning as for α_{aff}. The convergence may speed up if we choose τ to approach 1 as the iterates approaches the solution. Here we have used $\tau = 0.995$ fixed, as this is a representative value of τ [13, p. 567].

The next iterate is then obtained from equation (3.80) with $\alpha = \hat{\alpha}$.

Equation system (3.79) can be solved by eliminating Δy from the system and rearranging the equations. The following compact form is then obtained,

$$\begin{bmatrix} \boldsymbol{G} & \boldsymbol{A}_I^\top & \boldsymbol{A}_E^\top \\ \boldsymbol{A}_I & -\Lambda^{-1}\mathcal{Y} & 0 \\ \boldsymbol{A}_E & 0 & 0 \end{bmatrix} \begin{bmatrix} \Delta\boldsymbol{\phi} \\ -\Delta\boldsymbol{\lambda} \\ -\Delta\boldsymbol{\rho} \end{bmatrix} = \begin{bmatrix} -(\boldsymbol{G}\boldsymbol{\phi} + \boldsymbol{c} - \boldsymbol{A}_I^\top\boldsymbol{\lambda} - \boldsymbol{A}_E^\top\boldsymbol{\rho}) \\ -(\boldsymbol{A}_I\boldsymbol{\phi} - \boldsymbol{b} - \boldsymbol{y}) - \boldsymbol{y} + \sigma\mu\Lambda^{-1}\boldsymbol{e} \\ -(\boldsymbol{A}_E\boldsymbol{\phi} - \kappa) \end{bmatrix}, \tag{3.86}$$

where the coefficient matrix on the left hand side is symmetric. Since $\lambda_i \geq 0$ and $y_i \geq 0$ for all i, we know that matrices Λ and $\mathcal{Y}$ are nonsingular. The equation system can easily be solved by factorization methods. Equation system (3.81) is solved in the same manner.

Algorithm 1: Interior point method for convex QP; Predictor-Correcror Algorithm [13, p. 484].

Input: Matrix $\boldsymbol{G}$, inequality constraint matrix $\boldsymbol{A}_I$, equality constraint matrix $\boldsymbol{A}_E$, vectors $\boldsymbol{c}$ and $\boldsymbol{b}$, demand κ.
Output: Solution vector $\boldsymbol{\phi}$.
Compute $(\boldsymbol{\phi}_0, \boldsymbol{y}_0, \boldsymbol{\lambda}_0, \boldsymbol{\rho}_0)$ with $(\boldsymbol{y}_0, \boldsymbol{\lambda}_0) > 0$
for *k=0,1,2,...* **do**
  Set $(\boldsymbol{\phi}, \boldsymbol{y}, \boldsymbol{\lambda}, \boldsymbol{\rho}) = (\boldsymbol{\phi}, \boldsymbol{y}, \boldsymbol{\lambda}, \boldsymbol{\rho})_k$ and solve (3.79) with $\sigma = 0$ for $(\Delta\boldsymbol{\phi}, \Delta\boldsymbol{y}, \Delta\boldsymbol{\lambda}, \Delta\boldsymbol{\rho})^{\text{aff}}$;
  Calculate $\mu = \boldsymbol{y}^\top\boldsymbol{\lambda}/p$;
  Calculate $\hat{\alpha}_{\text{aff}}$ from equation (3.84);
  Calculate μ_{aff} from equation (3.83);
  Set centering parameter to $\sigma = (\mu_{\text{aff}}/\mu)^3$;
  Solve equation system (3.81) for $(\Delta\boldsymbol{\phi}, \Delta\boldsymbol{y}, \Delta\boldsymbol{\lambda}, \Delta\boldsymbol{\rho})$;
  Choose $\tau_k \in (0,1)$ and set $\hat{\alpha} = \min(\alpha_{\tau_k}^{\text{pri}}, \alpha_{\tau_k}^{\text{dual}})$ from (3.85);
  Set $(\boldsymbol{\phi}, \boldsymbol{y}, \boldsymbol{\lambda}, \boldsymbol{\rho})_{k+1} = (\boldsymbol{\phi}, \boldsymbol{y}, \boldsymbol{\lambda}, \boldsymbol{\rho})_k + \hat{\alpha}(\Delta\boldsymbol{\phi}, \Delta\boldsymbol{y}, \Delta\boldsymbol{\lambda}, \Delta\boldsymbol{\rho})$;
end

3.3.2 Expanding to several OD pairs

Expanding to several OD pairs is quite straight forward. When all paths between each OD pair is known, then matrix D is easily found. How to find all paths is explained in the next section. The only thing to remark is that the vector of OD demand $\boldsymbol{\kappa}$ now will have dimension equal to the number of OD pairs. And the equality constraint matrix A_E must be such that the sum over all paths connecting OD pair ν is equal to κ_ν, for all ν.

3.3.3 Programming in MATLAB

The interior-point method described above was implemented into Matlab, to solve the quadratic programming method. Some of the techniques used to find all paths and the $\boldsymbol{D}$ matrix will be described in this section.

In Matlab, each node was given a number, e.g. $o = 1$, $a = 2$, such that the links could be written as $u_1 = [1, 2]$ etc. The matrix of links $\boldsymbol{L}$ would then be,

$$\boldsymbol{L} = \begin{bmatrix} u_1 & u_2 & u_3 & u_4 & u_5 & u_6 \end{bmatrix}^\top = \begin{bmatrix} 1 & 2 & 1 & 3 & 2 \\ 2 & 4 & 3 & 4 & 3 \end{bmatrix}^\top,$$

for the Braess network example. Each path is written as a sequence of node numbers in a similar manner as the links, e.g. path U_{oad} in the Braess network example is written $[1, 2, 4]$. The matrix of paths $\boldsymbol{P}$ contains a path in each row. The OD pairs are given as a matrix, such that each row contains an origin in column one and a destination in column two.

To find all OD paths, a recursive function was made. The function traverses the network by finding the consecutive nodes in the network following all directed links out of a node. The method is described in Algorithm 2, and the MATLAB code is given in Appendix B.2. All necessary MATLAB codes to find all OD paths are given in Appendix B. The row and column indexes of matrix $\boldsymbol{P}$ of paths are denoted I_1 and I_2. The node in which, for each call of the function, we want to find links from is denoted a_F. For each iteration, the node we are jumping to is denoted a_T. For each call of the function, we need a variable containing the part of path I_1 which has been found so far, because several paths may begin with the same nodes. This part is denoted $\boldsymbol{P}_{part}$ in the algorithm.

The paths should not contain cycles. To avoid this, we check that no one-way link is repeated, or that no two-way link is used to go back and forth between the same two nodes.

Algorithm 2: Method to find all OD paths; NextNode().

Input: Node from a_F, matrix $\boldsymbol{L}$ of links, origin-destination pair OD_ν, row index I_1 of matrix $\boldsymbol{P}$, column index I_2 of matrix $\boldsymbol{P}$, matrix $\boldsymbol{P}$ of paths, vector of path-part $\boldsymbol{P}_{part}$.

Output: Matrix $\boldsymbol{P}$ of paths, row index I_1 of matrix $\boldsymbol{P}$.

```
Find all nodes a_j which are connected to node a_F by a directed link from a_F;
if no a_j exists AND last node in path I_1 is different from destination
OD_ν(2) then
    Remove row I_1 from P;
    I_1 = I_1 − 1;
I_2 = I_2 + 1;
for j = 1, 2..., number of a_j do
    a_T = a_j;
    if j > 1 then
        I_1 = I_1 + 1;
        Add P_part to row I_1 of P;
    if a_T == OD_ν(2) then
        Add node a_T to the end of path I_1, P(I_1, I_2);
    else
        if node a_T do not result in any cycle at current path I_1 then
            Add node a_T to the end of path I_1, P(I_1, I_2);
            Call NextNode with input {a_T, L, OD_ν, I_1, I_2, P, P(I_1, 1 : I_2)};
        else
            Remove row I_1 from P;
            I_1 = I_1 − 1;
        end
    end
end
```

3.4 Minimal system cost

The minimal system cost is obtained solving the non-linear program in equations (3.2) and (3.3) [19]. With linear travel time functions, objective function is equal to,

$$C(\boldsymbol{\phi}) = \sum_{\alpha} A_\alpha \phi_\alpha^2 + B_\alpha \phi_\alpha. \tag{3.87}$$

The objective function, written with matrices will then become,

$$\begin{aligned} C(\boldsymbol{\Phi}) &= \boldsymbol{\Phi}^\top (\boldsymbol{D}^\top \tilde{\boldsymbol{A}} \boldsymbol{D}) \boldsymbol{\Phi} + \boldsymbol{\Phi}^\top (\boldsymbol{D}^\top \boldsymbol{b}), \\ &= \boldsymbol{\Phi}^\top \boldsymbol{G} \boldsymbol{\Phi} + \boldsymbol{\Phi}^\top \boldsymbol{c}. \end{aligned} \tag{3.88}$$

The objective function for system cost differ only by one constant, the half in front of matrix G, from the objective function for user cost (Nash equilibrium) in equation (3.71). Since the objective functions are equal apart from a half, we can use the interior-point method described in Section 3.3.1.

Chapter 4

Results

In this chapter the results are presented. The methods described in Chapter 3 is used to find flow distributions and travel times at Nash equilibrium and system optimal flow.

Braess' paradox is investigated on four different networks. For each network, the parameters in the cost functions and travel demand are stepwise changed to see the effect on the flow distribution and the resulting path travel times.

To reveal occurences of Braess' paradox we remove one or several of the links from each network. In the case where travel times on used paths decrease when the link is removed, we may conclude that Braess' paradox occurs.

Turning the statement around, it is desirable to show that travel times on used paths increase when a link is added. Let $\tilde{\mathbf{\Phi}}$ be the flow distribution on paths after a link is removed, and $\mathbf{\Phi}^*$ be the flow distribution on the complete network. Since the programming problem used for the interior point method is based on Wardropes user equilibrium (equivalent to Nash equilibrium), then all used paths have the same path travel time, and travel times on non-utilized paths are greater or equal to this. Consequently, the minimum $\min_\beta T_\beta(\mathbf{\Phi})$ is understood to be the travel cost on all used paths. The increase in travel cost can then be illustrated by the ratio,

$$r = \frac{\min_\beta T_\beta(\mathbf{\Phi}^*) - \min_\beta T_\beta(\tilde{\mathbf{\Phi}})}{\min_\beta T_\beta(\tilde{\mathbf{\Phi}})}. \tag{4.1}$$

The Braess flow intervals presented in section 3.2 are calculated. The parameters in the cost functions and travel demand are stepwise changed to see the effect on the Braess flow intervals and distributions.

To investigate the impact of selfish routing, we compare the travel costs at Nash equilibrium and system optimal flow. Let the flow distribution at Nash equilibrium be denoted $\boldsymbol{\phi}_{\mathrm{N}}$, and let the flow distribution at system optimal flow be denoted $\boldsymbol{\phi}_{\mathrm{syst}}$. The ratio between system cost $C(\boldsymbol{\phi})$ at Nash equilibrium and

at system optimal flow will then be denoted,

$$\rho = \frac{C(\boldsymbol{\phi}_{\mathrm{N}})}{C(\boldsymbol{\phi}_{\mathrm{syst}})}. \tag{4.2}$$

4.1 Braess' network model

The network model originally used by Braess is studied in the analyses in this section. The network model is depicted in Figure 4.1. The network has five links denoted $\boldsymbol{u} = \{u_1, u_2, u_3, u_4, u_5\}$, and three routes between origin o and destination d denoted $\boldsymbol{U} = \{U_{oad}, U_{obd}, U_{oabd}\}$. The travel times for traversing each link are linear functions, denoted $t_\alpha(\boldsymbol{\phi}) = A_\alpha \phi_\alpha + B_\alpha$.

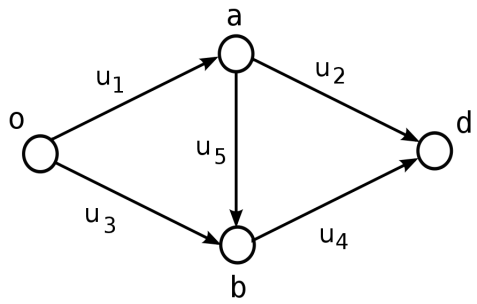

Figure 4.1: Braess' network model.

In the linear cost functions t_α, there are two parameters we can change. These are the value of parameter A_α and the value of parameter B_α. Parameter A_α decides how dependent the travel time is on traffic flow, while parameter B_α decides the travel cost on link u_α when traffic flow is zero. The values of the function parameters used by Braess are such that the travel time functions are symmetric over the links in the network. Consequently, the travel time functions on links u_1 and u_4 have equal parameters, and links u_2 and u_3 have equal function parameters. The symmetry property is used in most of the analyses.

The travel time functions used by Braess are,

$$t_1(\boldsymbol{\phi}) = A\phi_1, \tag{4.3a}$$
$$t_2(\boldsymbol{\phi}) = \phi_2 + B, \tag{4.3b}$$
$$t_3(\boldsymbol{\phi}) = \phi_3 + B, \tag{4.3c}$$
$$t_4(\boldsymbol{\phi}) = A\phi_4, \tag{4.3d}$$
$$t_5(\boldsymbol{\phi}) = \phi_5 + B_5, \tag{4.3e}$$

with,

$$A = 10, \qquad B = 50, \qquad B_5 = 10, \tag{4.4}$$

as presented in section 2.4. The values of function parameters A, B and B_5 used in the following analyses are equal to those given in equation 4.4, if nothing else i specified. Correspondingly, the travel demand used is $\kappa = 6$ when nothing else is specified.

4.1.1 Braess flow intervals

The critical intervals illustrate where Braess' paradox may occur given some travel cost functions on Braess' network model, as presented in section 3.2.4. The results of such intervals are given in this section.

The traffic flow may be distributed in several ways, depending on total demand and the cost function parameters. On the 4-link network, the traffic flow must be interior for a Braess flow to exist, meaning both paths must be utilized, as illustrated in Figure 4.2(a). On the 5-link network, link u_5 must be utilized for a Braess flow to exist. The possible flow distributions on this network are then interior flow, left boundary, right boundary and extreme boundary flow, which are all illustrated in Figure 4.2.

Below, we show examples of critical intervals for Braess flow on Braess' network model while changing some of the parameters. The travel cost functions are given in equation (4.4).

In the first analysis, the value of function parameter A is changed. Figure 4.3 gives the critical intervals for three different values of function parameter A, where $A = \{5, 10, 15\}$. The remaining function parameters are equal to the values given in equation (4.4). The black line represents the interval of demand where the flow distribution is extreme, and the green line is the interval for interior flow. We observe from Figure 4.3 that the Braess flow interval decrease when the value of A increase. The flow is distributed as extreme boundary flow (see Figure 4.2(e)) and interior flow (see Figure 4.2(b)). These distributions are expected as the travel functions are symmetric over the traffic network.

In the second analysis the value of function parameter B is changed. In Figure 4.4 the critical intervals with values $B = \{30, 50, 80, 110\}$. The remaining function parameters are equal to the original Braess example, as stated in equation (4.4). The black line is the interval of demand where flow distribution is extreme, and the green line is where the distribution is interior flow. We observe that the intervals of demand where Braess' paradox occurs increases when the value of B increases. The flow is distributed as extreme boundary flow (see Figure 4.2(e)) and interior flow (see Figure 4.2(b)), as expected.

In the third analysis the value of function parameter B_5 is changed. In Figure

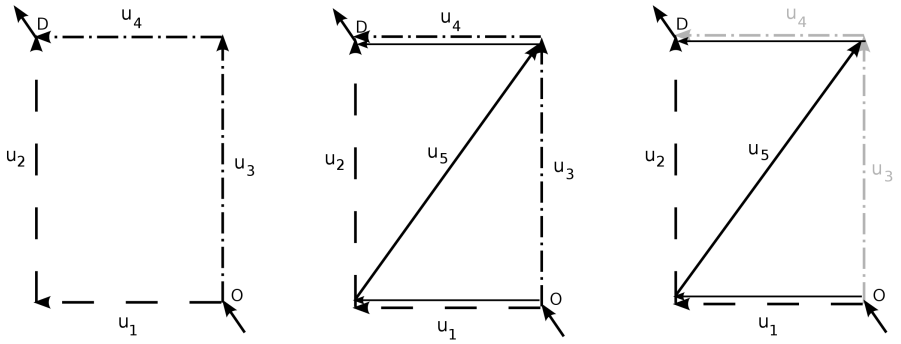

(a) Interior flow on 4-link network.

(b) Interior flow on 5-link network.

(c) Left boundary flow.

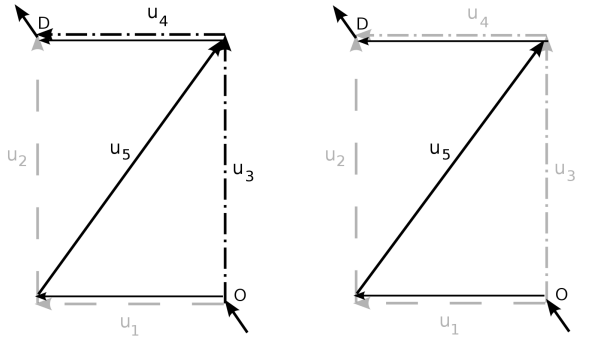

(d) Right boundary flow.

(e) Extreme boundary flow.

Figure 4.2: Flow distributions on the 4-link and 5-link network.

4.5 the critical intervals with values $B_5 = \{0, 20, 40\}$. The remaining function parameters are equal to the values given in equation (4.4). The black line is the interval of demand where flow distribution is extreme, and the green line is where the distribution is interior flow. We observe that the intervals of demand where Braess' paradox occurs increases when the value of B_5 increases. The flow is distributed as extreme boundary flow (see Figure 4.2(e)) and interior flow (see Figure 4.2(b)), as expected.

For the above examples the travel costs are symmetric over the links in the traffic network, in the sence that cost function $t_1 = t_4$ and $t_2 = t_3$. In the last analysis the travel functions are made nonsymmetric over the traffic network, and the results are shown in Figure 4.6.

First, travel time on link u_1 and u_4 are made nonsymmetric with $A_4 = 20 \neq$

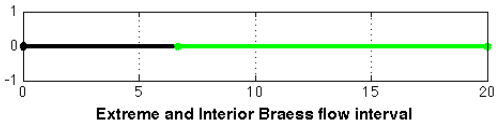

(a) Function parameter $A = 5$.

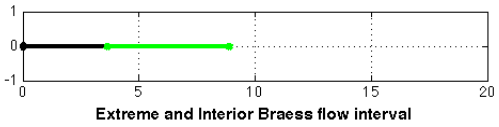

(b) Function parameter $A = 10$.

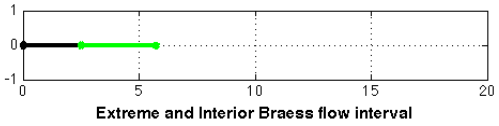

(c) Function parameter $A = 15$.

Figure 4.3: Extreme and interior Braess flow intervals, with various value of function parameter A.

$A_1 = 10$. The results are given in Figure 4.6(a). The flow distribution is extreme when demand is within the interval given by the black line, left flow when demand is within the interval given by the blue line, and interior in the interval by the green line. We observe from Figure 4.6(a) that the flow is distributed as left-boundary flow in a small interval of demand, which is different from the symmetrical cases. This is to be expected, since link u_4 is more expensive to traverse compared to link u_1.

In the second case travel time on link u_2 and u_3 are made nonsymmetric with $B_2 = 90 \neq B_3 = 50$. The results are given in Figure 4.6(b). The distribution is right flow when demand is within the interval given by the red line, and interior flow when demand is on the green line. In both examples the remaining function parameters are equal to the original Braess example, as stated in equation (4.4). We observe from Figure 4.6(b) that in a small demand interval the flow is distributed as right boundary flow, which differ from the above cases. This is also to be expected, since link u_2 is more expensive to traverse compared to link u_3.

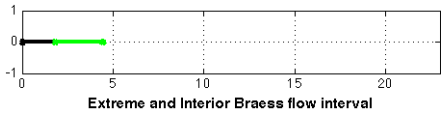

(a) Function parameter $B = 30$.

(b) Function parameter $B = 50$.

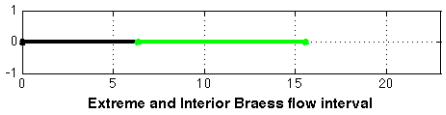

(c) Function parameter $B = 80$.

(d) Function parameter $B = 110$.

Figure 4.4: Extreme and interior Braess flow intervals, with various value of function parameter B.

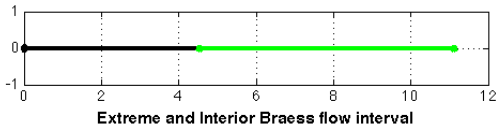

(a) Function parameter $B_5 = 0$.

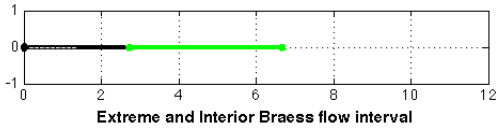

(b) Function parameter $B_5 = 20$.

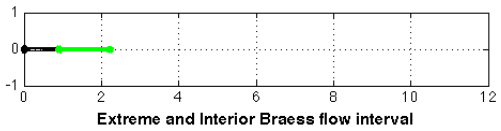

(c) Function parameter $B_5 = 40$.

Figure 4.5: Extreme and interior Braess flow intervals, with various value of function parameter B_5.

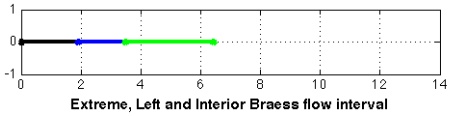

(a) Function parameter $A_4 = 20$.

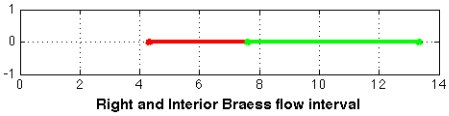

(b) Function parameter $B_2 = 90$.

Figure 4.6: Brass flow intervals when the link cost functions are non-symmetric on the traffic network.

4.1.2 Braess' paradox

In this section we investigate when Braess' paradox occurs depending on function parameters and demand. The travel functions are given in equation (4.3), and the parameter values are equal $A = 10$, $B = 50$ and $B_5 = 10$ as given in equation (4.4) if nothing else is specified. Correspondingly, the travel demand used is $\kappa = 6$ when nothing else is specified.

In the first analysis the OD demand κ is changed. The resulting ratio r of increased travel time defined in equation (4.1) is illustrated in Figure 4.7(a). Figure 4.7(b) shows the path travel cost on used paths for each of the network cases, with and without link u_5. The travel time at Nash equilibrium are on all paths equal to the minimal travel time over all path travel times. Consequently, we look at the minimal path travel time. The travel time on used routes on the 4-link network is given by the red line, and travel time on the 5-link network is given by the blue line.

Figures 4.7(c) and 4.7(d) show the path travel times on each of the networks. The black line represents path U_{oad}, path U_{oabd} is given by the blue dotted line, and path U_{obd} is given by the green dashed line. The routes of minimum travel times gives the paths which are used at Nash equilibrium, and therefore illustrates how the flow is distributed over the traffic network. The flow distributions on the complete network are illustrated in Figure 4.8.

Some of the results are given in Table A.2 and A.3 in Appendix A. The tables show the flow distributions on links and paths together with the path travel costs at some OD demands κ.

We observe from Figure 4.7(a) that the travel time for all users increases with at most 23 % when link u_5 is available in the traffic network. From Figure 4.7(b) we see that there is an interval $\kappa \in (2.5, 9)$ where travel time on used routes on the 5-link network exceeds the travel time on the 4-link network. From the results in Figures 4.7(a) and 4.7(b) we conclude that Braess' paradox occurs in the mentioned interval. When demand is 2.5 or less the traffic flow is distributed in route U_{oabd} and the travel time is less than on the 4-link network. However, when demand is equal or greater than 9 the path travel times and flow distributions are equal on both networks. Consequently, for large demands travel time is independent of whether link u_5 is available or not. Note that these intervals are specific for the used function parameters.

In the second analysis the value of function parameter A is changed. Figure 4.9(a) shows the ratio of increase in travel time depending on the value of function parameter A. The travel costs on used paths are given in Figure 4.9(b). The blue line represents travel time on the 5-link network, and the red line on the 4-link network. Some of the results of flow distributions on links and paths along with travel times are given in Table A.1 in Appendix A.

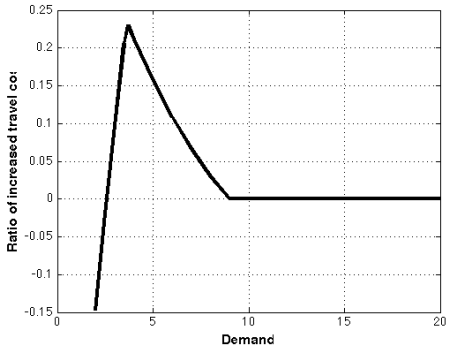

(a) Ratio of increased travel cost.

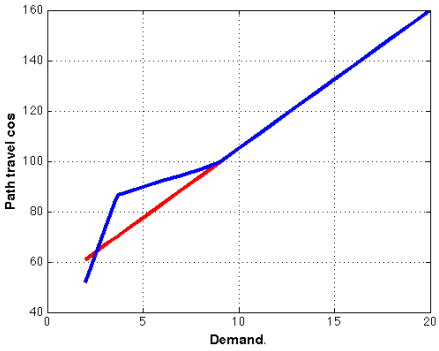

(b) Travel time on used paths, on the 4-link (red line) and 5-link network (blue line).

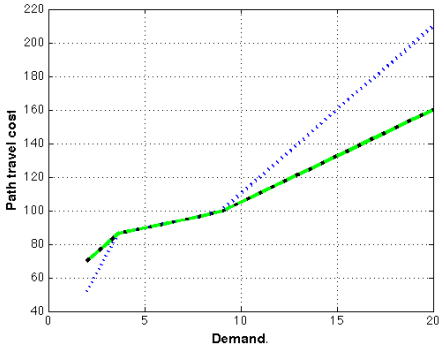

(c) Travel time on all paths, U_{oad} (black line), U_{oabd} (blue line), U_{obd} (green line), 5-link network.

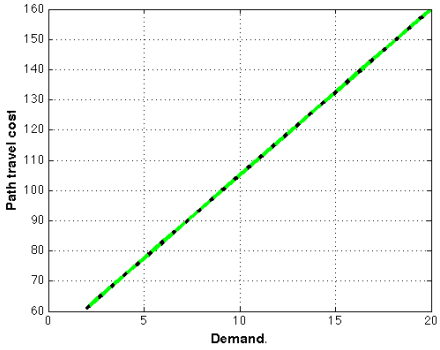

(d) Travel time on all paths, U_{oad} (black line), U_{obd} (green line), 4-link network.

Figure 4.7: Illustration of increased travel time between the 4- and 5-link Braess' network model depending on demand κ.

We observe from Figure 4.9(a) and 4.9(b) that Braess' paradox occurs when the value of A is in the interval $(4, 15)$. The increase in travel time is at most 20 %. Figures 4.9(c) and 4.9(d) show the flow distributions on paths on each of the networks. The black line represents path U_{oad}, path U_{oabd} is given by the blue dotted line, and path U_{obd} is given by the green dashed line.

While still letting the ratio of increased travel cost be dependent on parameter A, Figure 4.10 illustrates what happens when different values of demand κ is used. The values used for demand are $\kappa = 3$ (blue line), $\kappa = 6$ (green line), $\kappa = 9$ (red line) and $\kappa = 12$ (black line). We observe that small demands are more affected by large values of A, and when demand is higher the interval of A where Braess' paradox occurs is shorter.

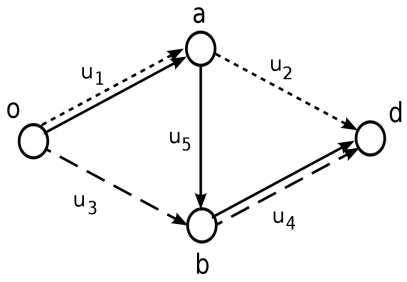

(a) Flow on all paths.

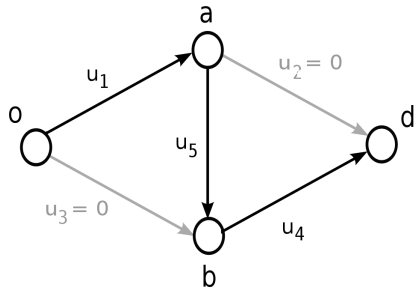

(b) Flow on path *oabd*.

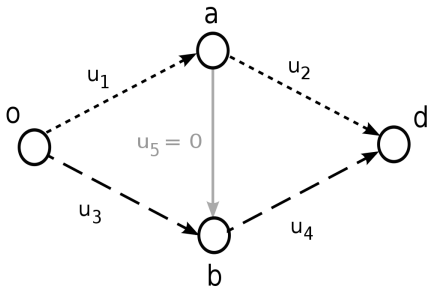

(c) No flow on link α_5.

Figure 4.8: Flow distribution on Braess' network example.

In the third analysis the value of function parameter B is changed. The results are given in Figure 4.11. Figure 4.11(a) gives the ratio of increased travel time defined in equation (4.1). The path travel costs on used paths are given in Figure 4.11(b) for the cases of the 4-link network (red line) and 5-link network (blue line). Some of the results are also given in Table A.4.

We observe from Figure 4.11(a) that the increase in travel time when link u_5 is added to the network is at most 25 %. From Figure 4.11(b) we observe that when parameter B is within the interval $B \in (35, 105)$ the travel time on the 5-link network is greater than the on the 4-link network, and we conclude that Braess' paradox occurs in this interval. Something to notice for this case is that the order of flow distribution, compared to the above analysis, is reversed. When the value is less or equal to $B = 35$ the flow is distributed on the outer links, equivalent to the 4-link network. For values larger or equal to $B = 105$ the flow is distributed on path U_{oabd}.

In the last analysis the value of function parameter B_5 is changed. The results are given in Figure 4.12. The ratio of increased travel cost defined in (4.1) is illustrated in Figure 4.12(a). The path travel costs on used paths are shown in

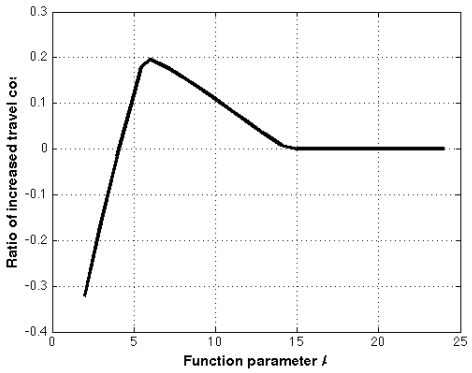

(a) Ratio of increased travel cost.

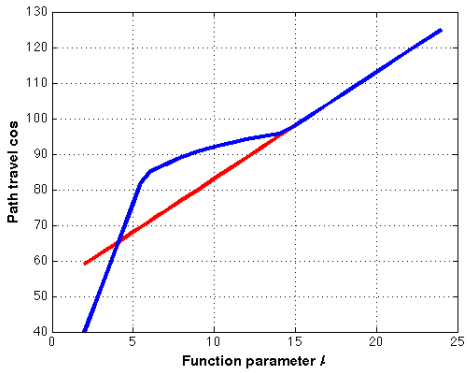

(b) Travel time on used paths, on the 4-link (red line) and 5-link network (blue line).

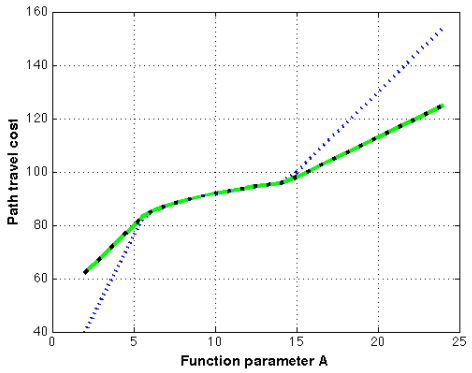

(c) Travel time on all paths, U_{oad} (black line), U_{oabd} (blue line), U_{obd} (green line), 5-link network.

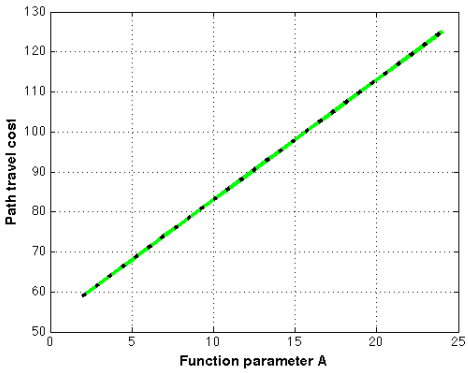

(d) Travel time on all paths, U_{oad} (black line), U_{obd} (green line), 4-link network.

Figure 4.9: Illustration of increase in travel time between the 4- and 5-link Braess' network depending on function parameter A, with demand $\kappa = 6$.

Figure 4.12(b), for both the 4-link network (red line) and the 5-link network (blue line). Some of the results are also given in Table A.5.

We observe from Figure 4.12(a) that the increased travel time after adding link u_5 is at most 19.2 %. When the value is $B_5 < 23$ (and larger than 0) we observe from Figure 4.12(a) and 4.12(b) that Braess' paradox occurs. From Figure 4.12(c) we observe that the flow is distributed on all paths when $B_5 < 23$. When the value is greater or equal to $B = 23$ the flow is distributed on the outer paths on the 5-link network, equivalent to the 4-link network.

In the above analyses all travel time functions have been symmetric on the traffic network. In the following analyses the two non-symmetric cases used in the

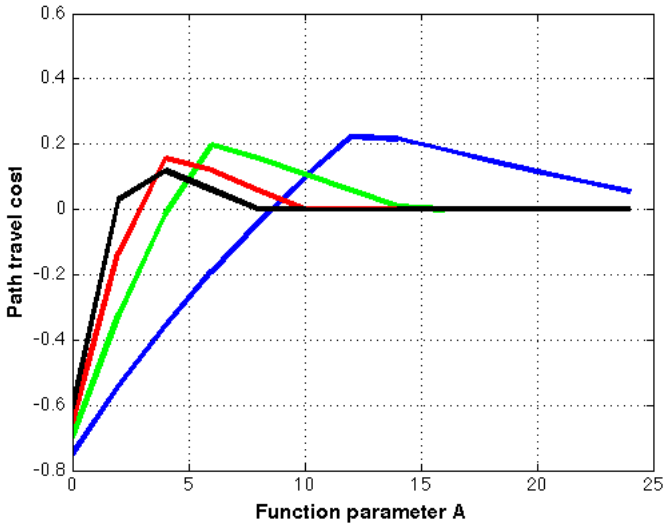

Figure 4.10: Illustration of increase in travel time depending on function value A, several demands. Each line represent the ratio of increase depending on the value of A. Each line represents different values of total demand; $\kappa = 3$ (blue), $\kappa = 6$ (green), $\kappa = 9$ (red), $\kappa = 12$ (black).

previous section are used.

In the first case the travel functions on links u_1 and u_4 are made non-symmetric with $A_4 = 20 \neq A_1 = 10$ while changing demand κ. The results are given in Figure 4.13. Figure 4.13(a) gives the ratio of increased travel time. The path travel costs on used paths are given in Figure 4.13(b) for the cases of the 4-link network (red line) and 5-link network (blue line). We observe from Figure 4.13(c) that the flow distributions are extreme, left boundary and interior flow, before the distribution is equivalent to interior flow on the 4-link network.

In the second case the travel functions on links u_2 and u_3 are made non-symmetric with $B_2 = 90 \neq B_3 = 50$ while changing demand. The results are given in Figure 4.14. Figure 4.14(a) gives the ratio of increased travel time. The path travel costs on used paths are given in Figure 4.14(b) for the cases of the 4-link network (red line) and 5-link network (blue line). From Figure 4.14(c) we observe that the flow distributions are extreme, right boundary and interior flow, before the distribution is equivalent to interior flow on the 4-link network.

Notice in each case that Braess' paradox occurs when the distributions are left boundary flow, right boundary flow and interior flow. When the distribution are extreme, when demands are small, the travel time is less than on the 4-link network.

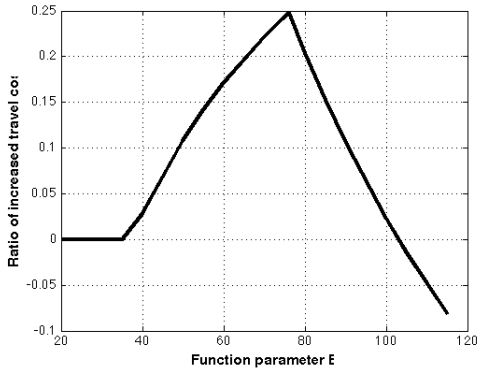

(a) Ratio of increase in travel cost.

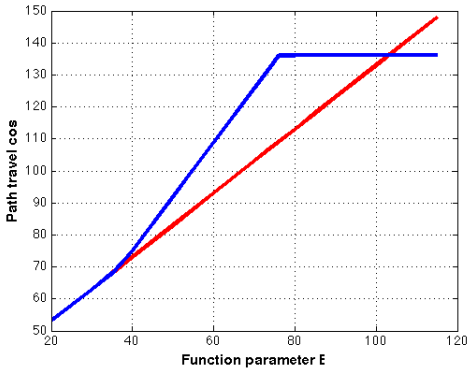

(b) Travel time on used paths, on the 4-link (red line) and 5-link network (blue line).

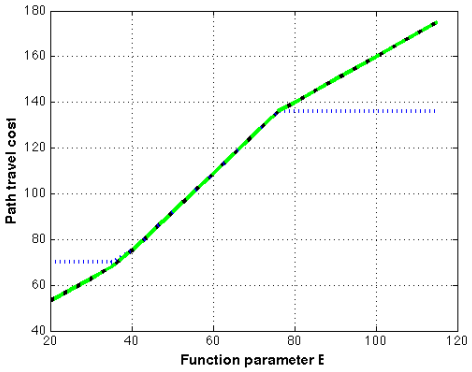

(c) Travel time on all paths, U_{oad} (black line), U_{oabd} (blue line), U_{obd} (green line), 5-link network.

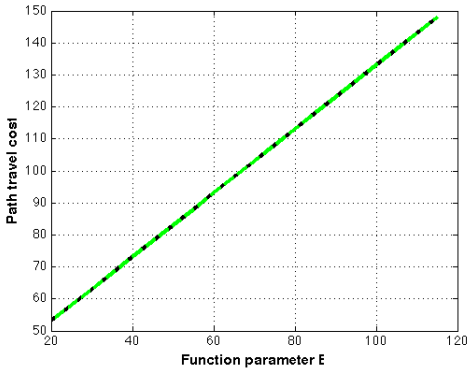

(d) Travel time on all paths, U_{oad} (black line), U_{obd} (green line), 4-link network.

Figure 4.11: Illustration of increase in travel time between the 4- and 5-link Braess' network depending on function parameter B with demand $\kappa = 6$.

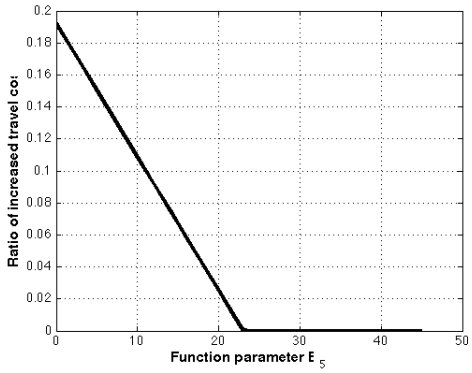

(a) Ratio of increased travel cost.

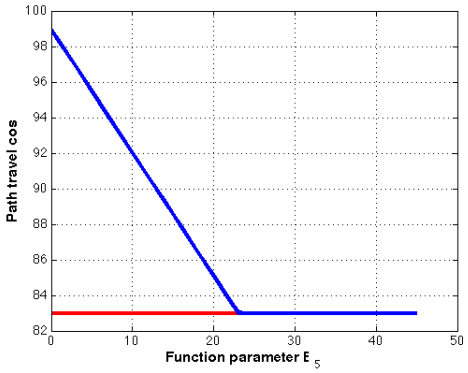

(b) Travel cost on used paths, on the 4-link (red line) and 5-link network (blue line).

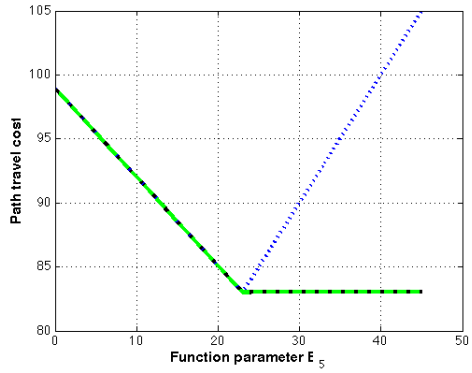

(c) Travel cost on all paths, U_{oad} (black line), U_{oabd} (blue line), U_{obd} (green line), 5-link network.

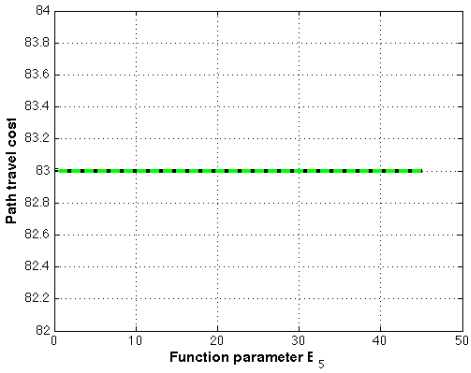

(d) Travel cost on all paths, U_{oad} (black line), U_{obd} (green line), 4-link network.

Figure 4.12: Illustration of increase in travel time between the 4- and 5-link Braess' network depending on function parameter B_5 with demand $\kappa = 6$.

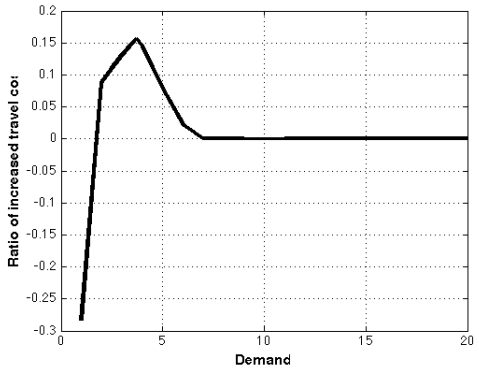

(a) Ratio of increased travel cost.

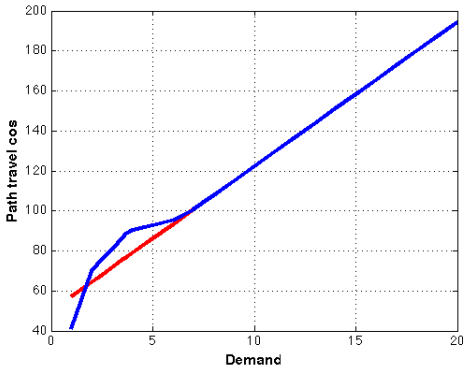

(b) Travel cost on used paths, on the 4-link (red line) and 5-link network (blue line).

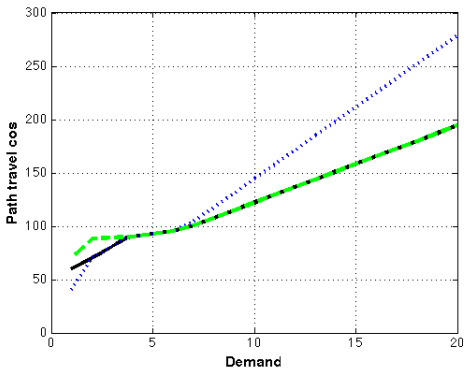

(c) Travel cost on all paths, U_{oad} (black line), U_{oabd} (blue line), U_{obd} (green line), 5-link network.

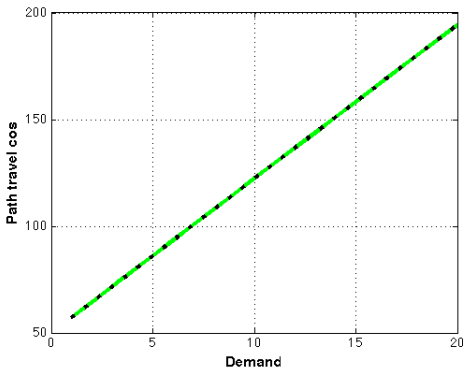

(d) Travel cost on all paths, U_{oad} (black line), U_{obd} (green line), 4-link network.

Figure 4.13: Illustration of increase in travel time between the 4- and 5-link Braess' network depending on demand with $A_4 = 20 \neq A_1$.

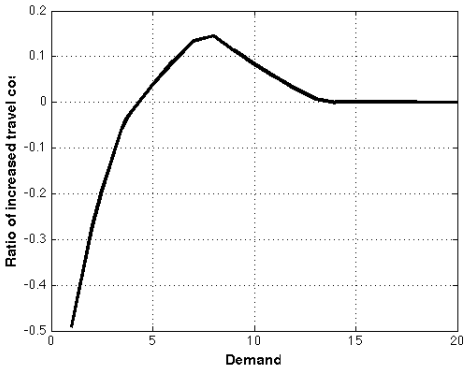

(a) Ratio of increased travel cost.

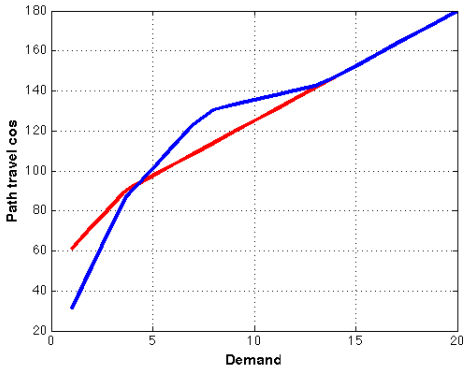

(b) Travel cost on used paths, on the 4-link (red line) and 5-link network (blue line).

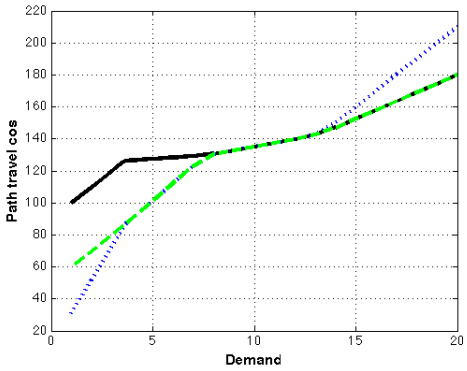

(c) Travel cost on all paths, U_{oad} (black line), U_{oabd} (blue line), U_{obd} (green line), 5-link network.

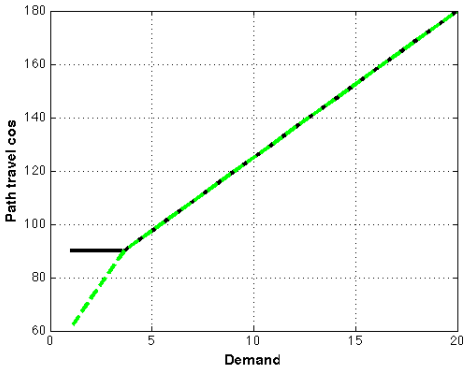

(d) Travel cost on all paths, U_{oad} (black line), U_{obd} (green line), 4-link network.

Figure 4.14: Illustration of increase in travel time between the 4- and 5-link Braess' network depending on demand with $B_2 = 90 \neq B_3$.

4.1.3 Selfish routing

In this section, we compare the Nash equilibrium and the system optimal flow to see how the distributions affect the travel costs. The comparisons include the ratio between system cost at Nash equilibrium and system optimal flow distribution, and show whether the ratio satisfy the upper limit of $\gamma = 4/3$ [19]. System cost is defined in equation 2.7. The path travel costs on used paths at these flow distributions are also shown.

In the first analysis the value of function parameter A is changed, the results are given in Figure 4.15. The ratio ρ between system cost at Nash equilibrium and system optimal flow is given by the blue line in Figure 4.15(a), while the black line is the upper limit $\gamma = 4/3$. Figure 4.15(b) illustrates the differences in path travel cost on used paths when flow is distributed at Nash equilibrium (the blue line) versus at system optimal flow (the red lines). At Nash equilibrium, all used paths have the same path travel time. At system optimal flow, the path travel times are not necessarily equal on all paths. The minimum path travel time of all used routes at system optimal flow, is therefore given by the solid red line, while the maximum value is given by the dashed red line.

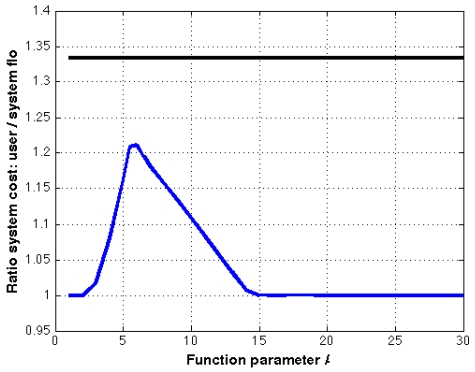

(a) Ratio ρ (blue line) between system cost at user and system optimal flow, and limit 4/3 (black line).

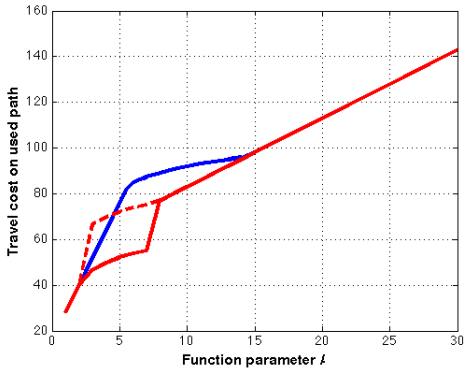

(b) Travel time on used paths at Nash equilibrium (blue line) and min. (red solid line) and max. (dashed line) at system optimal flow.

Figure 4.15: Comparison between user and system optimal flow distribution, changing value A with $\kappa = 6$ and $B = 50$.

We observe from Figure 4.15(a) that system cost at Nash equilibrium $C(\phi_{\mathrm{N}})$ is at the most 1.21 times as large as the system cost at system optimal flow $C(\phi_{\mathrm{syst}})$. The peak is below the upper limit $\gamma = 4/3$, and occurs when $A = 6$. The $C(\phi_{\mathrm{N}})$ at Nash equilibrium only exceeds $C(\phi_{\mathrm{syst}})$ at system optimal flow in a limited value

interval for A. These values are when A is within the interval $A \in (2, 15)$. In Figure 4.15(b) we observe that the minimum and maximum path travel time on used paths at system optimal flow are different in the interval $A \in (2, 8)$, while equal for any other value of A. The travel time on used paths at Nash equilibrium exceeds the minimum travel time at system flow in the interval $A \in (2, 15)$. Before and after this interval the travel times at each distribution seems to coincide. It is understood that outside the interval $A \in (2, 15)$ the flow distributions are equivalent.

In the second analysis the value of function parameter B is changed. The results are given in Figure 4.16. The ratio ρ is given by the blue line in Figure 4.16(a), with the limit $\gamma = 4/3$ (black line). Figure 4.16(b) illustrates the path travel cost at each of the flow distributions. The blue line is path travel cost at Nash equilibrium, and the red lines are minimum and maximum path travel cost at system optimal flow.

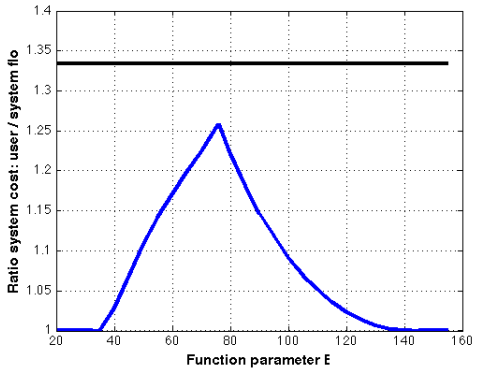

(a) Ratio ρ (blue line) between system cost at user and system optimal flow, and limit 4/3 (black line).

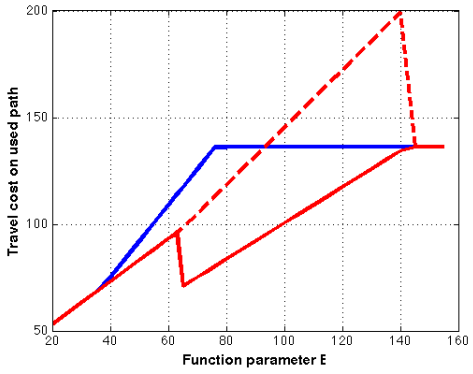

(b) Travel time on used paths at Nash equilibrium (blue line) and min. (red solid line) and max. (dashed line) at system optimal flow.

Figure 4.16: Comparison between user and system optimal flow distribution, changing value B with $\kappa = 6$ and $A = 10$.

From Figure 4.16(a) we observe that the system cost at Nash equilibrium $C(\phi_{\mathrm{N}})$ exceeds the system cost at system optimal flow $C(\phi_{\mathrm{syst}})$ when the value of B is within the interval $B \in (35, 140)$. The peak value is when $B = 76$ such that $C(\phi_{\mathrm{N}}) = 1.26C(\phi_{\mathrm{syst}})$. We observe from Figure 4.16(b) that distributions and travel times on used paths are equivalent when the value is in $B \in [20, 35]$ or $B > 145$. When the path travel time at Nash equilibrium is kept unchanged it is clear that the paths using link u_2 and u_3, which are affected by the value of B, is stops beeing utilized. This happens when $B = 76$. At this point only path U_{oabd}

is utilized. This is as expected.

The peculiar shape in Figure 4.16(b) for the system optimal flow is explained by changes in the flow distribution. The sharp jag at $B = 65$ is a result of link u_5 starting to be utilized, before this point the flow is only distributed equally over path U_{oad} and U_{obd}. The sharp jag at $B = 145$ is a result of change in flow distribution from using all paths to only using path U_{oabd}. The reason is that at system optimal flow there may exist nonutilized paths of less travel time. However, this is not possible at Nash equilibrium, because of the definition that nonutilized paths should have travel time greater or equal to the utilized paths.

In the third analysis the value of function parameter B_5 is changed. The results are given in Figure 4.17. Figure 4.17(a) shows the ratio ρ (blue line), with the limit $\gamma = 4/3$ (black line). The path travel times at each flow distribution are illustrated in Figure 4.17(b), where the blue line is path travel time at Nash equilibrium, and the red lines are minimum and maximum path travel time at system optimal flow.

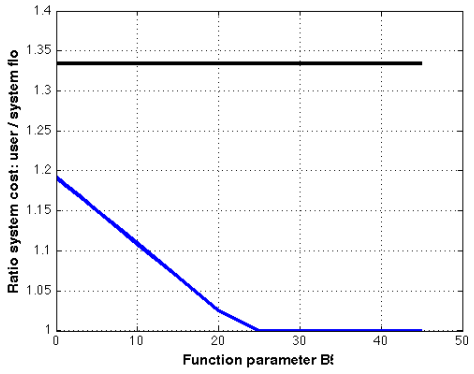

(a) Ratio *rho* (blue line) between system cost at user and system optimal flow, and limit 4/3 (black line).

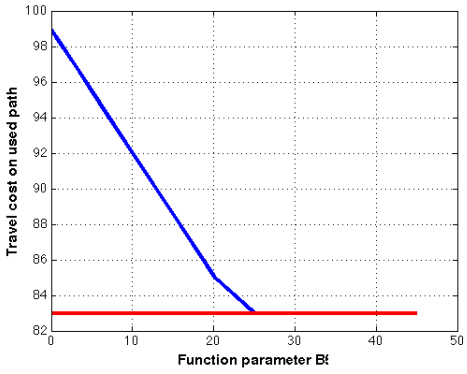

(b) Travel time on used paths at Nash equilibrium (blue line) and min. (red solid line) and max. (dashed line) at system optimal flow.

Figure 4.17: Comparison between user and system optimal flow distribution, changing value B_5 with $\kappa = 6$, $A = 10$ and $B = 50$.

We observe from Figure 4.17(a) that the system cost at Nahs equilibrium $C(\phi_{\mathrm{N}})$ exceeds $C(\phi_{\mathrm{syst}})$ at system optimal flow when the value of B_5 is below 25 (and above 0). At the most the ratio ρ is 1.19. From Figure 4.17(b) we observe that the path travel times and distribution coincides when the value of B is equal to or exceeds 25. From Figure 4.17(b) we observe that the flow distribution and path travel times does change with various values of B_5. If we combine this observation with previous discussion on the jagged line, it is clear that the flow at system optimal flow initially is distributed over paths U_{oad} and U_{obd}. When the value of

B_5 increases, it becomes less favourable to use link u_5. Consequently, the flow distribution at system flow is unchanged.

In the last analysis the value of demand κ is changed. The results are given in Figure 4.18. In this case we used the function values $A = 9$, $B = 70$ and $B_5 = 0$, which are different from the previous cases. The ratio ρ is given by the blue line in Figure 4.18(a), with the limit $\gamma = 4/3$. Figure 4.18(b) illustrates the differences in path travel times at each flow distribution, where the blue line is path travel time at Nash equilibrium, and the red lines are minimum (solid line) and maximum (dashed line) path travel time at system optimal flow.

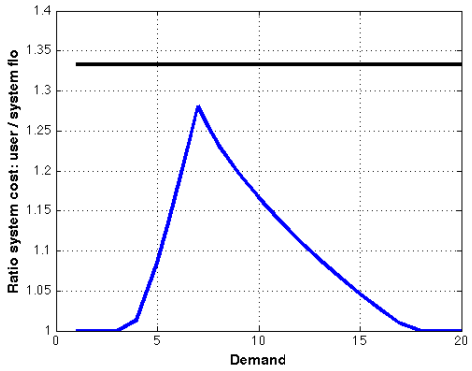

(a) Ratio ρ (blue line) between system cost at user and system optimal flow, and limit 4/3 (black line).

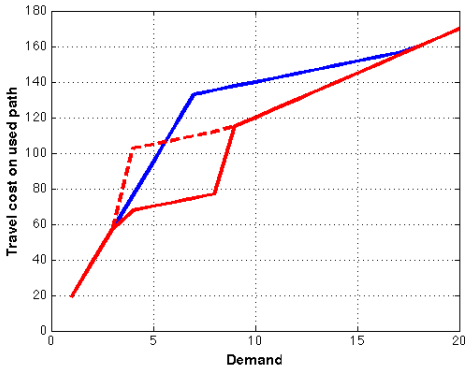

(b) Travel time on used paths at Nash equilibrium (blue line) and min. (red solid line) and max. (dashed line) at system optimal flow.

Figure 4.18: Comparison between user and system optimal flow distribution, changing demand κ with $A = 9$, $B = 70$ and $B_5 = 0$.

We observe from Figure 4.18(a) that the system cost $C(\phi_{\mathrm{N}})$ at Nash equilibrium is at most 1.28 times the value of $C(\phi_{\mathrm{syst}})$ at system optimal flow. Path travel times and distribution coincides when demand is outside the interval $(3, 18)$.

4.2 Network of one origin and two destinatons

In the following example, two Braess' network models are connected in such a way that they have the same origin but different destinations. In the traffic network illustrated in Figure 4.19(a), the networks have one link in common. The collective link is u_2, which results in 3 paths between each OD pair and 6 paths in total. In Figure 4.19(b) the middle links have opposite directions. Consequently, the paths between OD pairs (o, d_1) and (o, d_2) has in all five links in common. The collective links are u_1, u_2, u_3 u_8 and u_9, which results in 4 paths between each OD pair and in total 8 paths. In the following sections, the results for each of these traffic networks are presented.

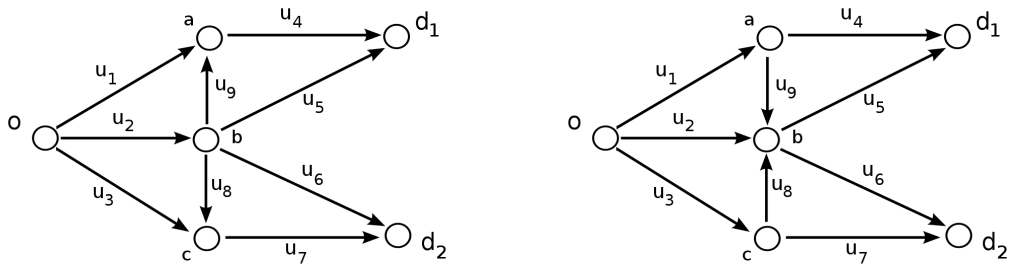

(a) Network of 6 paths, 1 link in common. (b) Network of 8 paths, 5 links in common.

Figure 4.19: Traffic networks of one origin o and two destinations d_1 and d_2.

4.2.1 Braess' paradox on 6-path network

The traffic network in Figure 4.19(a) has the following paths between the origin an each of the destinations,

$$\begin{aligned} U_{oad_1} &= u_1 - u_4, & U_{obd_2} &= u_2 - u_6, \\ U_{obd_1} &= u_2 - u_5, & U_{obcd_2} &= u_2 - u_8 - u_7, \\ U_{obad_1} &= u_1 - u_9 - u_4, & U_{ocd_2} &= u_3 - u_7. \end{aligned}$$

To get the example as similar to the Braess example as possible, we choose the following link cost relations,

$$t_\alpha = A\phi_\alpha, \qquad \alpha = 2, 4, 7, \tag{4.5a}$$
$$t_\alpha = \phi_\alpha + B, \qquad \alpha = 1, 5, 3, 6, \tag{4.5b}$$
$$t_\alpha = \phi_\alpha + B^*, \qquad \alpha = 8, 9. \tag{4.5c}$$

Let the travel time functions be given by equation (4.5), and let the function parameters be equal to $A = 10$, $B = 50$ and $B^* = 10$. With total demand between OD pair $o - d_1$ equal to $\kappa_1 = 6$ and zero demand to destiantion d_2, the resulting distribution is equal to the results in the Braess example. This is the expected result, and verifies that the method works on the network model. The result is not shown here as it is not relevant for the analyses.

In the following analysis the function parameters used are $A = 10$, $B = 50$ and $B^* = 10$, and we let OD demands be $\kappa_1 = \kappa_2 = \kappa = 6$ when nothing else is specified.

In the first analysis the value of OD demand κ is changed. The results are given in Figure 4.20, comparing the travel times between the case when the network contains all links (case 1), and the case when both link u_8 and u_9 are removed (case 2).

Figure 4.20(a) illustrates the ratio of increased travel cost defined in equation (4.1) between the two network cases. With the chosen network, travel time functions and demands, it can be seen that the network example is symmetric. Consequently, the flow distribution between the origin and destination d_1 is equal to the distribution between the origin and destination d_2. Therefore, Figures 4.20(b), 4.20(c) and 4.20(d) only illustrates the travel times between one of the OD pairs. The travel time on used routes, which is equivalent to the minimum travel time, is illustrated in Figure 4.20(b) for each of the cases. The minimal travel time on the complete network is given by the solid line, and the dashed line gives the minimal travel time after removing links u_8 and u_9.

Figure 4.20(c) shows the path travel times on all routes (between one OD pair) when the network contains all links. Path U_{oad_1} is given by the black line, path U_{obd_1} is given by the green dashed line, and path U_{obad_1} is given by the blue dotted line. Figure 4.20(d) shows the path travel times on all routes (between one OD pair) when links u_8 and u_9 are removed from the network. Path U_{oad_1} is still given by the black line and path U_{obd_1} is given by the green dashed line.

Some of the results from changing the OD demand between each OD-pair, with $\kappa_1 = \kappa_2$, are given in Table A.6.

From Figure 4.20(a) we observe that travel time increases with at most 15 % when links u_8 and u_9 are available in the traffic network. This increase is less than for the Braess network model, which was at most 23 %. This is probably because of the collective link u_2 between OD pair (o, d_1) and (o, d_2). Since paths between both OD pairs utilize link u_2 the travel time will consequently be higher than if only one OD pair used the link. We observe from Figure 4.20(b) that Braess' paradox occurs when demand κ is within the interval $(1.5, 7)$. It is evident that this interval is shorter than the interval for the Braess network model. From Figure 4.20(c) we notice that the flow distribution is not only the symmetric distributions

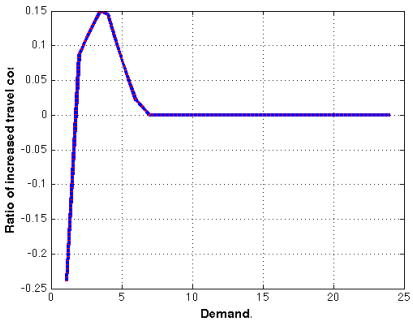

(a) Ratio of increased travel time.

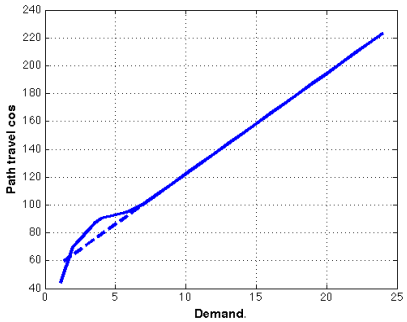

(b) Path travel times on used routes, on complete network (solid line) and without links u_8 and u_9 (dashed line).

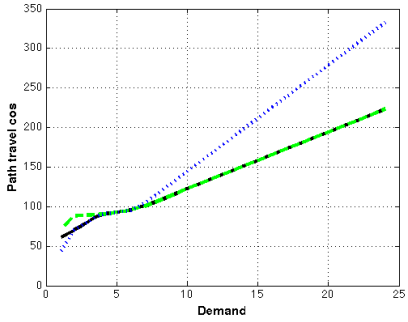

(c) Path travel times on complete network, U_{oad_1} (black line), U_{obd_1} (green line) and U_{obad_1} (blue line).

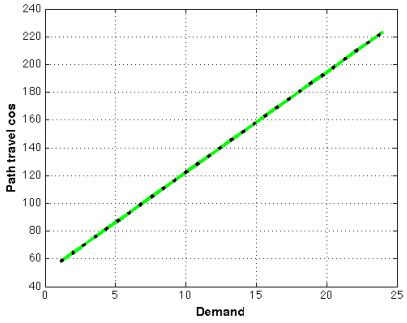

(d) Path travel time, without link u_8 and u_9.

Figure 4.20: Results on network of one origin and two destinations with 6 paths, changing demand κ, and removing both links u_8 and u_9.

as for the Braess network model. When demand is small, and in the short interval $(2, 4)$, the flow is distributed over the paths U_{obad_1} and U_{oad_1}. The distribution is similar to the right-boundary flow illustrated in Figure 4.2(d).

The different flow distributions are shown in Figure 4.21.

In the second analysis the value of function parameters A on links u_2, u_4 and u_7 is changed, and keeping demand fixed at $\kappa_1 = \kappa_2 = 6$. The results are given in Figure 4.22. The ratio of increased travel time is illustrated in Figure 4.22(a). Figure 4.22(b) shows the minimum travel time on the full network (solid line) and after removing links u_8 and u_9 (dashed line). The travel times on all paths in the full network are given in Figure 4.22(c). Path U_{oad_1} is given by the black line, path U_{obd_1} is given by the green dashed line, and path U_{obad_1} is given by the blue dotted line. The path travel times on the network in case 2 are given in Figure 4.22(d).

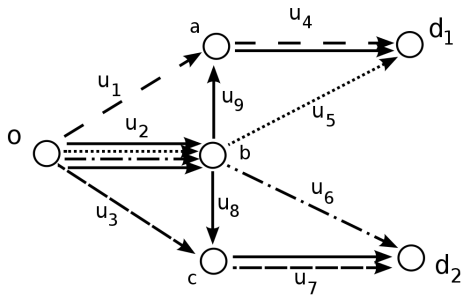

(a) All links used.

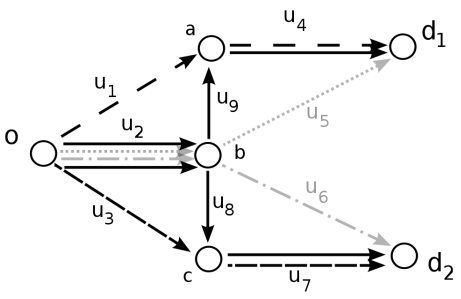

(b) Links u_5 and u_6 unused.

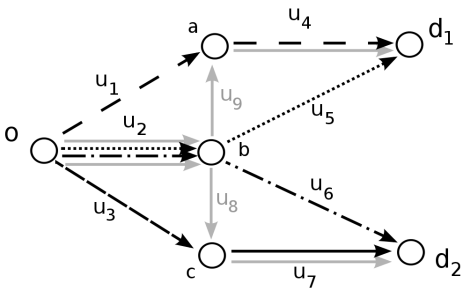

(c) Links u_8 and u_9 unused.

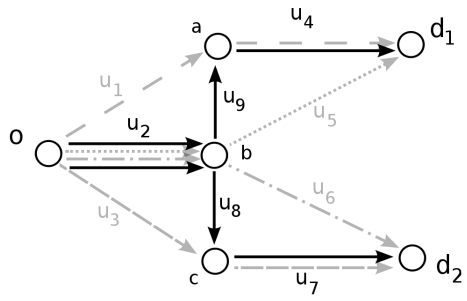

(d) Links u_1, u_3, u_65 and u_6 unused.

Figure 4.21: Flow distribution on traffic network of one origin o and two destinations d_1 and d_2.

As before, path U_{oad_1} is given by the black line and path U_{obd_1} is given by the green dashed line.

We observe from Figure 4.22(a) that travel time increases with at most 15 % when the traffic network is complete, compared to removing links u_8 and u_9. From Figure 4.22(b) we observe that when $A \in [3, 11)$ travel time on used routes in the complete network exceeds the time from when links u_8 and u_9 are removed. We notice from Figure 4.22(c) that traffic flow is distributed in four different manners.

In the last analysis, for the network of one origin and two destinations with 6 paths, the value of function parameter B on links u_1, u_3, u_5 and u_6 is changed. The results are given in Figure 4.23, with demand $\kappa_1 = \kappa_2 = 6$. The ration of increased travel time between case 1 and case 2 is illustrated in Figure 4.23(a). Path travel times on used paths in the full network (solid line) and after links u_8 and u_9 are removed (dashed line) are given Figure 4.23(b). Travel times on all paths in the full network is given in Figure 4.23(c). The black line illustrates path U_{oad_1}, path U_{obd_1} is given by the green dashed line, and path U_{obad_1} is given by

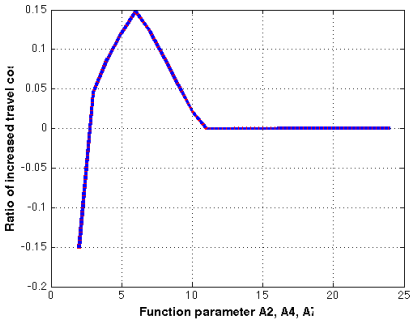

(a) Ratio of increased travel time.

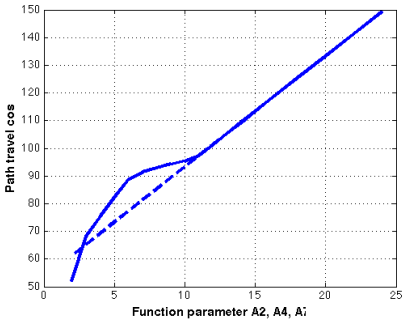

(b) Path travel times on used routes, on complete network (solid line) and without links u_8 and u_9 (dashed line).

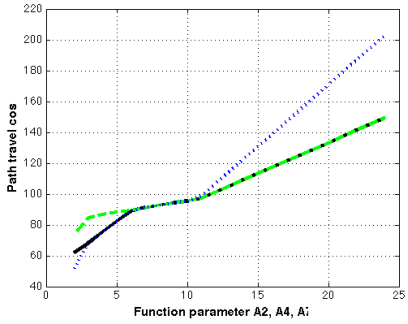

(c) Path travel times on the complete network, U_{oad_1} (black line), U_{obd_1} (green line) and U_{obad_1} (blue line).

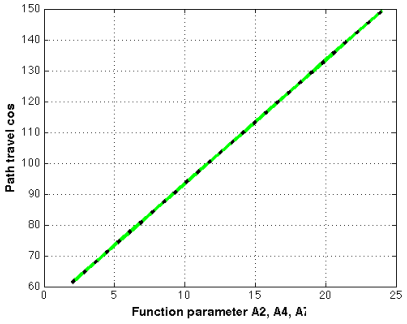

(d) Path travel times, without link u_8 and u_9.

Figure 4.22: Results on network of one origin and two destinations with 6 paths, changing function parameter A with demand $\kappa_1 = \kappa_2 = 6$, and removing both links u_8 and u_9.

the blue dotted line. The path travel times on the network in case 2 are given in Figure 4.23(d). As before, path U_{oad_1} is given by the black line and path U_{obd_1} is given by the green dashed line.

We observe from Figure 4.23(a) that the increase in travel time is at most 16.7 %. Braess' paradox occurs when $B \in (40, 150]$. The flow is first distributed on the paths U_{oad_1} and U_{obd_1}, then the flow is distributed on all paths, for larger values of B the distribution is right-boundary flow for each OD pair, and for even larger values only paths U_{obad_1} and U_{obcd_2} are used. We notice that Braess' paradox occurs when the flow is distributed on either all paths or as right boundary flow.

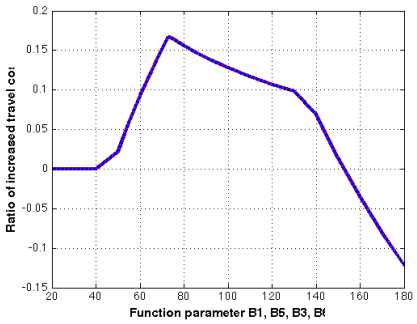

(a) Ratio of increased travel time.

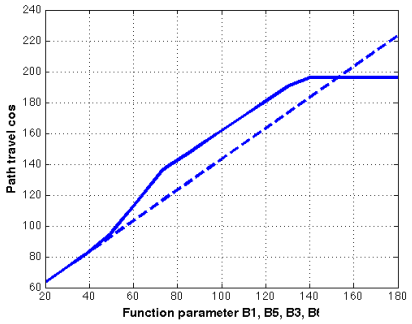

(b) Path travel times on used routes, on complete network (solid line) and without links u_8 and u_9 (dashed line).

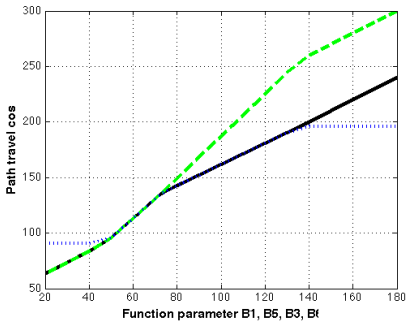

(c) Path travel times on the complete network, U_{oad_1} (black line), U_{obd_1} (green line) and U_{obad_1} (blue line).

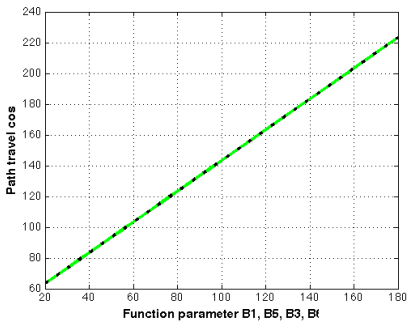

(d) Path travel times, without link u_8 and u_9.

Figure 4.23: Results on network of one origin and two destinations with 6 paths, changing function parameter B, and removing both links u_8 and u_9.

4.2.2 Braess' paradox on 8-path network

The traffic network in Figure 4.19(b) has the following OD paths from origin to each of the destinations,

$$\begin{aligned} U_{oad_1} &= u_1 - u_4, & U_{oabd_2} &= u_1 - u_9 - u_6, \\ U_{oabd_1} &= u_1 - u_9 - u_5, & U_{obd_2} &= u_2 - u_6, \\ U_{obd_1} &= u_1 - u_5, & U_{ocd_2} &= u_3 - u_7, \\ U_{ocbd_1} &= u_3 - u_8 - u_5, & U_{ocbd_2} &= u_3 - u_8 - u_6. \end{aligned}$$

To get the example as similar to the Braess example as possible, we choose the following link cost relations,

$$t_\alpha = A\phi_\alpha \qquad \alpha = 1, 5, 3, 6 \tag{4.6a}$$
$$t_\alpha = \phi_\alpha + B \qquad \alpha = 2, 4, 7 \tag{4.6b}$$
$$t_\alpha = \phi_\alpha + B^* \qquad \alpha = 8, 9. \tag{4.6c}$$

Notice that the link cost functions in equation (4.6) are different from those in equation (4.5).

Let the function parameters in equation (4.6) be equal to $A = 10$, $B = 50$ and $B^* = 10$. With these cost functions we change the value of demand with $\kappa_1 = \kappa_2 = \kappa$. The results are given in Figure 4.24. The ratio of increased travel time is given in Figure 4.24(a). Figure 4.24(b) shows the path travel times on used paths on the complete network (solid line) and the network after removing links u_8 and u_9 (dashed line). The travel times on all paths on the complete network are given in Figure 4.24(c). The black line illustrates path U_{oad_1}, path U_{oabd_1} is given by the blue line, path U_{obd_1} is given by the green dash-dotted line, and path U_{ocbd_1} is given by the red dotted line. The path travel times on the network in case 2 is given in Figure 4.24(d). As before, path U_{oad_1} is given by the black line and path U_{obd_1} is given by the green dash-dotted line.

After reversing the direction of links u_8 and u_9 the increase in travel time is at most 20 %, and the paradox occurs when demand in within $[3, 10)$. The flow is distributed on paths U_{oabd_1} and U_{ocbd_1} at small demands. For the interval of Braess' paradox the flow is distributed on all paths. For larger demands the flow distribution is equal to the network without links u_8 and u_9. The flow distributions are illustrated in Figure 4.25.

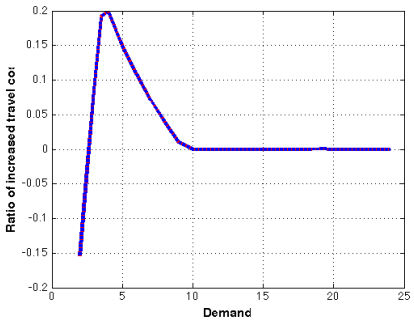

(a) Ratio of increased travel time.

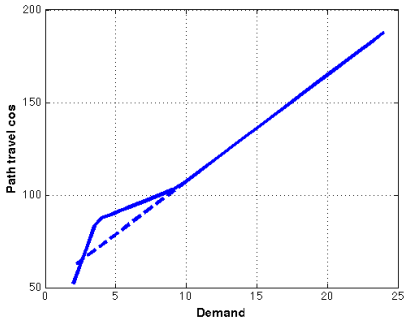

(b) Path travel times on used routes, on complete network (solid line) and without links u_8 and u_9 (dashed line).

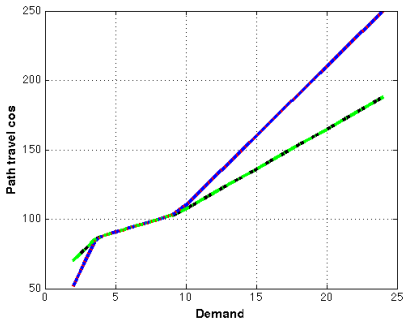

(c) Path travel times on the complete network, U_{oad_1} (black line), U_{obd_1} (green line), U_{obad_1} (blue line), U_{ocbd_1} (red line).

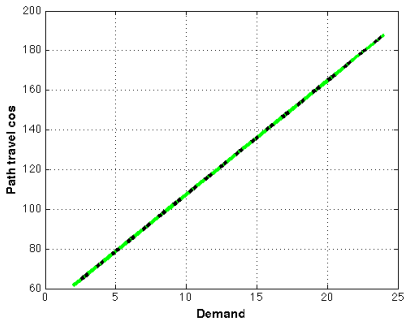

(d) Path travel time, without link u_8 and u_9, U_{oad_1} (black line), U_{obd_1} (green line).

Figure 4.24: Results on network of one origin and two destinations with 8 paths, changing demand κ, and removing both links u_8 and u_9.

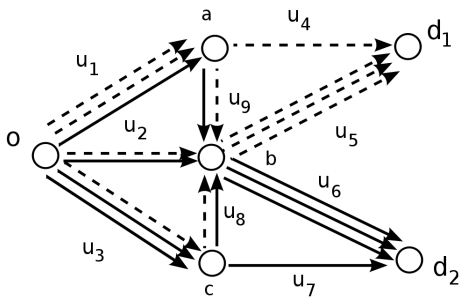

(a) All links used.

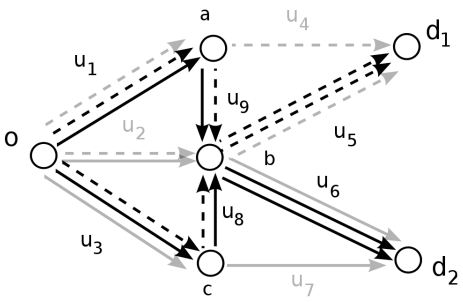

(b) Links u_4 and u_7 unused.

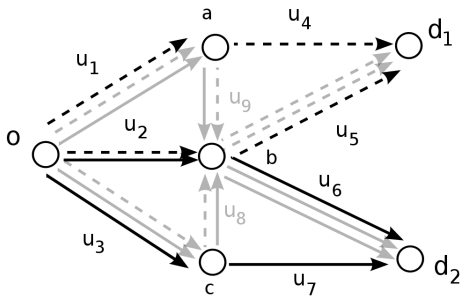

(c) Links u_8 and u_9 unused.

Figure 4.25: Flow distribution on traffic network of one origin o and two destinations d_1 and d_2.

4.2.3 Selfish routing on 6-path network

In this section we investigate selfish routing on the network of one origin and two destinations with 6 paths, and show how the distributions affect the travel costs. The comparisons include the ratio between system cost at Nash equilibrium and system optimal flow distribution, and show whether the ratio satisfy the upper limit of $\gamma = 4/3$ [19]. System cost is defined in equation 2.7. The path travel costs on used paths at these flow distributions are also shown.

In the first analysis the OD demands are changed, with $\kappa_1 = \kappa_2$. The results are given in Figure 4.26. The ratio ρ between system cost at Nash equilibrium and system optimal flow is given by the blue line in Figure 4.26(a), while the black line is the upper limit $\gamma = 4/3$. Figure 4.26(b) illustrates the differences in path travel cost on used paths when flow is distributed at Nash equilibrium (the blue line) versus at system optimal flow (the red lines). At Nash equilibrium, all used paths have the same path travel time. At system optimal flow, the path travel times are not necessarily equal on all used paths. The minimum path travel time of all used routes at system optimal flow, is therefore given by the solid red line, while the maximum value is given by the dashed red line.

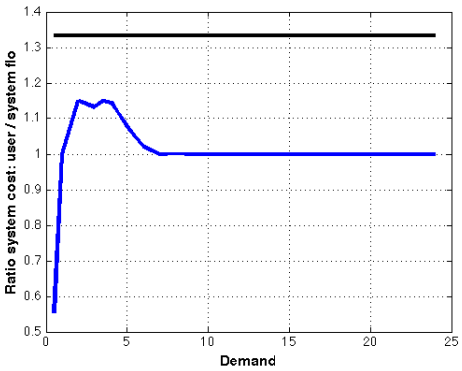

(a) Ratio (blue line) between system cost at user and system optimal flow, and limit 4/3 (black line).

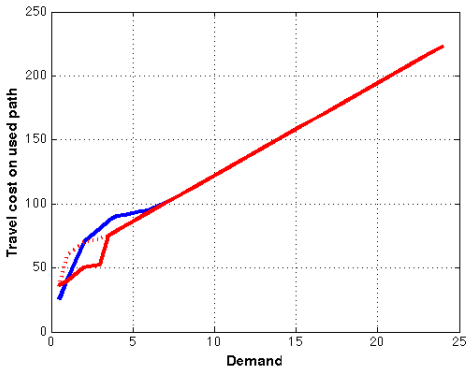

(b) Travel time on used paths at Nash equilibrium (blue line) and min. (red solid line) and max. (dashed line) at system optimal flow.

Figure 4.26: Comparison between user and system optimal flow distribution, changing demand κ.

We observe from Figure 4.26(a) that system cost at Nash equilibrium exceeds the system cost at system optimal flow when demand κ is within the interval $[1, 7)$. The ratio is at most $C(\phi_{\mathrm{N}}) = 1.15C(\phi_{\mathrm{syst}})$ at $\kappa = 2$ and $\kappa = 3.5$.

In the second analysis the value of A is changed. The results are given in Figure 4.27. The ratio between system cost at Nash equilibrium and system optimal flow

is shown in Figure 4.27(a). The travel times on used routes at Nash equilibrium are given by the blue line in Figure 4.27(b). System cost at system optimal flow is given by the red lines, where the solid line is minimum travel time and the dashed line is the maximum travel time.

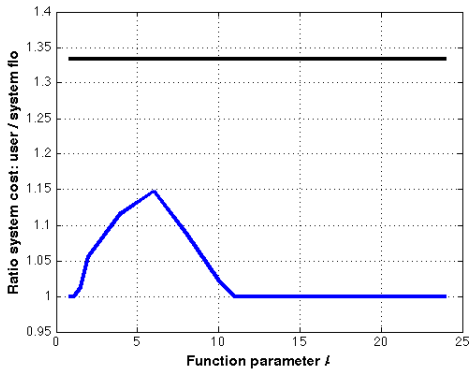

(a) Ratio (blue line) between system cost at user and system optimal flow, and limit 4/3 (black line).

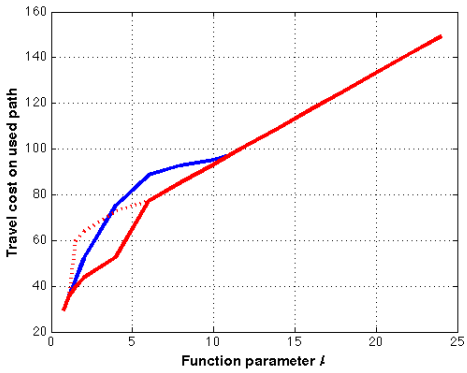

(b) Travel time on used paths at Nash equilibrium (blue line) and min. (red solid line) and max. (dashed line) at system optimal flow.

Figure 4.27: Comparison between user and system optimal flow distribution, changing A.

We observe that system cost at Nash equilibrium exceeds the value at system optimal flow in the interval $A \in (1, 11)$, and the ratio is at most $\rho = 1.15$.

In the last analysis the value of B is changed, and the results are given in Figure 4.28 The ratio ρ is shown in Figure 4.28(a). Figure 4.28(b) illustrates the travel time on used routes at Nash equilibrium (blue line) and at system optimal flow (red lines). The minimum travel time at system optimal flow is given by the solid line while tha maximum travel time is given by the dashed line.

We observe that the system cost $C(\phi_{\mathrm{N}})$ exceeds $C(\phi_{\mathrm{syst}})$ in the interval $B \in (40, 270)$, and the ratio is at most $\rho = 1.17$ at $B = 73$ and $\rho = 1.18$ at $B = 135$.

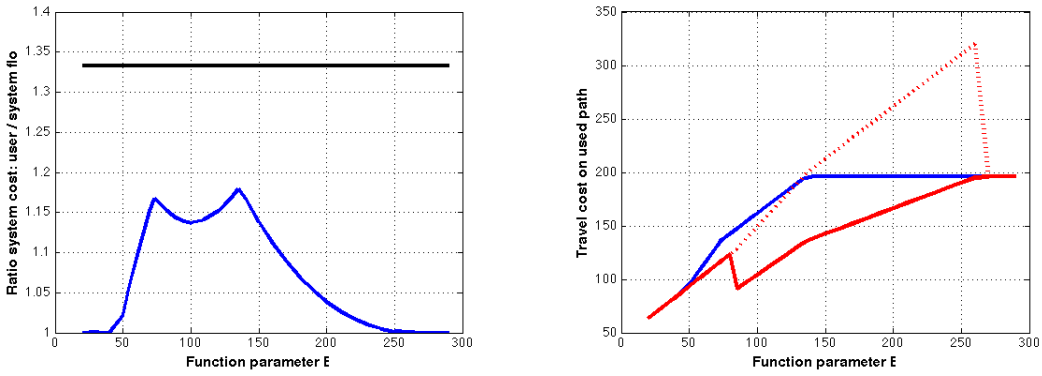

(a) Ratio (blue line) between system cost at user and system optimal flow, and limit 4/3 (black line).

(b) Travel time on used paths at Nash equilibrium (blue line) and min. (red solid line) and max. (dashed line) at system optimal flow.

Figure 4.28: Comparison between user and system optimal flow distribution, changing B.

4.3 Network of two origins and one destination

In the following example, two Braess' network models are connected in such a way that they have the same destination but different origins. In the traffic network illustrated in Figure 4.29(a), the networks have one link in common. The collective link is u_6, which results in 3 paths between each OD pair and 6 paths in total. In Figure 4.29(b), the middle links have opposite directions, such that the paths between OD pairs (o_1, d) and (o_2, d) has in all five links in common. The collective links are u_5, u_6, u_7 u_8 and u_9, which results in 4 paths between each OD pair and in total 8 paths. In the following sections, results for each of the traffic networks are presented. We only show the results from changing the OD demand because the results are similar to those for the network of one origin and two destinations.

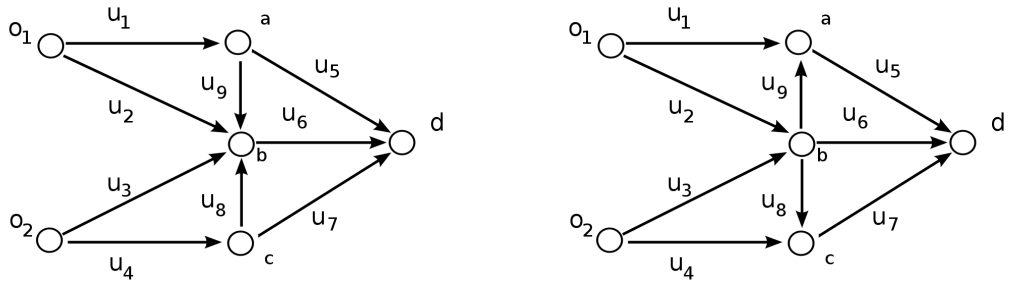

(a) Network of 6 paths, 1 link in common. (b) Network of 8 paths, 5 links in common.

Figure 4.29: Traffic network of two origin o_1 and o_2, and one destination d.

4.3.1 Braess' paradox on 6-path network

The traffic network in Figure 4.29(a) has the following OD paths,

$$\begin{aligned} U_{o_1ad} &= u_1 - u_5, & U_{o_2bd} &= u_3 - u_6, \\ U_{o_1abd} &= u_1 - u_9 - u_6, & U_{o_2cd} &= u_4 - u_7, \\ U_{o_1bd} &= u_2 - u_6, & U_{o_2cbd} &= u_4 - u_8 - u_6. \end{aligned}$$

To get the example as similar to the Braess example as possible, we choose the following link travel functions,

$$t_\alpha = A\phi_\alpha, \qquad \alpha = 1, 6, 4, \tag{4.7a}$$
$$t_\alpha = \phi_\alpha + B, \qquad \alpha = 2, 5, 3, 7, \tag{4.7b}$$
$$t_\alpha = \phi_\alpha + B^*, \qquad \alpha = 8, 9. \tag{4.7c}$$

Let the travel time functions be given by equation (4.5), and let the function parameters be equal to $A = 10$, $B = 50$ and $B^* = 10$. With total demand between OD pair $o_1 - d$ equal to $\kappa_1 = 6$ and zero demand from origin o_2, the resulting distribution is equal to the results in the Braess example. This is the expected result, and verifies that the method works on the network.

Let the OD demands be equal, such that $\kappa_1 = \kappa_2 = \kappa$. The results for different values of demand κ is then given in Figure 4.30, comparing the travel times between the case when the network contains all links (case 1) and the case when both link u_8 and u_9 are removed (case 2).

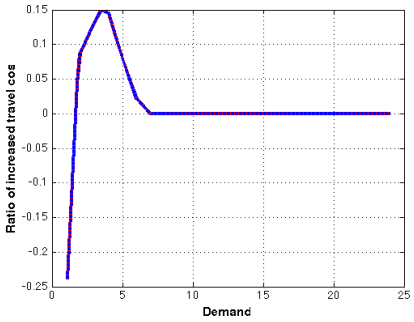

(a) Ratio of increased travel time.

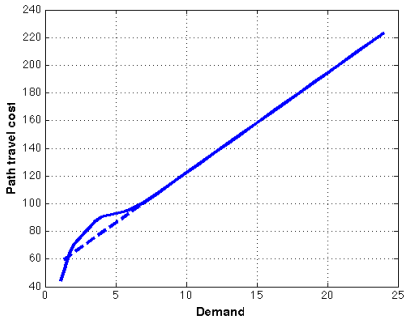

(b) Path travel times on used routes, on complete network (solid line) and without links u_8 and u_9 (dashed line).

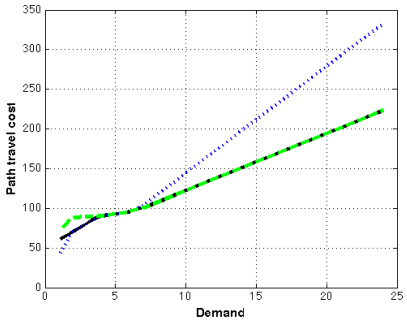

(c) Path travel times on the complete network, U_{o_1ad} (black line), U_{o_1bd} (green line) and U_{o_1abd} (blue line).

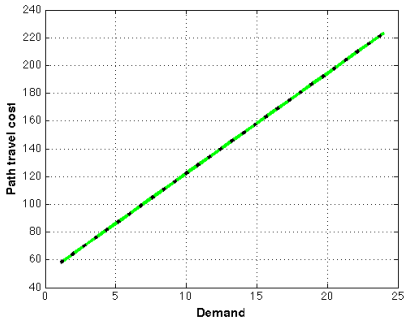

(d) Path travel times, without link u_8 and u_9.

Figure 4.30: Results on network of two origins and one destination, changing demand κ, and removing both links u_8 and u_9.

The ratio of increased travel time defined in equation (4.1) is illustrated in Figure 4.30(a). The minimal path travel times for each of the network cases are given in Figure 4.30(b). The solid line represents the minimum travel time when

the network contains all links, while the dashed line is minimal travel time after links u_8 and u_9 are removed. Figure 4.30(c) shows the travel times on all paths in the complete network. The black line represents path U_{o_1ad}, path U_{o_1abd} is given by the blue dotted line, and path U_{o_1bd} is given by the green dashed line. Figure 4.30(d) shows the travel times on all routes after links u_8 and u_9 are removed. The black line represents path U_{o_1ad} and path U_{o_1bd} is given by the green dashed line.

We observe from Figure 4.30(a) that travel time increases with at most 15 %. From Figure 4.30(b) we observe that Braess' paradox occurs when $\kappa \in [1.8, 7)$. From Figure 4.30(c) we notice that the flow is distributed as extreme, left boundary and interior flows, before it is equivalent to the distribution on the network without links u_8 and u_9. Particularly we notice that the flow is distributed in a small interval as left boundary flow.

4.3.2 Braess' paradox on 8-path network

The traffic network in Figure 4.29(b) has the following OD paths,

$$\begin{aligned}
U_{o_1ad} &= u_1 - u_5, & U_{o_2bd} &= u_3 - u_6,\\
U_{o_1bd} &= u_2 - u_6, & U_{o_2bcd} &= u_3 - u_8 - u_7,\\
U_{o_1bcd} &= u_2 - u_8 - u_7, & U_{o_2bad} &= u_3 - u_9 - u_5,\\
U_{o_1bad} &= u_2 - u_9 - u_5, & U_{o_2cd} &= u_4 - u_7.
\end{aligned}$$

To get the example as similar to the Braess example as possible, we choose the following link cost relations,

$$t_\alpha = A\phi_\alpha, \qquad \alpha = 2, 5, 3, 7, \tag{4.8a}$$
$$t_\alpha = \phi_\alpha + B, \qquad \alpha = 1, 6, 4, \tag{4.8b}$$
$$t_\alpha = \phi_\alpha + B^*, \qquad \alpha = 8, 9. \tag{4.8c}$$

Notice that the link cost functions in equation (4.8) are different from those in equation (4.7).

Let the function parameters in equation (4.8) be equal to $A = 10$, $B = 50$ and $B^* = 10$. With these cost functions we change the value of demand with $\kappa_1 = \kappa_2 = \kappa$. The results are given in Figure 4.31.

The ratio of increased travel times is given in Figure 4.31(a). Figure 4.31(b) shows the path travel times on used paths on the complete network (solid line) and the network after removing links u_8 and u_9 (dashed line). The travel times on all paths on the complete network is given in Figure 4.31(c). The black line illustrates path U_{o_1ad}, path U_{o_1bd} is given by the green dashed line, path U_{o_1bcd} is given by the blue dashed line, and path U_{o_1bad} is given by the red dotted line. The path travel times on the network after removing links u_8 and u_9 are given in Figure

4.31(d). As before, path U_{o_1ad} is given by the black line and path U_{o_1bd} is given by the green dashed line.

We observe from Figure 4.31(a) that the increase in travel time is at most 20 % when links u_8 and u_9 are included in the network. Braess' paradox occurs when $\kappa \in [3, 10)$ (see Figure 4.31(b)). From Figure 4.31(c) we notice that the flow is distributed as extreme and interior flow, before it is equivalent to the network without links u_8 and u_9. These distributions are the same as on Braess' network model.

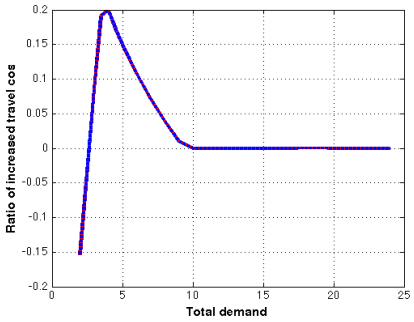

(a) Ratio of increased travel time.

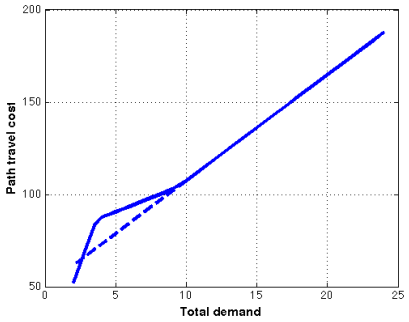

(b) Path travel costs on used routes, on complete network (solid line) and without links u_8 and u_9 (dashed line).

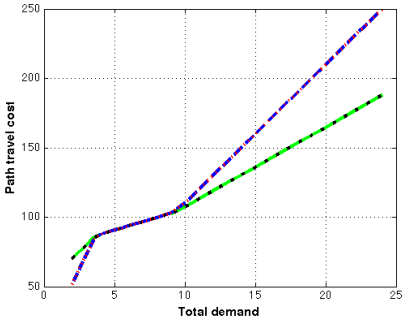

(c) Path travel times on the complete network, U_{o_1ad} (black line), U_{o_1bd} (green line) and U_{o_1abd} (blue line).

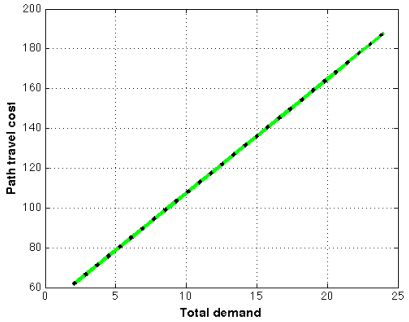

(d) Path travel times, without link u_8 and u_9.

Figure 4.31: Results on network of two origins and one destination, changing demand κ, and removing both links u_8 and u_9.

4.4 Three times symmetric Braess network model

In this section we expand the network into a three times symmetric Braess network model as illustrated in Figure 4.32 [9]. The network contains three origin-destination pairs. Each OD pair is connected with two paths, and has one link in common with each of the other OD pairs. In all there are nine links and 6 paths. The inner links, links u_1, u_4 and u_7, are each used by two OD pairs and in all three different paths.

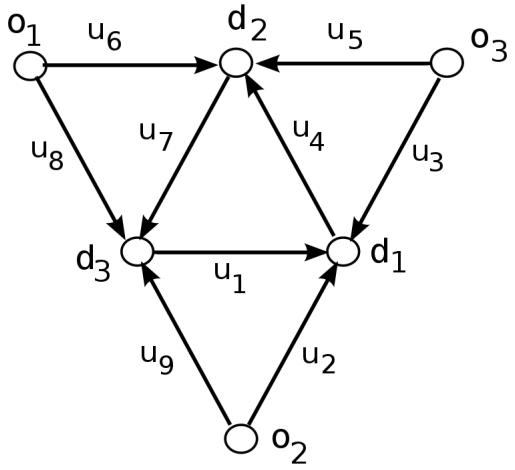

Figure 4.32: Three times symmetric Braess network example.

The network in Figure 4.32 contains the following paths,

$$U_1 = u_6 - u_7 - u_1, \qquad U_3 = u_2 - u_4, \qquad U_5 = u_3 - u_4 - u_7,$$
$$U_2 = u_8 - u_1, \qquad U_4 = u_9 - u_1 - u_4, \qquad U_6 = u_5 - u_7,$$

where paths U_1 and U_2 connects origin o_1 and destination d_1, paths U_3 and U_4 connects o_2 and d_2 and paths U_5 and U_6 connects o_3 and d_3

The following linear cost functions and function parameters are chosen,

$$t_\alpha(\boldsymbol{\phi}) = 10\phi_\alpha, \qquad \alpha = 1, 4, 7, \tag{4.9}$$
$$t_\alpha(\boldsymbol{\phi}) = \phi_\alpha + 70, \qquad \alpha = 2, 5, 8, \tag{4.10}$$
$$t_\alpha(\boldsymbol{\phi}) = 0, \qquad \alpha = 3, 6, 9. \tag{4.11}$$

Notice that the links u_3, u_6 and u_9 have zero travel times, and is therefore independent on the travel flow over the links. We let demand be equal for all of the OD pairs, such that $\kappa_1 = \kappa_2 = \kappa_3 = \kappa$. The results from changing demand is then given in Figure 4.33. We notice that the network, travel time functions and demands are symmetric, similar to the Braess network. Consequently, we only need to look at the travel times for one of the OD pairs.

4.4.1 Braess' paradox

To investigate if and when Braess' paradox occurs on the three times symmetric network, we remove the links of zero travel times which is links u_3, u_6 and u_9. The ratio of increased travel time defined in equation (4.1) between the travel time on the complete network and the travel time on the network after the three links are removed is given in Figure 4.33(a). The minimum travel times are given in Figure 4.33(b), where the solid line represents minimum travel time on the complete network and the dashed line is the travel time after the three links are removed. Figure 4.33(c) shows the travel times on all paths (between one OD pair) on the complete network. The green line represents path $U_1 = u_6 - u_7 - u_1$ and path $U_2 = u_8 - u_1$ is given by the red dashed line. The travel times on the network after the links are removed are given in Figure 4.33(d). Also in this plot path $U_2 = u_8 - u_1$ is given by the red dashed line.

We observe from Figure 4.33(a) that the increase in travel time is at most 30 %. Braess' paradox occurs when demand in within the interval $[3, 9)$ (see Figure 4.33(b)). The flow is first distributed on path U_1, then on both paths, and in the end on only path U_2. Braess' paradox occurs when the flow is distributed on both paths.

The different flow distribution are illustrated in Figure 4.34.

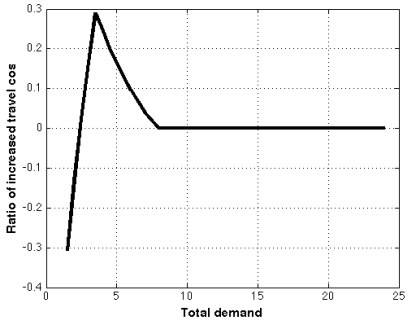

(a) Ratio of increased travel time.

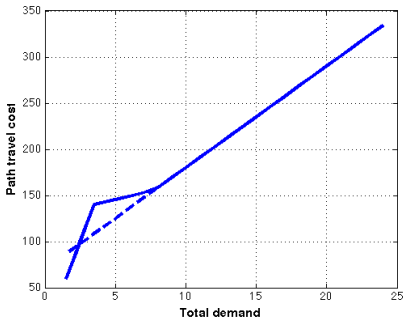

(b) Path travel times on used routes, on complete network (solid line) and without links u_3, u_6 and u_9 (dashed line).

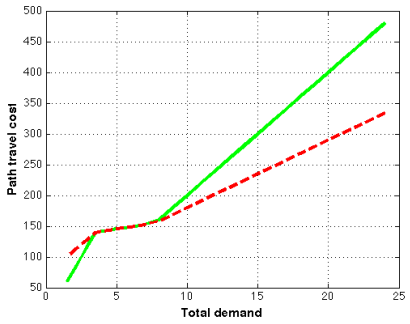

(c) Path travel times on full network, U_1 (green line) and U_2 (red dashed line).

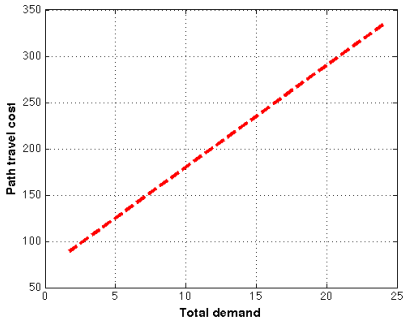

(d) Path travel times, without link u_3, u_6 and u_9, U_2 (red dashed line).

Figure 4.33: Results on the three times symmetric Braess network, changing demand κ, and removing all of links u_3, u_6 and u_9.

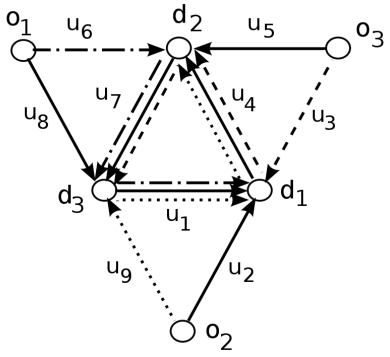

(a) All links used.

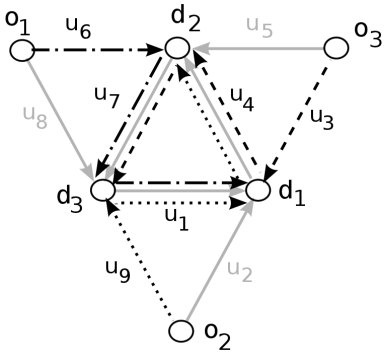

(b) Links u_2, u_5 and u_8 unused.

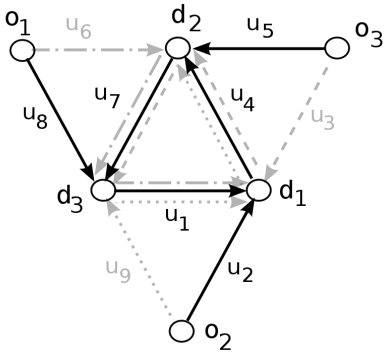

(c) Links u_3, u_6 and u_9 unused.

Figure 4.34: Flow distribution on the three time symmetric traffic network, with three origins o_1, o_2 and o_3 and three destinations d_1, d_2 and d_3.

Chapter 5

Discussion

By the results of the analyses of Braess' paradox presented in Chapter 4 we observe that Braess' paradox occurs on limited intervals of demand. It seems to exist an upper limit for the increase in travel time caused by the added road. The paradox occurs when all paths are used or the path with the additional link(s) (e.g. link u_5) is used together with one or several other paths. The path(s) with the additional link(s) is only favorable to use if demands are small, since the travel time on this path then is the smallest possible travel time at Nash equilibrium. Consequently, the flow is only distributed on the path with the added link at small demands.

If the value of parameter A is large (indicating narrow roads) the path with the additional link(s) is less favorable to use when demand is high, compared to when A is smaller. With large values of B (indicating long roads) the flow will favour the path with the additional link(s). We also notice that Braess' paradox does not occure when the value of B_5 (or equivalently) is large. This is reasonable and quite expected.

Braess' paradox can also occure if the road characteristics (values of A and B) are nonsymmetric on the network. Although the flow is distributed differently for some demands, we notice that the same "rule" apply; Braess' paradox occurs when the path(s) with the additional link(s) is used together with one or several other paths.

The paradox occurs on all networks investigated in this thesis, and all of the results discussed above applies on these networks.

For Braess' network model we compare the Braess flow intervals and the analyses of Braess' paradox. When changing the value of parameter A the results at demand $\kappa = 6$ coincides. The values of A which result in interior flow distributions are equal. For function parameter B with demand $\kappa = 6$ the results are equivalent as the flow is interior when $B = 50$ and extreme when $B = 80$ and higher. The results are similarly equivalent for different values of B_5. For the nonsymmetric analyses the intervals for each flow distribution coincides.

From the analyses of selfish routing we observe that each of the cases presented has a peak, where the ratio ρ of system cost reaches a maximum value before the ratio decreases. The value of ratio ρ is at all these peaks less than the limit $\gamma = 4/3$. For each case there is a limited interval where the system cost at Nash equilibrium exceeds the cost at system optimal flow. We observe that in some intervals the maximum and minimum path travel times on used routes are equal at system optimal flow, while at the same intervals the path travel time is larger at Nash equilibrium. This may seem strange since the travel time on all utilized paths at system optimal flow is equal, which is one of the criterias of Nash equilibrium. For system optimal flow this can be explained by an existence of nonutilized paths with less travel times. This is not possible at Nash equilibrium, because by definition nonutilized paths should have travel time greater or equal to the utilized paths. Outside the interval where $\rho > 0$ the path travel times on used routes and the flow distributions coincides.

In the case of selfish routing it is clear that for some combinations of travel functions and demands it is most unfavorable to use some of the paths, although the system cost is minimal. Specifically, this is when roads u_2 and u_3 in the Braess network model (or the roads corresponding to u_2 and u_3 in the other networks) have particularly large values of B. In these cases it is natural to assume that travelers would not utilize the unfavorable paths, and instead prefer travel time at Nash equilibrium.

We compare the intervals of occurences of Braess' paradox and the intervals of the selfish routing analyses. The intervals of parameter A is equivalent at the boundary $A = 15$, however the lower boundaries are slightly different. The differences occure when the system optimal flow is distributed differently from the 4-link network (or equivalently for the other networks). For the intervals of parameter B it is the lower boundary which coincides, while the upper boundary differ with 40 units. This is also due to differences in flow distributions.

In the Braess example presented in Section 2.4, flow distribution at system optimal flow on the 5-link network coincides with the flow distribution on the 4-link network. This could suggest that these distributions will always coincide. However, from the results presented in Chapter 4 and the discussion above it is clear that this is not a general occurence.

We remark that all networks used in the analyses in this thesis are symmetric in link functions, and in OD paths in the networks where there are more than one OD pair.

The traffic model used in this thesis has some restrictions and limitations. The traffic network is assumed to have reached an equilibrium state. This is a weakness in the model. The assumption relies on the prediction that traffic will experiment for a while, and then settle into an equilibrium. In a real world scenario, traffic

demand will change with time and influence the flow distribution.

Another weakness is that the traffic model relies on the assumption of an ideal traffic network, where all travelers are seeking to find for themselves the path of minimal travel cost. This requires that all travelers have knowledge about all roads and the traffic situation on all of them. This is not completely realistic, but it is a necessary and effective assumption for finding the user optimal flow.

Chapter 6

Conclusion

In this thesis it is shown that Braess' paradox occurs at some intervals of demand when the traffic network is similar to the networks investigated in this thesis. It seems to exist an upper limit for the increase in travel time caused by the added road connection. The intervals of demand are limited and dependent on the road characteristics, such as length and width of the roads. The paradox occurs when the path with the additional road (e.g. link u_5 in Braess' network model) is utilized together with and at the same time as one or several other paths.

It is shown that the paradox occurs on the networks with two and three origins and/or destinations. The routes between different origins and destinations in these networks have one or several collective links. The traffic networks contain long wide roads and short narrow roads in the same pattern as Braess' network model.

Selfish routing affects the travel time when demand is within a limited interval. In these intervals the travel time at Nash equilibrium is higher than at system optimal flow, while at demands outside the interval the flow distributions are equal at each of the optimal flows. The travel times at system optimal flow distribution is in some intervals most unfavorable for some of the travelers, compared to the travel time at user optimal flow.

Chapter 7

Further work

For further work it would be interesting to use suitable non-linear travel time functions. In this work the functions only take into consideration the travel time for traversing a road. A most relevant aspect of road networks is intersections, which can be time consuming when several roads merge. A modification for further work could be to inlcude travel costs at intersections. Such functions could possibly be dependent on the number of roads and the directions of the roads in the intersection.

One can also look into other traffic networks. In most real traffic networks there are more than one or two origins and destinations. Consequently, some roads, e.g. road u_5, could be a good road to use between other origins and destinations. Therefore, removing or closing a road may not in total give the best outcome. Will Braess' paradox occur on nonsymmetric networks? And is there any real traffic networks which could be relevant to analyse for Braess' paradox?

It could be relevant to look at the modified definition of Braess' paradox [9]. With the modified definition the results would for some cases be different from the original definition, and it could be interesting to compare the results.

Bibliography

[1] Abrams, R., Kerzner, L. A Simplified Test for Optimality. *Journal of Optimization Theory and Applications*, Vol. 25, 161-170. (1978)

[2] Ben-Israel, A., Ben-Tal, A., Zlobec, S. *Optimality in Nonlinear Programming: A Feasible Directions Approach*. Wiley, New York. (1981)

[3] Braess, D. Uber ein paradoxen der verkehrsplanung. *Internehmenforschung*, Vol. 12, 258-268. (1968)

[4] Braess, D., Nagurney, A. & Wakolbinger, T. On a Paradox of Traffic Planning. *Transportation Science*, Vol. 39, No. 4, 446-450. (2005)

[5] Cohen, J.E. and Horowitz, P. Paradoxical behavior of mechanical and electrical networks. *Nature*, Vol. 352(8), 699-701. (1991)

[6] Cohen, J.E. & Kelly, F.P. A Paradox of Congestion in a Queuing Network. *Journal of Applied Probability*, 27, pp. 730-734. (1990)

[7] Frank, M. The Braess Paradox. *Mathematical Programming*, 20, 283-302. (1981)

[8] Frank, M. & Wolfe, P. An algorithm for quadratic programming. *Naval Research Logistics Quarterly*, Vol 3, Issue 1-2, 95-110. (1956)

[9] Hagstrom, J.N. & Abrams, R.A. Characterizing Braess's Paradox for Traffic Networks. *IEEE Intelligent Transportation Systems Conference Proceedings*, Oakland (CA) USA. (2001)

[10] Hagstrom, J.N. & Abrams, R.A. Improving Traffic Flows at No Cost, *Mathematical and Computational Models for Congestion Charging*, Springer Science and Business Media, Inc, 1-22. (2006)

[11] Murchland, J.D. Braess's paradox of traffic flow. *Transportation Research*, Vol. 4, 391-394. (1970)

[12] Nash, J. Non-cooperative games. *Annals of Mathematics*, Vol. 54, No. 2, 286-295. (1951)

[13] Nocedal, J. & Wright, S.J. *Numerical Optimization*, 2nd edn, Springer Series in Operations Research, (2006)

[14] Pas, E.I. & Principio, S.L. Braess' Paradox: Some New Insights. *Transportation Research*, Vol. 31, No. 3, 265-276. (1997)

[15] Patriksson, M. *The Traffic Assignment Problem, Models and Methods*, VSP, Utrecht. (1994)

[16] Penchina, C.M. Braess Paradox: Maximum Penalty in a Minimal Critical Network. *Transportation Research*, Vol. 31, No. 5, 379-388. (1997)

[17] Rockafellar, R. T. Some Convex Programs Whose Duals are Linearly Constrained. In Rose, J.B., Magasarian, O.L., Ritter, K. (eds). *Nonlinear Programming*. Academic Press, 293-322. (1970)

[18] Roughgarden, T.*Selfish Routing and the Price of Anarchy*. MIT Press. (2005)

[19] Roughgarden, T. & Tardos, É. How Bad is Selfish Routing? *Journal of the ACM*, Vol. 49, No. 2, 236-259. (2002)

[20] Sheffi, Y. *Urban Transportation Networks*. Prentice Hall, Englewood Cliffs, New Jersey. (1985)

[21] Steinberg, R. & Zangwill, W.I. (1983), The Prevalence of Braess' Paradox. *Transportation Science*, Vol. 17, No. 3, pp.301-318.

[22] Sørensen, Anette Ø. A Survey of the Braess Paradox in Traffic Flow. TMA4500 specialisation project, NTNU. (2014)

[23] Wardrop, J.G. Some Theoretical Aspects of Road Traffic Research. *Proceedings of the Institute of Civil Engineering*, Part II, 325-378. (1952)

Appendix A

Tables and results

Table A.1: Varying variable $A_{1,4}$ on Braess' network example with and without link u_5, with linear travel functions and OD demand $\kappa = 6$.

	Flow Distribution									
Link	$A_{1,4} = 2$		$A_{1,4} = 5$		$A_{1,4} = 10$		$A_{1,4} = 15$		$A_{1,4} = 20$	
u_1	6	3	6	3	4	3	3	3	3	3
u_2	0	3	0	3	2	3	3	3	3	3
u_3	6	3	0	3	2	3	3	3	3	3
u_4	6	3	6	3	4	3	3	3	3	3
u_5	6	-	6	-	2	-	0	-	0	-
Route	Flow Distribution									
U_{oad}	0	3	0	3	2	3	3	3	3	3
U_{oabd}	6	-	6	3	2	-	0	-	0	-
U_{obd}	0	3	0	3	2	3	3	3	3	3
Route	Travel Times									
U_{oad}	62	59	80	68	92	83	98	98	113	113
U_{oabd}	40	-	76	-	92	-	100	-	130	-
U_{obd}	62	59	80	68	92	83	98	98	113	113

Table A.2: Varying OD demand κ on Braess' network model with and without link u_5, with original travel functions.

Flow Distribution														
Link	$\kappa = 2$		$\kappa = 3$		$\kappa = 4$	$\kappa = 6$			$\kappa = 8$		$\kappa = 9$		$\kappa = 10$	
u_1	2	1	3	1.5	3.69	2	4	3	4.31	4	4.5	4.5	5	5
u_2	0	1	0	1.5	0.31	2	2	3	3.69	4	4.5	4.5	5	5
u_3	0	1	0	1.5	0.31	2	2	3	3.69	4	4.5	4.5	5	5
u_4	2	1	3	1.5	3.69	2	4	3	4.31	4	4.5	4.5	5	5
u_5	2	-	3	-	3.39	-	2	-	0.62	-	0	-	0	-
Route	Flow Distribution													
U_{oad}	0	1	0	1.5	0.31	2	2	3	3.69	4	4.5	4.5	5	5
U_{oabd}	2	-	3	-	3.39	-	2	-	0.62	-	0	-	0	-
U_{obd}	0	1	0	1.5	0.31	2	2	3	3.69	4	4.5	4.5	5	5
Route	Travel Times													
U_{oad}	70	61	80	66.5	87.23	72	92	83	96.77	94	99.5	99.5	105	105
U_{oabd}	52	-	73	-	87.23	-	92	-	96.77	-	140	-	110	-
U_{obd}	70	61	80	66.5	87.23	72	92	83	96.77	94	99.5	99.5	105	105

Table A.3: Varying OD demand κ on Braess' network model with and without link u_5, with original travel functions.

	Flow Distribution									
Link	$\kappa = 15$		$\kappa = 20$		$\kappa = 25$		$\kappa = 40$		$\kappa = 75$	
u_1	7.5	7.5	10	10	12.5	12.5	20	20	37.5	37.5
u_2	7.5	7.5	10	10	12.5	12.5	20	20	37.5	37.5
u_3	7.5	7.5	10	10	12.5	12.5	20	20	37.5	37.5
u_4	7.5	7.5	10	10	12.5	12.5	20	20	37.5	37.5
u_5	0	-	0	-	0	-	0	-	0	-
Route	Flow Distribution									
U_{oad}	7.5	7.5	10	10	12.5	12.5	20	20	37.5	37.5
U_{oabd}	0	-	0	-	0	-	0	-	0	-
U_{obd}	7.5	7.5	10	10	12.5	12.5	20	20	37.5	37.5
Route	Travel Times									
U_{oad}	132.5	132.5	160	160	187.5	187.5	270	270	462.5	462.5
U_{oabd}	160	-	210	-	260	-	410	-	760	-
U_{obd}	132.5	132.5	160	160	187.5	187.5	270	270	462.5	462.5

Table A.4: Varying variable $B_{2,3}$ on Braess' network example with and without link u_5, with linear travel functions and OD demand $\kappa = 6$.

	Flow Distribution													
Link	$B_{2,3} = 10$		$B_{2,3} = 25$		$B_{2,3} = 40$		$B_{2,3} = 50$		$B_{2,3} = 75$		$B_{2,3} = 85$		$B_{2,3} = 100$	
u_1	3	3	3	3	3.23	3	4	3	5.92	3	6	3	6	3
u_2	3	3	3	3	2.77	3	2	3	0.077	3	0	3	0	3
u_3	3	3	3	3	2.77	3	2	3	0.077	3	0	3	0	3
u_4	3	3	3	3	3.23	3	4	3	5.92	3	6	3	6	3
u_5	0	-	0	-	0.46	-	2	-	5.85	-	6	-	6	-
Route	Flow Distribution													
U_{oad}	3	3	3	3	2.77	3	2	3	0.077	3	0	3	0	3
U_{oabd}	0	-	0	-	0.46	-	2	-	5.85	-	6	-	6	-
U_{obd}	3	3	3	3	2.77	3	2	3	0.077	3	0	3	0	3
Route	Travel Times													
U_{oad}	43	43	58	58	75.08	73	92	83	134.31	108	145	118	160	133
U_{oabd}	70	-	70	-	75.08	-	92	-	134.31	-	136	-	136	-
U_{obd}	43	43	58	58	75.08	73	92	83	134.31	108	145	118	160	133

Table A.5: Varying variable B_5 on Braess' network model with and without link u_5, with linear travel functions and OD demand $\kappa = 6$.

	Flow Distribution											
Link	$B_5 = 0$		$B_5 = 5$		$B_5 = 10$		$B_5 = 15$		$B_5 = 20$		$B_5 = 25$	
u_1	4.77	3	4.39	3	4	3	3.62	3	3.23	3	3	3
u_2	1.23	3	1.62	3	2	3	2.39	3	2.77	3	3	3
u_3	1.23	3	1.62	3	2	3	2.39	3	2.77	3	3	3
u_4	4.77	3	4.39	3	4	3	3.62	3	3.23	3	3	3
u_5	3.54	-	2.77	-	2	-	1.23	-	0.46	-	0	-
Route	Flow Distribution											
U_{oad}	1.23	3	1.62	3	2	3	2.39	3	2.77	3	3	3
U_{oabd}	3.54	-	2.77	-	2	-	1.23	-	0.46	-	0	-
U_{obd}	1.23	3	1.62	3	2	3	2.39	3	2.77	3	3	3
Route	Travel Times											
U_{oad}	98.92	83	95.46	83	92	83	88.54	83	85.08	83	83	83
U_{oabd}	98.92	83	95.46	-	92	-	88.54	-	85.08	-	85	-
U_{obd}	98.92	83	95.46	83	92	83	88.54	83	85.08	83	83	83

Table A.6: One origin and two destinations, with demands $\kappa_1 = \kappa_2$. With and without link u_9.

	Flow Distribution											
Link	$\kappa = 3$		$\kappa = 4$		$\kappa = 5$		$\kappa = 6$		$\kappa = 7$		$\kappa = 10$	
u_1	1.05	2.86	1.99	3.48	2.91	3.78	3.83	4.09	4.59	4.59	6.56	6.56
u_2	3.91	3.14	4.02	3.78	4.18	4.04	4.35	4.31	4.81	4.81	6.88	6.88
u_3	1.05	0	1.99	0.78	2.91	2.17	3.93	3.6	4.59	4.59	6.56	6.56
u_4	3	2.86	3.83	3.48	3.99	3.78	4.15	4.09	4.59	4.59	6.56	6.56
u_5	0	0.14	0.17	0.52	1.01	1.22	1.85	1.91	2.41	2.41	3.44	3.44
u_6	0	0	0.17	0.27	1.01	1.07	1.85	1.87	2.41	2.41	3.44	3.44
u_7	3	3	3.83	3.73	3.99	3.93	4.15	4.13	4.59	2.49	6.56	6.56
u_8	1.96	3	1.84	2.99	1.08	1.76	0.33	0.53	0	0	0	0
u_9	1.96	-	1.84	-	1.08	-	0.33	-	0	-	0	-
Route	Flow Distribution											
U_{oad_1}	1.05	2.86	1.99	3.48	2.91	3.78	3.83	4.09	4.59	4.59	6.56	6.56
U_{obd_1}	0	0.14	0.17	0.52	1.01	1.22	1.85	1.91	2.41	2.41	3.44	3.44
U_{obad_1}	1.96	-	1.84	-	1.08	-	0.33	-	0	-	0	-
U_{obd_2}	0	0	0.17	0.27	1.01	1.07	1.85	1.87	2.41	2.41	3.44	3.44
U_{obcd_2}	1.96	3	1.84	2.99	1.08	1.76	0.33	0.53	0	0	0	0
U_{ocd_2}	1.05	0	1.99	0.74	2.91	2.17	3.83	3.6	4.59	4.59	6.56	6.56
Route	Travel Times											
U_{oad_1}	81.05	81.5	90.32	88.28	92.83	91.63	95.35	94.98	100.53	100.53	122.19	122.19
U_{obd_1}	89.09	81.5	90.32	88.28	92.83	91.63	95.35	94.98	100.53	100.53	122.19	122.19
U_{obad_1}	81.05	-	90.32	-	92.83	-	95.35	-	104.06	-	144.38	-
U_{obd_2}	89.09	81.36	90.32	88.03	92.83	91.49	95.35	94.94	100.53	100.53	122.19	122.19
U_{obcd_2}	81.05	74.36	90.32	88.03	92.83	91.49	95.35	94.94	104.06	104.06	144.38	144.38
U_{ocd_2}	81.05	80	90.32	88.03	92.83	91.49	95.35	94.94	100.53	100.53	122.19	122.19

Appendix B

MATLAB codes

B.1 Finding all paths between each OD pair

```
function [ paths, E, P ] = Paths( Links, OD)
% Description:
%   - The function finds all paths between all origins and
%       destinations in  a traffic network
% Input
%   - Links     n x 2 matrix of links between nodes [node1 node2; ...]
%   - OD        m x 2 matrix of origin-destination pairs [o1 d1; ...]
% Output
%   - paths     matrix of paths between nodes [node1 node2 node3; ...]
%   - E         equality constraints matrix for demand on OD-paths,
%                   with entries 1 if path j goes between OD pair i
%   - P         n x 2 matrix of indexes for which paths (row number)
%               goes between each OD pair
[m, ~] = size(OD);
index1 = 1; %path
index2 = 1; %node
paths = 0; p = 1; E = 0;
for i = 1:m
    nodeFrom = OD(i);
    pathPart = OD(i,1);
    paths(index1,1) = pathPart;
    [ paths, index1 ] = NextNode( nodeFrom, Links, OD(i,:),...
        index1, index2, paths, pathPart );

    E(i,p:index1) = 1;
    P(i,1) = p;
    P(i,2) = index1;
    index1 = index1 + 1;
    p = index1;
```

```
end
end
```

B.2 Finding the next node on a path

```
function [ Paths, index1 ] = NextNode( nodeFrom, Links, OD, ...
    index1, index2, Paths, pathPart)
% Description:
%   -  The function finds the next node on a path between
%           origin OD(1) and destiantion OD(2).
% Input:
%   - nodeFrom:     the nodenumber one wants to go from
%   - Links:        n x 2 matrix, all directed links in the network
%   - OD:           1 x 2 matrix, origin and destination pairs
%   - index1:       row number (path) in matrix Paths
%   - index2:       column number (node) in matrix Paths
%   - Paths:        p x q in R, matrix of paths, p = # of paths,
%                   q = # of nodes (max) in Paths
% Output:
%   - Paths:        p x q in R, matrix of paths
%   - index1:       rox number (path) in matrix Paths
r = find(Links(:,1) == nodeFrom);
NodesTo = Links(r,2);
if isempty(r) == 1 && Paths(index1, index2) ~= OD(2)
    index1 = index1-1;
    Paths = Paths((1:index1),:);
    temp= index2;
    for j = 1:temp
        if Paths(:,end) == 0
            index2 = index2-1;
            Paths = Paths(:,(1:index2));
        else
            return
        end
    end
end
index2 = index2 + 1;
for i = 1:length(r)
    nodeTo = NodesTo(i);
    if i > 1
        index1 = index1 + 1;
        Paths(index1,1:(index2-1)) = pathPart;
    end
    if nodeTo == OD(2)
        Paths(index1,index2) = nodeTo;
    else
```

```
        NoCycles = noCycles( Paths(index1,:), nodeTo, OD );
        if NoCycles == 1
            Paths(index1, index2) = nodeTo;
            [ Paths, index1] = NextNode(nodeTo, Links, OD,...
                index1, index2, Paths, Paths(index1,1:index2));
        else
            index1 = index1-1;
            Paths = Paths((1:index1),:);
        end
    end
end
end
```

B.3 Check for cycles

```
function [ logical ] = noCycles( path, nextNode, od )
% Description:
%   - The function check that nextNode do not give a cycle,
%       either on one-way links or two-way links
% Input:
%   - path      1 x n vector in R
%   - nextNode  integer in R, want to be added to path at n+1
% Output:
%   - logical   1 = true, if nextNode may be added to the path
%               0 = false, if nextNode leads to cycle
logical = 1;
path = path(path ~= 0);
[~,n] = size(path);
temp = [path(n),nextNode];
for i = 1:(n-1)
    if path(i+1) ~= od(2)
        if temp(1) == path(i) && temp(2) == path(i+1)
            logical = 0;
            return
        elseif temp(2) == path(i) && temp(1) == path(i+1)
            logical = 0;
            return
        end
    end
end
end
```

Appendix C

Active-set method

This chapter presents the active-set method which was tried to solve the quadratic programming problem.

Active-set methods are a group of methods for solving quadratic programming problems [13, pp. 467-480]. A requirement to use this method on a convex problem is that G must be positive semidefinite.

Generally, we do not have knowledge about the active set in advance. So this is the main challenge when wanting to solve a QP problem with inequality constraints. Active-set methods solve QP subproblems with only equality constraints. The sets of equality constraints of these subproblems are called working sets, denoted $\mathcal{W}_k$ at iteration k, and will be further explained below.

There are three variations of active-set methods for QP, which are primal, dual and primal-dual. The primal methods 'generate iterates that remain feasible with respect to the primal problem, while steadily decreasing the objective function q(x)' [13, p. 468]. In the following calculations, a primal method was used.

C.1 KKT-conditions

Let x^* be any solution of the constrained QP problem in (3.65). Then x^* will satisfy the following KKT-conditions,

$$Gx^* + c - \sum_{i \in \mathcal{A}(x^*)} \lambda_i^* a_i = 0, \tag{C.1a}$$

$$a_i^\top x^* = b_i, \qquad \forall i \in \mathcal{A}(x^*), \tag{C.1b}$$

$$a_i^\top x^* \geq b_i, \qquad \forall i \in \mathcal{I} \backslash \mathcal{A}(x^*), \tag{C.1c}$$

$$\lambda_i^* \geq 0, \qquad \forall i \in \mathcal{I} \cap \mathcal{A}(x^*), \tag{C.1d}$$

for some Lagrange multipliers $\lambda_i^*, i \in \mathcal{A}(x^*)$, where a_i and b_i are the constraint parameters. As before, $\mathcal{E}$ and $\mathcal{I}$ are finite sets of indeces for equality and inequality

constraints, respectively. The index set $\mathcal{A}(x)$ is called the active set of x, and is defined as,

> The active set $\mathcal{A}(x)$ at any feasible point x consists of the equality constraint indices from $\mathcal{E}$ together with the indices of the inequality constraints $i \in \mathcal{I}$ for which $c_i(x) = 0$; that is
>
> $$\mathcal{A}(x) = \mathcal{E} \cup \{i \in \mathcal{I} | c_i(x) = 0\},$$
>
> [13, p. 308].

A point x is feasible if it satisfies the constraints of the constrained optimization problem. In the non-linear optimization problem on a traffic network, the inequality constraints in (3.2d) is said to be *active* if the path flow $\Phi_\beta = 0$ on path β, meaning path β carries no flow.

> If x^* satisfies the conditions (C.1) for some $\lambda_i^*, i \in \mathcal{A}(x^*)$, and G is positive semidefinite, then x^* is a global solution of (3.65) [13, p 464, Theorem 16.4].

For a QP problem of only equality constraints, the KKT-conditions may be written as matrices. Let λ^* be the vector of Lagrange mulitpliers which satisfies the KKT-conditions. Let A be the matrix whose rows are the gradients $a_i^\top$ of the constraints where $i \in \mathcal{E}$ (or $i \in \mathcal{A}(x)$), and equivalently let b be the vector of components $b_i, i \in \mathcal{E}$ (or $i \in \mathcal{A}(x)$).

Let Φ^* be the solution vector of path flows. The KKT conditions may then be written as

$$\begin{bmatrix} \mathrm{G} & -\mathrm{A}^\top \\ \mathrm{A} & 0 \end{bmatrix} \begin{bmatrix} \Phi^* \\ \lambda^* \end{bmatrix} = \begin{bmatrix} -c \\ b \end{bmatrix}. \tag{C.2}$$

Introducing $p = \Phi^* - \Phi$, where Φ is some estimate of the solution, and inserting into equation (C.2), the equation system can be rearranged such that,

$$\begin{bmatrix} \mathrm{G} & -\mathrm{A}^\top \\ \mathrm{A} & 0 \end{bmatrix} \begin{bmatrix} -p \\ -\lambda^* \end{bmatrix} = \begin{bmatrix} \mathrm{G} & -\mathrm{A}^\top \\ \mathrm{A} & 0 \end{bmatrix} \begin{bmatrix} \Phi \\ 0 \end{bmatrix} + \begin{bmatrix} c \\ -b \end{bmatrix},$$

which leads to

$$\begin{bmatrix} \mathrm{G} & \mathrm{A}^\top \\ \mathrm{A} & 0 \end{bmatrix} \begin{bmatrix} -p \\ \lambda^* \end{bmatrix} = \begin{bmatrix} g \\ h \end{bmatrix}, \tag{C.3}$$

where

$$g = \mathrm{G}\Phi + c \qquad h = A\Phi - b.$$

The matrix of equation (C.3) is called the Karush-Kuhn-Tucker matrix, denoted K.

C.2 Approach

The working set $\mathcal{W}_k$ at iteration k is a subset of constraints, both equality and inequality. All constraints in the working set is imposed as equality constraints and is the assumed active constraints at iteration k. An important requirement for the working set is that all gradients of constraints a_i in the set, $i \in \mathcal{W}_k$, are linearly independent. The requirement is equal to the linear independence constraint qualification (LICQ) [13, p. 320], which must be satisfied to apply KKT-conditions to the problem.

As usual, the next iterate is given by a step direction p and a step length α, such that $\Phi_{k+1} = \Phi_k + \alpha_k p_k$. In the active-set method, step p is found by solving a QP subproblem of equality constraints from the working set $\mathcal{W}_k$. To find the QP subproblem, let p and g_k be defined as,

$$p = \Phi - \Phi_k, \qquad g_k = G\Phi_k + c,$$

where Φ_k is the iterate at step k. Substituting Φ into the objective function (3.71) (or (3.65a)), we obtain

$$C(\phi) = \frac{1}{2}p^\top G p + g_k^\top p + \frac{1}{2}\Phi_k^\top G \Phi_k + \Phi_k^\top c.$$

Since the two last terms are independent of p, these may be neglected when solving the minimization problem with respect to p. So, the QP subproblem becomes

$$\begin{aligned} \min \quad & \frac{1}{2}p^\top G p + g_k^\top p && \text{(C.4a)} \\ \text{subject to} \quad & a_i^\top p = 0, \qquad i \in \mathcal{W}_k, && \text{(C.4b)} \end{aligned}$$

with solution p_k. As the subproblem only has equality constraints, the KKT-conditions can be written as matrices, such that

$$\begin{bmatrix} \mathrm{G} & -\mathrm{A}^\top \\ \mathrm{A} & 0 \end{bmatrix} \begin{bmatrix} p_k \\ \lambda_k \end{bmatrix} = \begin{bmatrix} -g_k \\ 0 \end{bmatrix}. \tag{C.5}$$

This system of equations can be solved directly or iteratively. We have used a direct solution, which is found as following: From the first equation in (C.5) we have that

$$\mathrm{G}p_k - A^\top \lambda_k = -g_k. \tag{C.6}$$

As G is positive definite, we multiply the above equation by AG^{-1}, such that

$$\mathrm{A}p_k - \mathrm{AG}^{-1}\mathrm{A}^\top \lambda_k = -\mathrm{AG}^{-1} g_k.$$

From the second equation in (C.5), $\mathrm{A}p_k = 0$, so λ_k is found by

$$(\mathrm{A}\mathrm{G}^{-1}\mathrm{A}^\top)\lambda_k = \mathrm{A}\mathrm{G}^{-1}g_k. \tag{C.7}$$

Inserting the solution of λ_k into (C.6), gives

$$\mathrm{G}p_k = (\mathrm{A}^\top\lambda_k - g_k), \tag{C.8}$$

which can be solved to obtain the solution p_k of the QP subproblem (C.4).

As long as $p_k \neq 0$, the next iteration step will be $\Phi_{k+1} = \Phi_k + \alpha_k p_k$, for some step-length parameter α_k. This step-length is selected as the largest value in the range [0,1], for which all constraints are satisfied. If $\Phi_k + p_k$ is a feasible point, then $\alpha_k = 1$. If not, α_k will be decided by the following equation,

$$\hat{\alpha}_k = \min_{i \notin \mathcal{W}_k, a_i^\top p_k < 0} \frac{b_i - a_i^\top \Phi_k}{a_i^\top p_k}. \tag{C.9}$$

And so, the step-length parameter will be

$$\alpha_k = \min\left(1, \hat{\alpha_k}\right). \tag{C.10}$$

The iteration is continued until a point $\hat{\Phi}$ is reached, which minimizes the objective function over its working set $\mathcal{W}_k$. At this point we have that the solution of the subproblem is $p_k = 0$.

The solution $p_k = 0$ satisfies the optimality conditions in equation (C.3) and (C.4). The Lagrange multipliers $\hat{\lambda}_i$ will then satisfy

$$\hat{A}^\top\hat{\lambda} = g, \tag{C.11}$$

at iteration k with working set $\hat{\mathcal{W}} = \mathcal{W}_k$, where

$$\hat{A}^\top\hat{\lambda} = \sum_{i \in \hat{\mathcal{W}}} a_i\hat{\lambda}_i, \qquad g = G\hat{\Phi} + c. \tag{C.12}$$

The value of λ_i must be greater or equal to zero.

With a bad initial feasible point x_0, the method needs too many iterations to find the solution. The challenge is to find a good initial guess, to ensure a smaller number of iterations.

The stepwise procedure is given in Algorithm 3.

Algorithm 3: Active-set method for convex QP [13, p. 468].

Input: Matrix G, c and OD demand κ.
Output: Solution flow distribution x^* at Nash equilibrium.
for *k=0,1,2,...* **do**
  Solve the QP subproblem (C.4) to find p_k
  if $p_k = 0$ **then**
    Compute Lagrange mulitipliers λ_i from (C.11)
    if $\lambda_i \geq 0$ *for all* $i \in \mathcal{W}_k \cap \mathcal{I}$ **then**
      return with solution $x^* = x_k$
    else
      $j \leftarrow \arg\min_{j \in \mathcal{W} \cap \mathcal{I}} \lambda_j$;
      $x_{k+1} \leftarrow x_k$;
      $\mathcal{W}_{k+1} \leftarrow \mathcal{W}_k \backslash \{j\}$;
    end
  else
    Compute α_k from equations (C.10) and (C.9);
    $x_{k+1} \leftarrow x_k + \alpha_k p_k$;
    if *there are blocking constraints* **then**
      Obtain $\mathcal{W}_{k+1}$ by adding one of the blocking constraints to $\mathcal{W}_k$;
    else
      $\mathcal{W}_{k+1} \leftarrow \mathcal{W}_k$;
    end
  end
end